UNIVERSITÀ DEGLI STUDI DI PALERMO

Department of Biomedicine, Neuroscience and Advanced Diagnosis (BiND)

RESEARCH DOCTORATE IN BIOMEDICINE AND NEUROSCIENCE

Glioblastoma: development of new diagnostic tools based on EV-associated proteins

PhD student

Giusi Alberti

Academic Tutor

Prof.ssa Claudia Campanella

Doctorate Coordinator

Ch.mo Prof. Fabio Bucchieri

CICLO XXXIII

Year of Graduation 2020/2021

Contents

Abstract

Glioblastomas multiforme (GBM) are the most common malignant primary brain tumors in adults. They are highly aggressive and have an overall survival of <15 months despite maximal surgical resection and chemoradiation (Ostrom, 2019). GBMs are typically heterogeneous with a wide range of genetic and epigenetic variations among tumor cells. Extracellular vesicles (EVs) represent one of the plausible ways through which can be obtained a better understanding of the heterogeneous subpopulations of GBM / molecular signatures. EVs hold promise for the discovery of potential tumours biomarkers useful in clinical managment for GBM patient diagnosis and follow-up. Isolating EVs from body fluids and screening their protein content may serve as a complementary approach to assess the heterogeneous molecular landscape of GBM as tumors evolve.

Many reports support the idea that Hsps are implicates in the pathogenesis and in the progression of different human neoplasms, by uncertain metabolic mechanism. Athough Hsps perform their canonical “chaperoning” functions in both prokariotic and eukaryotic cells, they have also acquired, probly during evolution, “extra-chaperoning” roles. Among these roles, there are some involved in the mechanism of cancerogenesis.

In this study, we evaluate the exspression of some Hsps (in particular Hsp10, Hsp27, Hsp60, Hsp70, and Hsp90) through experiments of immnohistochemistry in samples of GBM and healthy controls, and also by immunofluorescence analysis on priamry and secondary cell lines of GBM. We also focused to research these proteins in EVs isolated from plasma obatained from patients with GBM, before and after surgery. The isolation was followed by a morphological and biochemical characterization of the EVs, in order to better study the characteristics of these potential natural carriers for the tool development for diagnostic and, possibly, also follow-up biopsy.

Introduction

1 Glioblastoma multiforme

1.1 General overview of the Glioblastoma

Primary brain tumours comprise a wide range of histological and pathological entities, each with a distinct natural history. For simplicity, central nervous system (CNS) tumours are classified as gliomas or non-gliomas. Glioma is a general term used to describe the tumors that affect the glial portion of the brain parenchyma, and they represent a group of neoplasms with multiple histologic types and malignancy grades (Ostrom, 2018) (***Figure 1***). Gliomas of astrocytic, oligodendroglial, oligoastrocytic and ependymal origin account for more than 70% of all brain tumours, with glioblastoma multiforme (GBM) being the most frequent (65%) and malignant of all adult gliomas (Chen, 2017). A shared characteristic of all grades of diffuse glioma is their extensive infiltration in the CSN parenchyma along white matter tracts and pre-existing blood vessel (Sharifi, 2020).

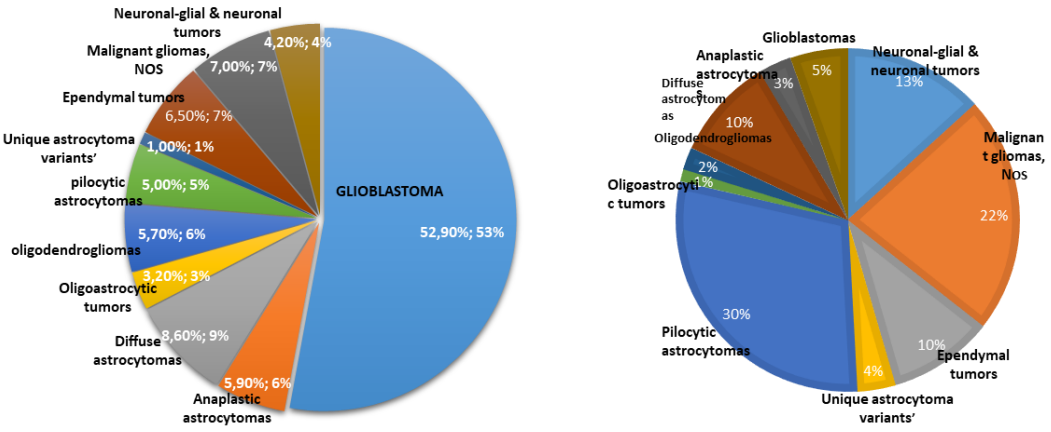

Figure 1. *Relative frequency of tumor types within the overarching categories of glial, neuronal-glial, and neuronal central nervous system neoplasms: left, in the overall population (based on diagnosis in 99.761 cases); on the right, in children and adolescents, ages 0–19 years (11 824 cases). (Reproduced from Ostrom, 2018).*

Following the histopathological diagnosis, patients undergo surgery, chemotherapy, radiotherapy, or a combination of these treatments, although the chances of cure are reduced. Without, survival of patients with GBM is approximately 6-9 months after diagnosis, and even with current standard treatment, the survival rates remain dramatically poor (Tan, 2020).

In 1979 the World Health Organisation (WHO) published the first edition of "Histological Typing of Tumours of the Central Nervous System" to establish a comprehensive four-tiered malignancy grading guideline for the evaluation of brain tumour progression. The WHO system is based on the appearance of specific characteristics, such as nuclear atypia, mitotic activity, florid microvascular proliferation (MVP), and necrosis. By reflecting the malignant potential of the tumour, these features help assess the choice of therapies (Wesseling, 2018) (Jovcevska, 2013). The four grades are detailed as follows: (i) grade I, gliomas relate to lesions that have low proliferative potential and can be cured by surgical procedure; (ii) grade II, gliomas are also considered low grade, but they are infiltrative in nature and often recur despite surgical resection; (iii) grade III, gliomas carry histological evidence of malignancy, such as atypia and fast mitotic activity, and are considered intermediate to high-grade lesions; (iv) grade IV, gliomas are considered high grade and are cytologically malignant, mitotically active, necrosis-prone neoplasms often associated with rapid pre- and post-operative disease evolution and a fatal outcome.

GBM is the most aggressive, invasive and undifferentiated type of tumor and has been designated Grade IV by WHO, accounting for approximately 12-15% of all intracranial neoplasms and 60-75% of astrocytic cancers (Louis., 2016). GBM rarely metastasize, instead, it induces death through invasion into normal brain tissue, and by striking resistance to current therapies (JS, 2021) (de Gooijer, 2018). The morphological hallmark of GBM is its widespread intratumoral heterogeneity, as the moniker "glioblastoma multiforme" implies, with different cell types within a single GBM is characterized by numerous properties and levels of resistance to therapy (Bergmann, 2020). The histopathological features of GBM include nuclear atypia, cellular

pleomorphism, mitotic activity, vascular thrombosis, microvascular proliferation and necrosis (Hambardzumyan, 2015). This complexity, combined with a putative cancer stem cell subpopulation and an incomplete atlas of epigenetic and genetic lesions, has contributed to making this cancer one of the most difficult to understand and treat. So far, multidisciplinary approaches are actually employed in the treatment of patients with GBM, as radical surgery, fractionated beam photon radiation and chemotherapy using temozolomide (TMZ) (Villà, 2014). This therapy could improve the median overall survival of not more than a few months even with best efforts. Indeed, researches are pushed into assessing new putative targets to be tested in clinical trials and into defining new biomarkers to support the decision-making process. Up to these days, anti-angiogenic therapies and immunotherapy are now under evaluation in several clinical trials. Regarding anti-angiogenic treatments, results have not been encouraging, but it is undeniable that the exploitation of the pathways through which angiogenesis inhibitors act, might be fundamental for a better understanding of tumor growth and drug resistance processes (Anthony, 2019).

1.2 Pathogenesis of Glioblastoma

1.2.1 Epidemiology

GBM is rare tumor with an age-adjusted incidence rate of 3.22 per 100,000 population, which accounts for 57.3% of all gliomas and 48.3% of all malignant brain tumors (Ostrom, 2019). The incidence of GBM increases significantly with age and the median age at diagnosis is 65 years (Ostrom, 2018) (Ostrom, 2019). Its prognosis is a constantly poor prognosis with survival rate of 14-15 months after diagnosis makes that it a crucial public health issue (Thakkar, 2014). Of note, the advanced age is a well-established negative prognostic factor. In a phase 3 randomized controlled trial, the median survival of GBM patients is less than 10 months among elderly subjects with short-course radiotherapy plus temozolomide (Perry, 2017). Consequently, elderly patients with GBM represent an important subgroup since they have worse prognosis. Still, limited studies have focused on the incidence trend of elderly with GBM. Research conducted from 2000 to 2008 in Australia reported an increasing incidence of GBM in patients over the age

of 65 with an annual percentage change of 3.0 (95% confidence interval [CI], 0.5-5.6) (Dobes, 2011). Besides, it has been reported an increase in the percentage (from 24 to 27%) of patients over 70 years of age with GBM between 2000 and 2013 in Finland (Korja, 2019). Specifically, the 2019 report from the Central Brain Tumor Registry of the US (CBTRUS) provided the incidence rates and incidence trends of GBM by age group (0-14 years, 15-39 years and 40+ years) (Ostrom, 2019). Moreover, the ratio of incidence is higher in men as compared to women (Thakkar, 2014). The males in the US have a 1.57 increased chance of suffering from GBM, while the western world has higher incidence of gliomas then less developed countries (Thakkar, 2014), probably due to under reporting of gliomas cases, limited access to health care and differences in diagnostic practices. Few studies have shown that blacks are less prone, and incidence of GBM is higher in other ethnic groups including Asians, Latinos and Whites (Bohn, 2018) (Chen., 2001).

1.2.2 Etiology

The etiology of GBM is unknown with the only identifiable risk factor being exposure to ionizing radiation (Grech, 2020). It has been calculated that exposure to ionizing radiation from CT scans increases the overall risk of developing GBM by 2.5% (Davis F. , 2011). However, the risk of radiation-associated cancer persists and is not dependent on age of exposure in patients with GBM (Grech, 2020). A Working Group met in 2011, at the International Agency for Research on Cancer, assessed another possible risk factor for development of GBM, i.e. RF-EMF (include the sun and the earth itself, while artificial sources include satellite devices, broadcasting devices and mobile phones), concluding that there may be an association between RF-EMF (level 2B evidence) and glioma predisposition. Growing evidence have found a correlation between GBM and another possible contributing factor, i.e. air pollution (Yoon, 2020). Nevertheless, there are not substantial evidence of association with lifestyle characteristics, such as cigarette smoking (Holick, 2007), alcohol consumption (Qi, 2014), drug use (Gramatzki, 2020), or dietary exposure to nitrous compounds (Dubrow, 2010). Prognostic factors contributing to the survival of patients with GBM include tumor location, size, as well as advanced age, comorbidities, and the patient's general condition.

1.2.3 Site

The common site of onset of the GBM is the supratentorial region (frontal, temporal parietal, and occipital lobes), with the highest incidence in the frontal lobe, multiple lobes (overlapping tumors), followed by the temporal and parietal lobes (Chakrabart, 2005). A few percent of these tumors occur in cerebellum, brainstem and spinal cord with different tumor behavior found at these locations (Engelhard, 2010). Specifically, supratentorial location of GBM is in older patients (62-64 years of age), in which the cerebellar one is quite rare, as it is more common in younger patients (50–56 years of age) (Babu, 2013). Regarding spinal cord, have been observed in subjects under 18 years of age (Konar, 2016).

1.2.4 Morphological aspects of GBM

The current gold standard diagnosis of these tumours relies on histopathological classification, which provides a grading of malignancy as a predictor of biological behavior. An adequate microscopic diagnosis carries important prognostic information and forms the basis for further patient management. However, histopathological classification of GBM is not always easy due to problems such as tissue harvesting and the biological diversity characteristic of these tumors which make it difficult to capture in precise histopathological criteria.

Histologically, GBM shows significant inter-tumor and intra-tumor heterogeneity, different mutations and phenotypic states, as well as indistinct epigenetic states reflect the genomic instability that leads to therapeutic choices and variable clinical outcomes (Ohgaki, 2013). GBM commonly shows dense proliferation of highly atypical and pleomorphic cells, necrosis, microvascular proliferation. Glioblastoma multiforme cells have shown extensive variability of cell morphology that is characterized by the coexistence of small cells and multinucleated giant cell, polygonal to spindle-shaped with increased nuclear to cytoplasmic ratios, moderate nuclear pleomorphism, coarsely clumped hyperchromatic chromatin, irregular nuclear membranes, and distinct nucleoli. Moreover, GBM presents binucleated and multinucleated cells, as well as lymphocytes, neutrophils, macrophages and necrotic cells. Some cells could contain intranuclear

inclusions and have proliferation of fibrillary extending from the atypical cells. Besides, a few cells resemble adipocytes due to the presence of large lipomatous vacuoles and they may constitute 5–10% of all the tumor cells and even 80% in single cases (Zhang P. , 2020).

Necrotic foci are one of the most characteristic features of the GBM. Histologically, two types of necrosis are typically encountered, depending on localization and size of the necrotic area. The first one consists of large areas of necrosis within the central area of the tumor, resulting from insufficient blood supply. The other type contains small, irregularly shaped necrotic foci surrounded by densely packed, somewhat radially oriented small tumour cells (‘pseudopalisading areas). The pseudopalisading cell population could represent rapidly proliferating neoplastic cells that have “outgrown their blood supply” and undergone central necrosis; a population resistant to apoptosis, which has accumulated because of increased cell survival; a mixed population of tumor and inflammatory cells adjacent to necrosis; or a population of cells migrating to or from a central focus. Cell density of pseudopalisades is almost twice as high, but proliferation activity is from 5 to 50% lower than in other tumor zones. The presence of necrosis leads to a diagnosis of the GBM (Parsons, 2008).

Several studies have shown that GBM shares common molecular features with metastatic cancers (Stoddard, 1993) (Al-Khallaf, 2017). Sequential switching between proliferation and invasion responsible for the formation a dense network of vessels tortuous and hyperpermeable, with increased excessive production of pro-angiogenic factors, resulting in uncontrolled proliferation, infiltration and progression of tumor mass. Therefore, the surface of these newly vessels is covered with a discontinuous layer of pericytes, without any contact with astrocyte processes (Núñez, 2019). Glioblastoma cells undergo a series of molecular and conformational changes shifting the tumor towards mesenchymal traits, including extracellular matrix (ECM) remodeling, cytoskeletal re-patterning, and stem-like trait acquisition (Reinhard, 2016). Importantly, glioblastoma cells have the ability of phenotypic shifts that are conducing to their proliferation, angiogenesis and invasion. Actually, clinical evidence suggests that some GBMs are more disseminated than others (Louis, 2016). For example, mesenchymal-subtype GBM show an

increased potential to invade in comparison to its neural, proneural and classical counterparts (Hartmann, 2010) (classification described below). In light of the overall poor outcome from current therapies, a better understanding of the unique biology of glioma invasion may provide brain-specific interventions for this rapidly progressing disease.

1.2.5 Genetic and molecular alterations based classifiaction

GBMs have been classified into two subtypes, primary or de novo and secondary. Primary tumors represent the majority of diagnosed cases and they develop very rapidly without clinical or histopathological evidence of a less malignant precursor. Secondary tumors, on the other hand, have a history of malignant progression from a lower-grade tumour such as diffuse astrocytoma (WHO grade II) or anaplastic astrocytoma (WHO grade III), with more than 70% of WHO grade II gliomas transforming into WHO grade III/IV diseases within five to 10 years of diagnosis (SongTao, 2012). The majority of GBMs (90%) are primary, and they tend to pertain to an older cohort of patients (mean age = 55 years) than those with secondary GBM (mean age = 40 years) (Stancheva, 2014). It is important to note that, despite their distinct clinical histories, primary and secondary GBMs are morphologically and clinically indistinguishable and their prognosis is equally poor after performing age-adjusted analysis (Mondesir, 2016). In this regard, it is necessary to consider genetic and molecular biomarkers as analysis for their predictive and prognostic significance.

The genetic events involved in the initiation and progression of GBM are still unknown because of the limited availability of early-stage neoplastic tissue. Interestingly, some important and aberrant genetic events drive malignant transformation of GBM, highlighting the importance of molecular classification (***Figure 2***). In a study conducted in 2008, the mutating mutation present in a small number of samples with GBM was found to be in the active site of the isocitrate dehydrogenase 1 (IDH1) gene on the long arm of chromosome 22, a gene never previously associated with GBM (Rohle, 2013). IDH1 encodes an isocitrate dehydrogenase, which catalyzes the carboxylation of isocitrate to α-ketoglutarate and nicotinamide adenine dinucleotide

phosphate (NADPH), a coenzyme used as a reducing agent in anabolic processes. Five isocitrate dehydrogenase genes exist in humans and three are localised in the mitochondria, while IDH1 is localised within the cytoplasm and peroxisomes (Brennan, 2013). The function of IDH1 is to help release cellular stress from oxidative damage through the generation of NADPH. IDH1 may function as a tumour suppressor and, when inactivated by mutation, may contribute to tumourigenesis through induction of the HIF1 pathway (Brennan, 2013). Different researches have shown that patients with IDH1 mutations are significantly different from those without IDH1 mutations in molecular and clinical characteristics, including prognosis. In 2016, the WHO divided it into two: IDH1 mutation and IDH1 wild type the GBM patients (Park, 2019) (***Figure 2***). Mutations in IDH1, which corresponds to the so-called secondary GBM, were observed preferentially in younger glioblastoma patients, on average 33 years of age. The IDH1 mutations are noted in the vast majority of grade II and grade III gliomas, and are associated with better clinical outcomes (Park, 2019). Multivariate analyzes that show that the status of the IDH mutation is as strong a predictor of survival as the histological classification that differentiates high-grade astrocytomas (Bell, 2018). IDH wild type is the most frequent tumor subtype (almost 90% cases), and with a late onset over 55 years of age, typically present in patients with primary GBM. Moreover, there are those not otherwise specified (NOS) for which the IDH status could not be determined. These patients had a longer median survival time of 3.8 years as compared to 1.1 years for patients with wild-type IDH1 (Noushmehr, 2010) (Venkatesan, 2016). The inhibitor of the IDH mutation, which has been applied in preclinical models, shows activity to retard glioma cell growth (Verhaak, 2010).

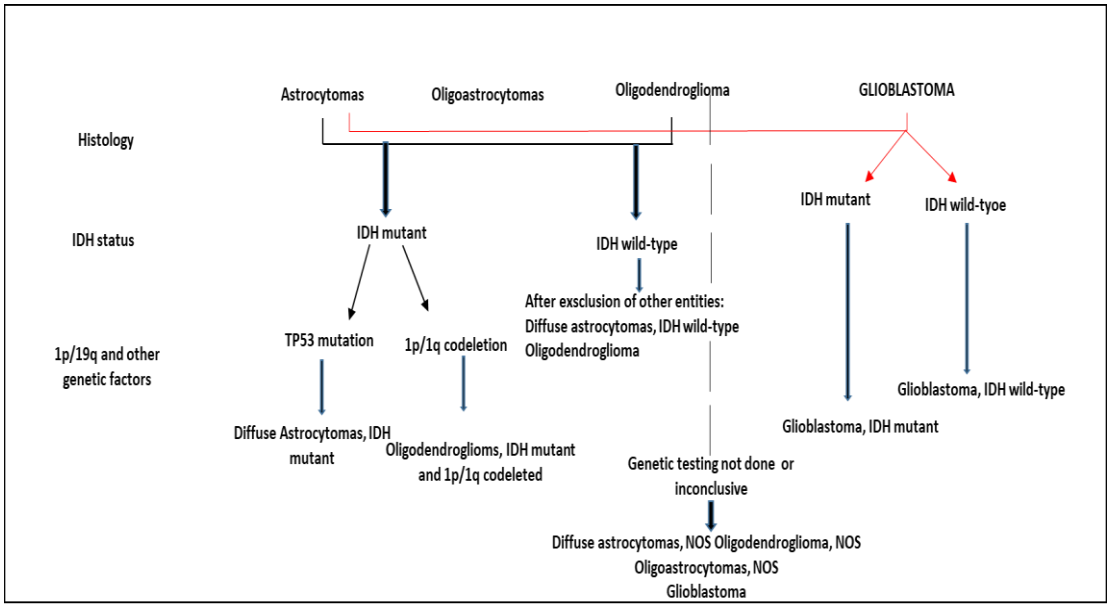

Figure 2. *Simplified algorithm for the classification of GBMs based on histological and genetic characteristics.*

Multi-omics studies from the landscape of GBM in the Cancer Genome Atlas Research Network (TCGA), revealed the complicated genetic profile (Verhaak, 2010). The aim was to "catalogue and discover major cancer-causing genome alterations in large cohorts of human tumours through integrated multi-dimensional analyses". The presently most aberrant molecules in GBM including TP53 (34.4%), Phosphatase and TENsin homolog (PTEN) (32%), NF1 (Neurofibromin 1, 13.7%), EGFR (32.6%), RB1 (Retinoblastoma-associated protein 1, 9.3%), PIK3R1 (Phosphatidylinositol 3-kinase regulatory subunit alpha, 11.7%), PDGFRA (Platelet-derived growth factor receptor A, 4.5%), and the cyclin-dependent-kinase (CDK) CDK4 and CDK6 (Verhaak, 2010) (Colman, 2010) (***Figure 2***). Therefore, the TCGA GBM project states that TP53 mutation is a common event in primary tumors. Interestingly, uncommon focal alterations were also found, such as the amplification of the serine/threonine protein kinase AKT3, known to represent central nodes in a variety of signaling cascades that regulate normal cellular process such as cell size and growth, proliferation, survival, and neo-vascularization (Behnan, 2019). Another key predictive and prognostic marker for the treatment of GBM is the epigenetic changes in O-6-methylguanine-DNA methyltransferase (MGMT) promoter. MGMT is involved in DNA repair and its promoter methylation status has already been associated to sensitivity to the

temozolomide alkylating agent, which is the current standard of care for patients with GBM. Specifically, MGMT promoter methylation is a prognostic factor for patients with GBM and has a significant correlation with worse survival rates (16.9 months vs. 12.7 months) (Sharma, 2017). Moreover, global changes in CpG islands methylation are frequently occur in a subset of GBMs (Brennan, 2013).

Researches on GBMs have highlighted those specific genetic lesions are more commonly observed in certain subclasses of GBMs. Primary tumors typically harbours mutations in the EGFR receptor tyrosine kinase gene, tumour suppressor PTEN and CDKN2A, while secondary tumors harbours mutations in platelet-derived growth factor (PDGF) and tumour suppressor TP53 (Rickert, 2009). However, the latter association is now starting to be considered a historical one, since an increasing number of studies are showing that TP53 mutations occur in a significant amount of primary GBM (Liu, 2017). These alterations can become predictive of glioma subclasses. GBMs with intact expression of the PTEN and EGFR vIII17 proteins, for example, correlate with increased EGFR kinase inhibitor response as compared to tumours expressing EGFR vIII but lacking PTEN. In the past few years, gene expression based studies have successfully identified transcriptional profiles that define the main GBM subclasses: proneural (PN), neural (N), classical (CL) and mesenchymal (MES). Classical GBMs are also characterized by EGFR amplification, lack of TP53 mutations, and oftentimes homozygous deletion of the CDKN2A (Arvold, 2014). Proneural GBMs, sometimes demonstrating alterations in PDGFRA pathway, are usually associated with a better outcome, particularly when harboring mutations in the IDH gene (Phillips, 2006). Mesenchymal GBMs are enriched in mesenchymal markers such as YKL40 and MET (Phillips, 2006) and PTEN genes, which parallels alterations seen in the epithelial-to-mesenchymal transition described in several other tumors (Thiery, 2002). This subtype is commonly associated with a poor prognostic outcome (Phillips, 2006). Finally, neural GBMs strongly resemble the signature of neural cells, with strong expression of neuronal markers such as NEEL, GABRA1, SYT1 and SLC12A5 (Verhaak, 2010) to the point that subsequent studies suggest this group may have arisen from contamination from non-tumor resident cells in

the initial analyses (Wang Q. , 2017). Overall, the mesenchymal and the proneural subtypes tend to be the most robust and reproducible signatures in GBM.

Given the differences between GBM subtypes, it is also important to understand whether there are corresponding differences in their immune landscapes. Initial analyses of the publicly available gene expression data from the Cancer Genome Atlas (TCGA) for GBM showed that mRNA expression for various cytokines, immune cell markers, and immune-associated signaling pathways were found to be increased in the mesenchymal subtype, suggesting that this subtype was the most proinflammatory (Doucette, 2013). TCGA GBM RNA-seq data and other publicly available datasets showed that both the M2 macrophage and neutrophil gene signatures were significantly associated with the mesenchymal subtype (Wang Q. , 2017). These findings, using gene expression, suggest that the GBM subtypes are different in their immune component; but they do not address immune phenotype heterogeneity, nor do they provide a quantitative analysis of the preponderance of immune cells in the tumor microenvironment.

1.2.6 Glioblastoma stem cells

The concept of cancer stem cell initially arose from the observation that cancer tissues resembled developing tissues and self-renewal mechanisms were common to cancer cells and stem cells. For many solid tumours within the CNS, evidence has emerged to support the cancer stem cell hypothesis. In GBM, two different studies (Bao, 2006) (Piccirillo, 2006) separately sought to discern the stem cell nature of this tumor, already identified in a pioneering work by Singh et al (Singh., 2003). Of note, GBMs contain a rare subpopulation of cells with stem cell-like properties, so-called cancer stem cells or tumour-initiating cells expressing or not Prominin as CD133+ stem cells, or more differentiated CD133-cells that include GBM progenitor cells, respectively (Lee., 2006). The historically adopted use of tumor cell lines to delineate tumor biology needs to be re-evaluated in light of the recently discovered stem cell component, in order to assess how well tumor cell lines reflect this characteristic among others compared to primary cells tumor cultures. GBM stem cell (GSC) lines show a remarkable degree of genetic stability (Lee., 2006) and

represent the best available *in vitro* model to study the biology of GBM. Notably, GSC lines mimic the intertumoural molecular heterogeneity of human GBM, and GSC lines resembling all major molecular subtypes have been described, including GSC lines with proneural and mesenchymal expression patterns (Lottaz, 2010). In addition, GSCs recapitulate the intratumoral heterogeneity of the parental tumor in *vivo*, and their biological relevance is demonstrated by their functional role in tumor growth and recurrence, thus representing an important therapeutic target (Verhaak, 2010). Specifically, GSCs thrive in complex microenvironmental niches, nested in the heart of the tumor primarily, as well as unencumbered by stringent checkpoints on proliferation and survival that limit their normal counterparts (Keerthikumar, 2016). The characteristic multipotency of GSCs is determined by a permissive and constant epigenetic landscape, as well as by a low and fluctuating expression of a large number of genes (Théry, 2018). Important contributors to the induction of quiescence including the hypoxic-necrotic nucleus and the perivascular niche. Hypoxic and necrotic regions are a hallmark of GBMs, and support GSC maintenance, proliferation, and therapy resistance. In particular, hypoxic stress generates a subpopulation of cells that are adapted to survive in nutrient-restricted conditions, and promotes shifts towards aerobic glycolysis and glutamine-mediated fatty acid production (Xie, 2014). The effects of hypoxia is mediated in large part through hypoxia-inducible factor 1 (HIF-1) (Gourlay, 2017), localized in perinecrotic niches within tumoral tissue (De la Garza-Ramos., 2016). Among the many roles, HIF-1 also promotes the expression of VEGF, thus inducing angiogenesis in the hypoxic regions (Klekner, 2019). Accordingly, the hypoxic niche prepares the cells to regenerate the perivascular niche, a prime example of how the multiplicity of subpopulations and signaling pathways induced by different attracting states promotes dynamic heterogeneity within the tumor. In fact, GSCs are thought to localize in close proximity to perivascular niches where produce high levels of proangiogenic factors, such as VEGF, that drive endothelial cells proliferation, as well as survival, migration, and blood vessel permeability (Sheng, 2017). Interestingly, GSCs can give rise to pericyte-like cells, key regulators of vascular remodeling and stabilization, indicating an active role in the building of an appropriate niche supplied with additional vasculature and nutrients (Sharifi, 2020).

Overall, understanding the complex intratumoral interactions that facilitate cell resilience GSCs can provide novel therapeutic strategies aimed not only at a snapshot of cellular state but also a topographical landscape of cellular potential.

2 Heat shock proteins

Heat shock proteins (Hsps) are a family of ubiquitous molecules present in the cells of all organisms, and are an important class of molecules essential for cell life and survival (Cappello., 2005). Primarily discovered in the salivary glands of Drosophila following heat stress (Lee J. , 2017), thus the term "heat shock protein". However, is a misnomer because many agents other than heat induce the expression of the heat shock protein gene, such as: ischemia (Ramp, 2007), heavy metal ions (Hasan, 2017), ethanol (Mandrekar, 2008), and surgical stress (Santos-Junior., 2018). This family of genes is highly conserved across species, from Prokaryotes to Eukaryotes. Hsp proteins are critically important because they appear to be necessary in the critical step of three-dimensional folding of some newly formed proteins, as well as in the degradation of damaged-denatured proteins, helping new polypeptides reaching their final functional structure, or re-folding, as well as degrading damaged proteins once exposed to stress events. In addition, they are also important players in other cellular mechanisms such us protein translocation, protein degradation, cell differentiation and signal transduction (Campanella, 2016) (Vilasi, 2018). The swift induction of Hsps expression in response to multiple stress factors is collectively called the heat shock response (HSR), which is regulated at the transcription level by heat shock factors (HSFs), the upstream transcriptional regulators of Hsps (Garrido, 2006). Under non-stress conditions, Hsps are less expressed, but their cytoprotective functions are activated in response to stress through their greater expression of Hsps. Interestingly, compared to normal cells, cancer cells with higher metabolic demands and inappropriately activated signaling pathways showed a greater demand for chaperone machinery to survive. The development of cancer occurs through a radical dysregulation of cellular functions, overcoming the homeostasis of tissues to resume growth and mobility (Hanahan, 2011). In tumor conditions, the increase of oncoproteins require

high levels of Hsps chaperonage for their folding, stabilization, aggregation, activation, function and proteolytic degradation (Chatterjee, 2016) (Neckers, 2012). Importantly, inhibition of Hsps and the chaperonage machinery offers the critical advantage of targeting multiple oncoproteins as well as different signaling pathways crucial for tumor progression (Wang X. , 2014).

Hsps are subdvided into several families on the basis of molecular weight expressed in KiloDalton (kDa) (***Table 1***), namely HSPH (Hsp110), HSPC (Hsp90), HSPA (Hsp70), DNAJ (Hsp40), HSPB (small Hsps), and the chaperonin family's HSPD/E (Hsp60/10). In the list, the first name refers to the new nomenclature system of Hsp human families introduced by Kampinga et al in 2009 (Kampinga, 2009) with the aim of eliminating inconsistencies in their labeling, while the denotation in brackets complies with the common names of the main Hsps. The 27 kDa heat shock protein (Hsp27) belongs to the small heat shock proteins and acts as an ATP-independent molecular chaperone during cellular heat shock (Arrigo, 2007). The 60 kDa heat shock protein (Hsp60), the 70 kDa heat shock protein (Hsp70), and the 90 kDa heat shock protein (Hsp90) are ATP-dependent chaperones that facilitate the folding of unfold or incorrectly aggregated proteins, or, delivery to additional proteostasis machinery for degradation or sequestration of the protein unable to refold, but differ in substrate specificity, localization and in some mechanistic details (D'Souza, 1998) (Sreedhar, 2004).

Chaperone family	Molecular weight (kDa)	Main function(s)
Heavy	100 or higher	Prevents protein aggregation, helps protein folding.
Hsp90	81-99	Protein folding, cytoprotection; intracellular signaling (e.g., steroid receptor); cell-cycle control.
Hsp70	65-80	Prevents protein aggregation, protein folding, cytoprotection and anti-apoaptotic function.
Hsp60	55-63	Protein folding.
Hsp40	35-54	Protein folding and refolding together with Hsp70/Hsc70
Small Hsp	34 or less	Anti-apoptotic function; cytoprotection
Hsp10	10	Protein folding together with Hsp60; modulation of immune system.

Table 1. *Classification of Hsps according to their molecular mass. From* (Rappa, 2012).

2.1.1 Hsp27

Hsp27 (also denoted HspB1) is a well-known member, together with alphaB-crystallin, of the small heat-shock proteins (sHsps) (20–40 kDa). Hsp27 is an ATP-independent molecular chaperone, systemically expressed under basal conditions and upregulated by oxidative stress conditions (Acunzo, 2012), during aging (Lee C. , 2000), and in cancer (Ciocca, 2005). Structural studies reported that, Hsp27 assembles to form a wide range of oligomers, whose constituent monomers and dimers freely exchange between oligomers (Haslbeck, 2015). However, the activity of Hsp27, once activated, remains unclear, with large oligomers, small oligomers, and dimers all involved (Bepperling, 2012) (Fleckenstein, 2015). Intriguingly, the variants of Hsp27 that have a greater tendency to form free monomers show hyperactivity both in *vitro* and in *vivo* (Almeida-Souza, 2010). Furthermore, it has been observed that post-translational dynamic changes, such as phosphorylation, lead to the heterogeneous oligomerization of Hsp27, and are linked to pathological conditions such as tumor (Acunzo, 2012). In details, non-phosphorylated Hsp27 is capable of forming multimers, while the phosphorylation causes conformational changes leading to a significantly reduced oligomeric size, with complex dissociation and subsequent loss of chaperone activity. Nevertheless, its phosphorylation state in cancer cells compared to healthy cells are only starting to be examined. In actual fact, the future challenge lies in a deeper understanding of Hsp27 phosphorylation state in cancer cells in order to develop and/or improve therapies, specific to cancer cells. Of note that, phosphorylation of Hsp27 could present modified subcellular localization which may account for specific roles in cancer cells, considering the diversity of functions that it exerts in normal cells.

2.1.2 Hsp60

Hsp60 is a mitochondrial protein belonging to the group of chaperonins, evolutionarily most conserved among species, from prokaryotes to eukaryotes (Gupta, 1995) (Gammazza, 2012). Despite this, much of information that we have about the structure and function of these

chaperonins derives from studies on their bacterial counterpart, chaperonin groEL and its co-chaperonins groES (Brocchieri, 2000).

In humans, Hsp60, together with its co-chaperonin protein 10 (Hsp10), are encoded by nuclear genes and not mitochondrial (Hansen, 2003). Hsp60 / Hsp10 chaperone complex function consists in helping the folding of the client's proteins forming a tetradecameric structure with two heptameric rings responsible for its barrel shape (Vilasi, 2014). In particular, the monomeric Hsp60 present an equatorial domain responsible for ATP / ADP binding and inter-ring interaction, an intermediate domain, and an apical domain implicated in the interacting with substrate proteins and with co-chaperone. The binding of ATP, substrate and mtHsp10 to both rings simultaneously leads to the typical "football" conformation of Hsp60, which only dissociates following the ATP hydrolysis. Studies in the literature suggest that, rings catalyze the folding of client proteins independently of each other, and that the release of ATP leads to the removal of mtHsp10 and the folded substrate, resulting in a return to the conformation of the double ring (Vilasi, 2014). Unique catalytic cycle of Hsp60 led to deduce that it also does its work in cooperation with Hsp10 in an ATP-dependent process, but it does not shows much affinity for its co-chaperone, preferring the formation of a single hepatmeric ring over the barrel-shaped double ring (Enriquez, 2017). Under normal conditions, Hsp60 molecular chaperonin is present in both mitochondria and cytoplasm (Vilasi, 2014). In mitochondria, Hsp60, together with its co-chaperone Hsp10, assists the importing and folding of newly polypeptides from the cytoplasm to the mitochondrion, and aids the folding of specific client proteins present in the mitochondrial matrix space (Vilasi, 2014). Instead, the isoform of cytosolic Hsp60 has a contradictory role on the regulation of apoptosis, i.e. it may have a pro-survival or pro-apoptotic function according to specific stimuli (Chun, 2010). Accumulating data in literature support that, Hsp60 is localized in extramitochondrial compartments such as cytosol, nucleus, cell surface, and extracellular space and even in blood circulation under stress conditions (Cappello., 2008).

2.1.3 Hsp70

Hsp70 is a structurally and functionally conserved protein, and is one of the most abundant chaperones. The bacterial homolog of human Hsp70 is DnaK, with 50% sequence identity (Hunt, 1985). Hsp70 is encoded by the HSP70 gene and includes protein products that differ in amino acid sequence, level of expression and subcellular localization (Brocchieri, 2008). The Hsp70 family consists of constitutively expressed isoforms (HspA8 / Hsc70), highly stress inducible (HspA1A / Hsp70) and isoforms that perform compartment specific functions (e.g. HspA5 / GRP78 and mtHsp70 / Grp75 are confined to the lumen of the ER and mitochondrial matrix, respectively) (Radons, 2016). Under physiological conditions, the function intracellular of Hsp70 is based in folding of misfolded polypeptides by using ATP binding and hydrolysis (Clerico, 2015), which may be divided into three related activities: prevention of aggregation, promotion of folding to the native state, and solubilization and refolding of aggregated proteins. Hsp70 works together with their co-chaperones of the J-domain protein (JDP) family through association with hydrophobic patches of substrate molecules, which shields them from intermolecular interactions ('holder' activity). An increasing number of regulatory proteins of eukaryotes are known to be controlled in their biological activity through transient association with Hsp70 (Kampinga, 2019). These proteins include nuclear receptors (steroid hormone receptors), kinases (Raf, eIF2α-kinase, CyclinB1/Cdk1) and transcription factors (HSF, c-Myc, pRb) (Kampinga, 2019). Moreover, Hsp70 interacts with Hsp90 and a number of co-chaperones. Multi-faced appearance of Hsp70 is represented by its ability to change its conformations through its functional cycle, allowing Hsp70 to operate in different states and in different condions. In the context of pathological, its ability to suppress apoptosis, senescence, immune responses and promote angiogenesis and metastasis are not yet fully understood. Attempts to develop small molecule inhibitors targeting its two major domains in different states showed promising results, however, it is not yet clear how it can be translated into clinics (Albakova, 2020).

2.1.4 Hsp90

Hsp90 chaperon is highly conserved, its homologue in Escherichia coli is named HtpG (Shiau, 2006). According to the guidelines for Hsps nomenclature detated by Kampinga et al, the human Hsp90 family includes five members classificated as HSPC (Kampinga, 2009). On the basis their location are distinguished in: (i) Hsp90α and Hsp90β, the two major isoforms in the cytoplasm and nucleus, (ii) GRP94 (94-kDa glucose-regulated protein) in the endoplasmic reticulum, and (ii) TRAP-1 (tumor necrosis factor receptor-associated protein 1) in the mitochondrial matrix (Csermely, 1998). Hsp90α is inducible under stress conditions, while Hsp90β is constitutively expressed (Sreedhar, 2004). Like Hsp70, molecular structure comprises a domain of binds to the ATP, middle domain of interaction with a client proteins, and the C-terminal domain involved in the protein dimerization and anchoring of various co-chaperones containing tetratricopeptide domains (TPR) (Li, 2013). The function of Hsp90 is binding and stabilizing specific mutated proteins over their wild-type counterpart, such as p53, a known tumor suppressor gene, thus contributing to mutagenesis. Besides, several clients of Hsp90 are involved in important cellular processes such as cell cycle control, protein stability, angiogenesis, cell proliferation; and tumorigenesis, Hsp90 is observed onto cell membrane of a variety of cells as opposed to its canonical intracellular localization. Furthermore Hsp90 may to be found in the extracellular environment, as well as in extracellular vesicles (Rong, 2018).

3 Extracellular vesicles

Cells can communicate with each other by releasing extracellular vesicles (EVs), which interact with and modify the behavior of target cells at close or distant sites. The first observations of EVs and their relevance occurred in 1946 by Chargaff (Chargaff, 1946) as procoagulant platelet-derived particles in normal plasma and referred to as “platelet dust” by Wolf in 1967 (Wolf, 1976). They represent a highly heterogeneous and dynamic population that differs in cell origin, size, morphology, contents, and membrane composition depending on the cellular source, state and environmental conditions. On the basis of their size, at least 3 main subgroups of EVs have been

defined: (a) apoptotic bodies (1-5µm), (b) cellular microparticles/microvesicles/ectosomes (from 0.1-1 µm), and (c) exosomes (40-50nm) (Gould, 2013) (***Figure 3***).

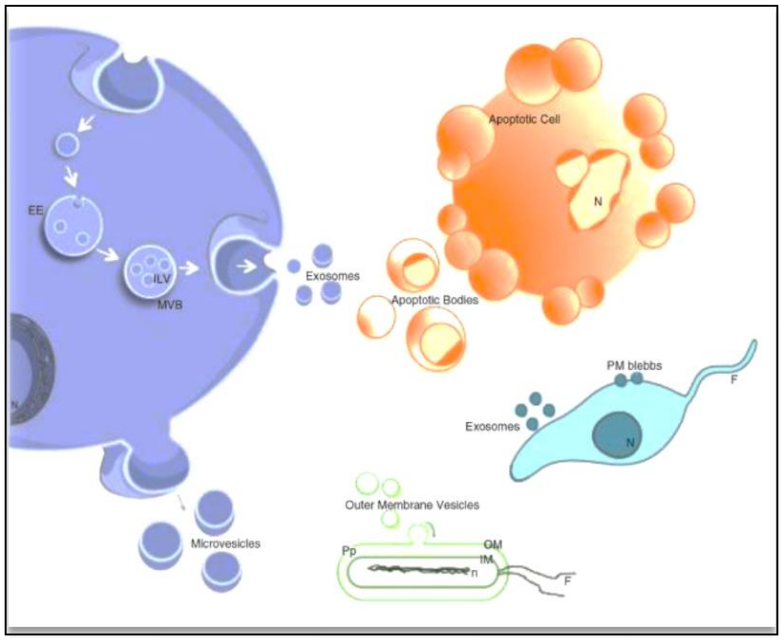

Figure 3. *Biogenesis and release of extracellular vesicles. EE=early endosome; MVB=multi-vesicular body; ILV=intraluminal vesicles; N=Nucleus; OM=outer membrane; Pp=periplasm; IM=inner membrane; n=nucleoid; F=flagella. From* (Yáñez-Mó M. , 2015)

Despite this first classification, EVs were also grouped on the base their tissue of origin, (e.g. oncosomes), their function, or their presence outside the cells, one of their last classification mainly focuses on their mechanism of biogenesis (LM., 2019). So far, there are few studies detailing the classification of EVs with subsequent in-depth characterizations on the markers that can be used as unique references for their classification into different subgroups (i.e. micro- or nano- vesicles). Consequently, allocate a vesicles to a particular biogenesis pathway is still very difficult, unless it is captured during its release in live imaging techniques (Colombo, 2014). An important step in the recent developments of the EVs field has been the collaborative work since 2011 by the members of the International Society of Extracellular Vesicles (ISEV: www.isev.org/), with the aim to unify the nomenclature and the methodologies of EVs (MISEV 2018). They suggested to sort vesicles based on several parameters, such as: size (“small EVs”

(sEVs) and “medium/large” m/l –EVs), density (low, middle, high), biochemical composition (CD63C, CD81C, Annexin A5), description of their tissue of origin (prostasomes, oncosomes), their function outside the cells, and their biogenesis pathway (Théry, 2018).

The EVs molecular composition is cell-type specific and is represented by several molecules, such as proteins, lipids, nucleic acid, metabolites, and even DNA fragments, all reflecting the similar composition of the cell from which they originated (Gutiérrez-Vázquez, 2013). EVs contain proteins that are considered to be pan-EV markers (i.e. common for most EVs), and their proteins and protein post-translational modifications that specifically reflect the vesicle localization, cellular origin and mechanism of secretion (Ostergaard, 2012). In general, EVs are highly abundant in cytoskeletal-, cytosolic-, heat shock- and plasma membrane proteins, as well as in proteins involved in vesicle trafficking, whereas the intracellular organelle proteins are less abundant (Mondal, 2019). However, the protein content may be also on how EVs were isolated (biofluids, cell culture medium, and tissues) (Théry, 2018). Different methods yield EVs and EV sub-fractions of variable homogeneity, which makes it difficult to extrapolate findings between different proteomic studies of EVs. While protein profiles may be characteristic of different EV subgroups, there is, nevertheless, no single marker that can uniquely identify EVs. These vesicles are best isolated, defined and characterized based on multiple techniques, such as differential ultracentrifugation, density gradient centrifugation (sucrose or iodixanol gradients), filtration and size-exclusion chromatography. Due to the small differences in physical properties and composition, discrimination between different EV subgroups after their cellular release remains difficult (Lässer, 2018). Instead, characterization of EV protein content is commonly conducted by, for example, immunoblotting. Proteins enriched in EVs sub-populations that are used as markers include tetraspanins (CD9, CD63, CD81 and CD82), 14-3-3 proteins, major histocompatibility complex (MHC) molecules and cytosolic proteins such as the Hsps, Tsg101 and the Endosomal Sorting Complex Required for Transport (ESCRT-3) binding protein Alix (Yánez- Mó M., 2015). Overall, CD9 and CD81 belong to the top 200 most frequently identified EV proteins (Witwer, 2013).

EVs lipid composition is least known, mainly due to the few standardized isolation methods currently used, that have also caused some confusion in the scientific community in the interpretation of results. However, despite these limitations, it is now known that the lipidomic profiling of EVs isolated from cell cultures and biofluids includes differences in lipid composition between them and the releasing cells (Yáñez-Mó M. , 2015; Acunzo, 2012). Based on the studies present in literature so far, EVs are mainly made up of membrane lipids, although small amounts of other lipids could be captured by the cytosol during intraluminal vesicles (ILV) formation. Consequently, the lipid composition of the EVs should reflect the composition of a lipid bilayer (Elsharkasy, 2020). Since lipids are essential structural and functional constituents of EVs, additional lipidomic studies of EVs from different cell types and body fluids are required to elucidate the role of lipids in the biogenesis and biological functions of EVs.

EVs are released by virtually all cell types in the body and they have been found in various biofluids, including blood, urine, saliva, bile and cerebrospinal fluid (Yáñez-Mó, 2015) (Murillo, 2019). Importantly, EVs isolated from cancer patients' biofluids have been shown to contain cancer-associated molecules such as amplified oncogenes, oncoproteins, specific miRNA signatures, and mutated mRNA or DNA fragments (Al-Nedawi, 2008) (Broggi, 2019). Moreover, it is increasingly recognized that cancer-derived EVs contribute to cancer progression via transferring phenotypic traits among cancer cells and mediating crosstalk with the tumor microenvironment (TME), pre-metastatic niche and immune system (Becker, 2016). TME is a complex dynamic system, made up of several cells (e.g.cancerous cells, fibroblasts, endothelial cells, adipocytes and immune cells) who coexist in the same environment under the regulation of soluble growth factors and other molecules of the extracellular matrix (Hirata, 2017). EVs take part in the modulation of the TME, carrying altered molecules that can modify the physiology of the surroundings, increasing tumor growth (Choi, 2014). Interactions among EVs, cancer cells and the surrounding micro-environment may occurs in several ways: by directly binding the cellular surface of the cell (via the interaction between ligand-membrane receptors), through the release of their luminal content near the target cells, or by simply merging with the plasma

membrane of the cells (partially or totally endocytosed) and delivering their cargo within the lumen of the recipient cell. Through these interactions, cancer-EVs may transfer their metastatic phenotype to different cells, influencing their fate. For instance, cancer EVs carry glycolytic enzymes and metabolites that may provoke a series of endothelial cell alterations, modifying the metabolic activity of cells and enhancing the development of a pro-metastatic micro-environment (Lawson, 2017). Cancer-EVs may also affect the proliferative capacity of donor cells in an autocrine manner, through the interaction with their own plasma membrane (Raimondo, 2015). Cancer-EVs also regulate tumor angiogenesis processes (an essential pathway for tumor growth), controlling the formation of new blood vessels and delivering growth factors and cargo to the cells (Raimondi, 2020). TME is highly hypoxic, due to the excessive consumption of glucose by tumor cells; under these conditions, levels of alterated EVs increase (as compared to EVs released from normoxic cells) and carry proteins and microRNA transcripts involved in pro-angiogenesis processess (Patton, 2020). Therefore, as a consequence of excessive hypoxia, cancer-EVs stimulate the production of new vessels that will positively affect tumor growth (Ko, 2019). However, tumor angiogenesis may also occur indirectly, through the interaction of EVs with other cells (i.e. fibroblasts), causing the secretion of several pro-angiogenic factors that guide endothelial cells migration and vessels formation (Ko, 2019). Cancer-EVs are also implicated in the development of cancer-related thrombi, where they carry coagulant proteins (i.e. tissue factor -TF-) that interact with other clotting factors within the blood and cause the development of a thrombus (Hisada, 2019). However, among all these activities, one of the main roles of cancer-EVs occurs during mechanisms of tumor invasion and metastasis (Endzeliņš, 2017). During these processes, cells have to colonize new different cellular sites through a series of events (e.g. disruption of the cellular matrix and interaction with endothelial cells) that end with the passage of cells into the circulation (bloodstream or lymph) and the colonization of a new distinct site. The rupture of the extracellular matrix may be also promoted by the activity of metastatic EVs that, thanks to the presence of surface integrins and metalloproteinases, interact with the extracellular matrix and guide the migration of other EVs through this latter (Nawaz, 2018). Metastasization may be also stimulated through the communication between EVs and stromal

cells, by the regulation of inflammation processes that increase tumor malignancy and growth (Gener Lahav, 2019). For instance, tumor derived-EVs are able to acquire features similar to those of cancer fibroblasts (the principal cell type within the microenvironment of solid tumors), which can then regulate the activation of these stromal cells for the release of stromal-EVs into the microenvironment, thus contributing in the development of tumor fibroblasts (Vu, 2019). Therefore, EVs act as intercellular communicators between tumor cells and distant organs during metastatic colonization; for instance, some kind of metastatic cells preferably colonize precise organs (lung, liver, brain) releasing EVs that, through the blood, migrate to these new sites and prepare them to the metastatic colonization (Valencia, 2014). This is also possible because during tumor growth, the newly formed blood vessels have a weak structural organization, letting cancer cells enter into the circulation for the colonization of distant areas of the body ring these steps, EVs promote cellular proliferation by transferring specific cargoes that may enhance the expression (or mutation) of oncogenes, as well as activate intracellular signaling pathways, or inhibit negative feedback mechanisms (Maacha, 2019). Metastatization may be also caused by the treatment of tumors with specific chemotherapy drugs that may affect the activity of cancer-EVs. For instance, after these treatments, EVs released by cancer cells may deliver resistance proteins and nucleic acids that stimulate the development of a multi-drug resistance phenotype (MDR) in tumor cells (Lopes-Rodrigues, 2017). According to this hypothesis, it has been shown that cells treated with different type of therapies (e.g. ionizing radiation and chemo-therapeutics), secrete vesicles that may interact with distant cells and provoke stress response or proliferative processes (Kim M. , 2016). Another reason could be that EVs block cancer toxin drugs through the exposition of specific antigens that are targeted by specific antibody (Markov, 2019). Cancer EVs play also an important role during immune evasion, impacting the activity of immune system cells (e.g. NK- and T- cells) and inhibiting their natural functions of killing tumor cells (Ricklefs, 2018). It seems that they regulate the interaction between tumor cells and immune system, promoting many pro- and anti-tumoral effects, such as the immunosuppression of dendritic and T-cells, or the decrease of cytotoxicity of NK-cells (Al-Samadi, 2017). Unlike to all these pro-tumor processes, cancer-EVs can also exert anti-tumor effects, acting as antigen vesicles that

promote anti-tumor immune responses and activate dendritic, NKs- and macrophages cells (Zhang B. , 2014). For instance, once dendritic cells have absorbed tumor cells and tumor antigens, they release EVs loaded with those antigens that may positively increase immune responses (Zeng, 2018).

These findings have raised the idea that the analysis of molecular content of EVs could inform about the presence molecular profile and behavior of cancer and therefore they could serve as liquid biopsies. There is conflicting evidence regarding the levels of EVs in cancer patients as opposed to healthy controls (Cappello., 2017) (Xu, 2018), since some studies show that cancer patients have increased EV levels in their blood (Matsumoto, 2016) (Rodríguez-Martínez, 2019); whereas other studies show that there is no statistical difference in EV plasma levels between cancer patients and healthy individuals (Menck, 2017). These conflicting results may be due to the lack of technical standardization between laboratories, including differences in EVs isolation and quantification protocols. Athough, increased EV levels in the blood have been found in patients with various other diseases including ischemic stroke (Chiva-Blanch, 2016), coronary heart disease (Cui, 2013), diabetic kidney disease (Rodrigues, 2018), and others. Thus, increased release of EVs appears to be a common feature of many diseases and is likely to be triggered by common stress factors. There are several factors that is well known to stimulate EV release from various cell types including cancer cells is hypoxia (Lowry, 2018), oxidative stress (Hedlund, 2011), as well as tumor acidity (Logozzi M. , 2018). One of the main features that makes EVs particularly attractive as analytes for liquid biopsies is that tumor-derived EV's cargo bares a strong pathological resemblance to the intracellular status of the cancer cell of origin (Tanaka, 2013). Despite this, several recent studies suggest that the sorting of molecular cargo into EVs is a regulated process leading to the enrichment or depletion of EVs in specific proteins, nucleic acids or lipids (Gangoda, 2017). Comprehensible, these sorting mechanisms modulate the physiological and pathological effects elicited by EVs both in recipient cells and parental cells (Chen Y. , 2017). Moreover, the existence of specific sorting mechanisms implies that the levels of some molecules in the cells and their EVs are not directly related. Thus, some biomarkers that

are highly expressed in tissues may not be detectable in EVs and vice versa – deregulation of cargo sorting mechanisms in cancer cells may lead to the enrichment of EVs with molecules that are not overexpressed in cancer c ells, thus rendering them useful biomarkers enrichment of EVs with molecules that are not overexpressed in cancer cells, thus rendering them useful biomarkers. Several EV-based technologies, it is of utmost importance to fulfil their potential into clinically useful enabling tools for diagnosis and treatment of cancer patients. Actually, EVs-derived products have the potential to fulfil two major unfinished clinical needs in a new era of precision medicine: their use as (i) biomarkers for diagnosis, prognosis, and monitoring tumor evolution and as (ii) naturally engineered drug-delivery for improved cancer therapy (Roy, 2018). To day, more of 120 clinical studies are registered at https://clinicaltrials.gov/involving the use of EVs for cancer diagnosis, prognosis or therapeutic purposes.Of note, most of these studies are related with cancer biomarkers compared to fractions EVs- based therapeutics. Despite this advancement in R&D EV-based companies, there are still very few EV-products approved for clinical use and commercialization. The first Evs-based products for clinical use includes ExoDx Prostate (IntelliScore), a urine-based test used in combination with PSA for prostate cancer (McKiernan, 2018), ExoDx™ Lung(ALK), i.e. a plasma-based liquid biopsy for lung cancer (De Rubis, 2019). Overall, between the observed market investment in EV technologies and the actual commercialization of EV products for cancer diagnosis, the EV global market worth's nearly $91 million in 2019 (Singh, 2018). Most importantly, this value is projected to increase to nearly $265 million in 2024 at an estimated 5-year. Compound Annual Growth Rate (CAGC) of 23.8%. Strikingly, EV diagnostic-based biomarkers represent the largest sector of this market, expected to grow from $56.5 million in 2019 to $250 million in 2024 at a CAGR of 29.4% (Singh, 2018).

4 Extracellular vesicles in cancer

The role of EVs in the development of various pathological conditions has aroused a lot of interest in the recent years, demonstrating their active involvement in several diseases (Gao, 2017). In

particular, the mammalian EVs are involved in the regulation of different diseases mechanisms, such as: coagulation, immunity, metabolomic alterations, cancer, etc.

Carcinogenesis is a process in which unlimited/uncontrolled cell division occurs, leading to the formation of malignant tumors. Compared to normal cells, cancer cells acquire malignant properties through genetic mutations and other aberrations that give them adaptive and proliferative advantages. This malignant transformation is a multi-stage process involving the gradual accumulation of abnormalities necessary for cell tumor progression (Martincorena, 2018). Sequential selection of variant subpopulations within the neoplastic clone are responsible for the progression of the neoplasm, and the development of intra-neoplastic diversity is emerging as an important feature. In fact, heterogeneity allows cells to develop characteristics that allow them to proliferate, evade apoptosis, undergo angiogenesis, alter metabolism, and form metastases (Qian, 2017). Findings suggest that cancer progression is related to altered protein expression and changes in metabolic pathways, which gives cancer cells the ability to survive and expand in a hostile microenvironment. Cancer cells use a variety of mechanisms through which they develop an extraordinary ability to adapt and expand in the microenvironment, including the release and uptake of EVs. Cancer-derived EVs are important players in cancer progression, being able to facilitate intercellular communication with cells near and far away (e.g., stromal cells), promoting the formation of pre-metastatic niches. EVs are involved in different stages of tumorigenesis and metastasis by increasing angiogenesis and remodeling the extracellular matrix. For this reason, molecular profiling of EVs can help us understand the behavior of the cancer, in order to obtain an early diagnosis and develop targeted therapies.

Factors, such as hypoxia, inflammation, and extracellular acidification in the tumor microenvironment (TME) may contribute to the increased secretion rate of EVs (Boussadia, 2018). In fact, it has been reported that malignant cells secrete an increased number of EVs with an altered composition to those from non-malignant cells of the same type (Keller, 2019).

However, diagnostic and prognostic evaluations using the total abundance of EVs may be subject to confounding effects from non-malignant cells responsible for circulating EVs in some disease conditions. Even so, studies have demonstrated that EVs are enriched with a highly heterogeneous pool of biological cargo, i.e., proteins, lipids, RNA, and metabolites that modulate target cells (Hayashi, 2020). As previously mentioned, these tumor-derived EVs are released into circulation in order to carry out functions that support tumorigenesis, such as stimulating angiogenesis and promoting metastatic diffusion. This, along with their ability to act as powerful cell-cell communication mediators, has contributed to their emergence as biomarkers of numerous diseases, including cancer (Simeone, 2020). For istance, it has been shown that levels of carbonic anhydrase IX (CA-IX) increase with progressive acidification of the tumor microenvironment in human prostatic cancer (PCa) cell line and in exosomes released from them, whereas decrease following alkalinisation (Logozzi, 2019). Furthermore, EVs isolated from plasma samples of patients with PCa are enriched in CA IX, making them the most powerful prognostic biomarker of cancr progression together with exerting a CA IX-related activity (Logozzi, 2020).

Proteins are an important class of molecules that are transported by EVs, and some of them are integral constituents of EV structures. Analysis of EV protein composition is crucial to understanding the mechanisms of their biogenesis and function under physiological and pathological conditions. It is well-known that EVs are highly enriched in membrane proteins, such as tetraspanins (Brzozowski, 2018), proteins involved in EVs biogenesis as well as ESCRT-related proteins, and syntenin (Xu, 2018). Other typical EV proteins include cell adhesion-related proteins (integrins, LFA-1, and ICAM -1) ((Reina, 2017), and those participating in cytoskeletal construction (actin and tubulin) and vesicle trafficking (e.g., Rab family proteins). MHC class I and II complexes, involved in antigen presentation, have been also reported (Gutiérrez-Vázquez, 2013), as well as heat shock proteins, which facilitate protein folding and balance of proteostasis (i.e., Hsp60, Hsp70, and Hsp90) (Taha, 2019).

In addition to self-proteins, EV content reflects the physiological state of the cell from which they originated. Since EVs are normally isolated in small amounts, highly sensitive analyses are

needed. In recent years, technology have been widely used to allow the massive identification and relative quantification of proteins present in EVs from different biological samples (Kreimer, 2015) (Shao, 2018). Moreover, many public databases have been created to share data among the scientific community, such as EVpedia, ExoCarta, and Vesiclepedia (Kim, 2013) (Keerthikumar, 2016) (Pathan, 2019). Current proteomic technology based on mass spectrometry (MS) is the basis for the study and discovery of specific non-invasive biomarkers in the oncology field and beyond. Its high sensitivity makes it capable of identifying low abundance proteins over wide dynamic ranges, including post-translational changes. Additionally, ELISA and Western blotting can be used to identify potential biomarkers. Although many analytical methods have been standardized, unique challenges are associated with different applications of proteomics.

Several studies have contributed to identifying potential biomarkers in cancers through showing increased serum EVs. For istance in PCa, there is a need to identify new markers, due to the fact that prostate specific antigen (PSA), both in free form and in EVs derived from plasma of PCa lacks spec-ificity and sensitivity (Logozzi, 2017), and therefore could lead to overdiagnosis (Loeb, 2014). However, a breakthrough in the clinical management of PCa with a minimally invasive test was demonstrated by Logozzi and coworkers that reported an enrichment in exo-PSA levels in the plasma obtained from PCa patients when compared to the levels in plasma of both healthy donors and patients with benign prostatic hyperplasia (BPH) (Logozzi, 2019), which along with smaller sizes of them, thus promising new tool for early-stage cancer detection. A large number of biomarkers is currently being investigated in other cancers, as in hepatocellular carcinoma (HCC), breast cancer, melanoma, esophageal squamous cell carcinoma (ESCC), GBM, etc. So, EVs obtained from high- and low-grade metastatic HCC cell lines discriminated intrahepatic carcinoma from other tumors, highlighting adenylate cyclase associated protein 1 (CAP1) as enriched in metastatic tumor cells when compared to non-tumor/primary cell lines (Wang X. , 2014). In breast cancer, EVs from cell culture have also provided a potential biomarker candidates, including heat shock protein 71 (Palazzolo, 2012). An alternative and more intriguing hypothesis is that EVs could be a hallmark of more aggressive tumors, and thus high EVs plasma

levels could identify patients with unfavorable prognosis despite early disease stage. Indeed, the unique biochemical properties of these organelles and the peculiar lipid composition of their membranes may determine their long-term persistence in plasma also in patients whose tumor has been surgically removed. Because of the lack of a reliable quantitative assay, no study has so far addressed whether the amount of EVs in plasma may associate with a different disease course in cancer patients. This is an even more important issue in melanoma, which is a rather heterogeneous disease, with subsets of patients undergoing unexpectedly poor prognosis despite the presence of good prognostic factors and vice versa. Nonetheless, analysis of the EVs in plasma from melanoma patients with respect to healthy individuals are significantly increased expressing tumor markers such as caveolin-1 (Logozzi, 2009). Caveolin-1 was also identified as a biomarker in EVs purified from plasma of patients with oral squamous cell carcinoma before and after surgery (Zorrilla, 2019).

In regard to GBM, Naryzhny and colleagues (2020) provided a list of potential biomarkers by secretome profiling through LC-MS/MS, which included annexin A2, vimentin, and tenascin-C, among others (Naryzhny, 2020). Vimentin is an intermediate filament protein that plays a central role in GBM progression (Zhao, 2018) , and tenascin-C is a non-filamentous protein that mediates cell-cell and cell-matrix interactions, which affects negatively proliferation and invasion in GBM (Xia, 2016). In recent years it has begun to take hold the knowledge that GBM cells secrete “heterogeneous” EVs which mirror the molecular features of parental cells and are able to escape from tumor microenvironment, reaching cerebrospinal fluid and systemic blood circulation. Such information led to consider the possibility to use extracellular vesicles in biological fluids as markers of GBM pathology and to use them as a more feasible "liquid-biopsy" to gain diagnostic information, follow the disease progression and the response to clinical treatment, just through a blood test or cerebrospinal fluid collection. Recently, proteomic analyses has confirmed that plasma EVs from GBM patients was higher in pathological conditions when compared with healthy controls, brain metastases, and extra-axial brain tumors, thus confirming it as biomarkers useful per diagnosis and prognosis, as well as for the progression of GBM (Osti, 2019).

5 Methods of isolation and characterization of extracellular vesicles

Currently, characterization of EVs is a combination of several methods that include: microscopy (TEM, SEM, CrioTEM), dynamic light scattering techniques (Nanoparticle Tracking Analysis-NTA and Zetasizer), Tunable Resistive Pulse Sensing (TRPS), Western Blot, -omics analysis (proteomic, lipidomic, metabolomic), as well as immunohistochemical and flow cytometry analysis of specific EVs markers, used to describe their morphology, biochemical composition and receptors localized on their membranes (Momen-Heravi, 2012). However, one of the main issue when purifying these particles is that, currently, there is no consensus for a unique standard isolation protocol (Szatanek, 2015).

Ideally, the method used for their isolation should be simple, fast and inexpensive. Overall, three main methodologies are currently used for their isolation: (i) differential centrifugation coupled to ultracentrifugation with, or without, a sucrose gradient/cushion (Iwai, 2016); (ii) size exclusion chromatography (Gámez-Valero, Size-Exclusion Chromatography-based isolation minimally alters Extracellular Vesicles' characteristics compared to precipitating agents. , 2016); (iii) adsorption to magnetic/non-magnetic micro-beads (Koliha, 2016). Each method has its own advantages and disadvantages, and the choice of one rather than another can result in different EV subpopulations with different properties (Davis, 2019). Therefore, at the moment there is no single standardized method for 23 the isolation of EVs, which could be also able to minimize co-isolating protein aggregates and other membranous particles from a sample of EVs.

In order to compare different isolation methods, several researchers have isolated EVs using 4 of the most common methods (ultracentrifugation, density gradient, exo-kit and total exosome isolation) for the evaluation of yield, size, morphology, protein and RNA content of vesicles (Deun, 2014). They demonstrated that density gradient ultracentrifugation gave the purest exosome preparations as respect to the other three techniques which have also co-isolated

contaminating factors. Skottvoll et al evaluated the performance of different isolation methods based on differential ultracentrifugation and a commercial isolation kit (total exosome isolation reagent), demonstrating that the two isolation methods had similar performance with only some differences based on the origin of the cell (Skottvoll, 2018).

In another study, size-exclusion chromatography (SEC) was suggested as capable of eliminating most of the abundant proteins contained in body fluids, also maintaining the vesicular structure and conformation of EVs, thus making this procedure ideal for biomarker discovery, as well as for therapeutic applications (Gámez-Valero, 2016). These data were also confirmed by another research group, which showed that ultrafiltration followed by size exclusion chromatography (UF-SEC) provides well-concentrated EVs for proteomic and functional analysis (Benedikter, 2017). Thanks to its efficient capability to separate EVs from contaminant proteins (especially from large initial volumes), UF-SEC seemed to give a higher yield of pure vesicles if compared to those isolated by simple ultracentrifugation (Nordin, 2015).

For these reason, Several EV protein detection assays have been developed that use the affinity of specific antibodies for EV membrane proteins to capture and subsequently detect (specific) EVs. In these immunosorbent assays (ISAs), derived from the classical enzyme-linked immunosorbent protein assays (ELISA), EVs are typically captured on a supporting surface that is coated with an antibody targeting a common EV surface protein such as the tetraspanins CD63, CD9 or CD81 (Musante, 2016) (Logozzi, 2020). The membrane proteins of interest, present on the surface of captured EVs, are detected using antibodies targeting the same epitope of the same protein or other (disease-) specific EV surface proteins. These antibodies are directly or indirectly labelled with an enzyme like horseradish peroxidase (HRP) that induces an enzymatic conversion of a fluorescent/coloured substrate that can be quantified using a spectrophotometer (as in an ELISA). Alternatively, fluorescent antibody conjugates are used for the detection of the captured EVs in the more sensitive fluorophore-linked immunosorbent assay (FLISA) or time-resolved-fluorescence immunoassay (TR-FIA) (Duijvesz, 2015). Especially the prolonged (time resolved) fluorescence emission of Europium (Eu) in the TR-FIA results in minimal fluorescence levels

from other sources (e.g., auto-fluorescence of the sample) and thus a superior sensitivity. These assays have shown to be valuable tools for the quantification of EV surface proteins in complex samples such as urine or blood, without prior EV isolation and/or purification (Musante, 2016) (Logozzi, 2020). Adding a gentle lysis step before binding of the detection antibodies allows quantification of EV cargo proteins in the TR-FIA. The immunosorbent EV assays can easily be carried out in a 96-well format making large scale analysis accessible and affordable. This can even be extended by miniaturization of the assay. The "ExoChip" assay, for example, makes use of a microfluidic device fabricated from silicone elastomer (Kanwar, 2014) to capture fluorescently-labelled EVs within small chambers coated with anti-CD63 antibodies, followed by EV detection using a multi-purpose plate reader. This configuration also enables recovering the EVs for further downstream analysis (e.g., RNA analysis). Assay miniaturization also allows multiplexing of EV analysis using a series of antibodies against surface targets. For example, a microarray was generated by spot-printing a panel of selected antibodies for EV capture on an epoxy-coated slide in a multi-well cassette, the "EV array" (Jørgensen, 2013). After washing away the unbound EVs, the captured ones were labelled with a cocktail of biotinylated detection antibodies against three common tetraspanins CD9, CD63 and CD81, followed by labelling with streptavidin-Cy5 for detection using a microarray reader. More recently, the authors increased the number of capture antibodies to 60 which enables in-depth surface protein profiling of EVs (Jørgensen, 2015). In addition to the classical immunosorbent approach in which a flat surface is used to capture EVs, several assays use (magnetic) beads for EV capture, e.g., the integrated microfluidic exosome analysis platform (IMEAP) (Zarovni, 2015). The main advantage of using immuno-magnetic beads is that the capture surface is mobile which potentially increases the capture efficiency. Moreover, magnetic beads simplify labelling and washing procedures and make the assay more flexible for subsequent analyses. The use of functionalized capture beads also allows flow cytometric analysis of the bead-captured EVs using general membrane dyes and/or fluorescent antibodies (Kowal, 2016). Despite the extensive quantitative use of immunosorbent EV assays, it must be realised that these approaches only quantify the EV-associated target proteins. Although the detection level of an EV-related protein is often used as

an indication of EV concentration, observed variations in detection levels can also reflect the heterogeneous EV protein composition between biological samples, for example due to different levels of expression in the cells of origin (Koliha, 2016) (Kowal, 2016). Moreover, the use of specific capturing and detection antibodies implies that only a specific subset of EVs that carry the targeted proteins is being quantified and characterized. Additionally, although recent findings hint to predominant protein markers for several different EV types, no protein targets have yet been identified that cover the full spectrum of EVs or are even specifically present on every vesicle within a vesicle type (Kowal, 2016). The high level of standardization, the ease of use and general availability make immunosorbent EV assays very suitable for diagnostics. However, although these assays are commonly used in EV research and several immunosorbent EV assays including the TR-FIA are commercially available, their future clinical application relies on the ongoing research programs to identify essential disease markers on the EV surface (Fais, 2016).

6 Aim the study

This thesis is part of a previous project PRIN 2012, concerning the role of cancer-derived EVs that may serve as a source of biomarkers for diagnosis and monitoring cancer progression. The aims of this PhD thesis have been to evaluate:

1. the levels and the espression of Hsp10, Hsp27, Hsp60, Hsp70, and Hsp90 in samples human of GBM and in healthy controls by immunomorphology analysis both on tissue and in primary and secondary cell cultures (i.e. by IHC and IF)
2. the presence and the levels of GFAP and Hsp70 in EVs isolated from plasma of patients with GBM before and after surgery, compared to controls, by immunoblotting and proteomic analysis
3. the research on EVs to translate it into the development of reliable tools for the clinical management of cancer patients, by to identify cancer-derived EVs or EVs subpopulations that are enriched in relevant biomarkers and decoding the "messages encrypted" in the molecular cargo of EVs.

The first set of experiments (1) showed that Hsp70 is not significant among the researched Hsps in terms of expression and levels, both in the tissue and in primary cell cultures, and this was why we continued our experiments (2, 3) fusing on this protein.

Our goal was to(dis)prove the utility of GFAP and Hsp70 in diagnostics, assessing the prognosis and follow-up in patients affected by GBM. Moreover, our results should shed light on the usefulness of GFAP and Hsp70 as target for a novel tool diagnostic able to support the notion that circulating EVs can reflect, to some extent, the tumor landscape being feasible to use them as a real-time monitoring tool.

Understanding the morphology of tumor cells and the functional characteristics of these vesicles will allow the development of tools wihch may have some advantages over other exploited in liquid biopsies.

7 Materilas and Methods

7.1 Patients recruitment

The patients enrolled in this study underwent surgery for supratentorial, hemispheric GBM at the Neurosurgery Department, Policlinico P. Giaccone, University of Palermo. In all cases, total tumor removal was achieved-namely, a resection of the entire contrast-enhancing lesion confirmed by magnetic resonance imaging (MRI). All patients gave their written informed consent to study participation.

Patients	Sex	Anatomical Site	IDH1	Ki67	Synaptophysin
1	M	Left frontal lobe	-	67.40%	-
2	F	Left parieto-occipital region	+	67.40%	-
3	F	Right frontal lobe	NOS	67.40%	-
4	F	Right frontal lobe	NOS	67.40%	-
5	M	Right frontal lobe	+/-	17%	-
6	F	Left frontal lobe	-	67.40%	-
7	M	Left frontal lobe	-	67.40%	-
8	M	Left frontal lobe	-	60.40%	-
9	F	Right temporal lobe	+	60.40%	-
10	M	Right temporal lobe	+	67.40%	-
11	M	Right frontal lobe	-	67.40%	-
12	M	Left frontal lobe	-	60.40%	-
13	M	Left frontal lobe	-	60.40%	-
14	M	Left frontal lobe	-	60.40%	-
15	M	Left parieto-occipital region	+	67.40%	-

***Table 2**. Diagnostic analysis of enrolled patients for IDH1, Ki67, and synaptophysin.*

This study was approved by the local human research ethics committee and was performed in accordance with current legislation and the ethical standards laid down in the 1964 Declaration of Helsinki and its later amendments. The samples were collected between 2020 and 2021; hence, tumor diagnosis was performed according to the fourth edition of the World Health Organization (WHO) classification of tumors of the central nervous system. In our study, 15 patients with GBM were enrolled at the Policlinico P. Giaccone. The mean age of the patients enrolled in this study was 57.75 years (ranging from 53 to 64) and the clinical characteristics such as, diagnosis, DH1 wild type (WT) or mutant, Ki67, and synaptophysin markers of the patients recruited into the study have been evaluated by the Institute of Pathological Anatomy, Policlinico P. Giaccone, and are summarized in ***Table 2***. In addition, 10 non-pathological samples of cortex from age-matched subjects as healthy controls were used for comparative analysis, obtained from U.O.S. Forensic Medicine, Policlinico P. Giaccone. In our experimental study, we therefore used biopsies of selected patients for the isolation of primary cell lines, as described below. At the same time, we collected blood samples before and after surgery to obtain liquid biopsies (plasma) for the study of EVs.

7.2 Immunohistochemistry

Immunohistochemical staining was performed using formalin-fixed paraffin-embedded blocks provided the Institute of Pathological Anatomy, Policlinico P. Giaccone. Briefly, 4-µm-thick tissue sections, obtained by microtome cutting, were deparaffinized in xylene and hydrated by immersing in a series of graded ethanol. Antigen retrieval was performed in agitation by placing the sections in epitope retrieval solution (0.01 M citrate buffer, pH 6.0) at 95°C for 8 minutes and immersed for 8 min in acetone at -20 C to prevent the detachment of the sections from the slide. All subsequent reactions were conducted at room temperature. After washing the sections with Dulbecco's phosphate buffered saline (DPBS, pH 7.4) for 5 min at 22 C, the immunohistochemical reaction was performed by the streptavidin–biotin complex method using a Histostain®-Plus Third Gen IHC Detection Kit (Life Technologies, Frederik, MD, USA; Cat. No. 85–9073) for 10' to block non-specific antigenic sites. The sections were treated for 5' with

Peroxidase Quencing Solution (reagent A of Histostain®-Plus 3rd Gen IHC Detection Kit, Invitrogen) to inhibit any endogenous peroxidase activity. Endogenous peroxidase was inhibited by immersing the sections in 0.3% hydrogen peroxide for 10 minutes. Subsequently, the sections were incubated overnight, with a primary antibody against Hsp10, Hsp27, Hsp60, Hsp70, and Hsp90 (***Table 3***). The sections were observed with an optical microscope (Microscope Axioscope 5/7 KMAT, Carl Zeiss) connected to a digital camera (Microscopy Camera Axiocam 208 color, Carl Zeiss). All the observations were made at a magnification of 400X and the percentage of positive cells was calculated in a high-power field (HPF) and repeated for 10 HPF. The immunopositivity was expressed as the average percentage of all immuno-quantifications performed in each case for each Hsp.

7.3 Cell lines

7.3.1 Primary cell lines

From patients, nine biopsy tissues were obtained, and we successfully established four primary cell lines derived from GBM with continuous proliferation that could be passed regularly. Tumor tissue of GBM patients was collected during resection and transferred cooled to the laboratory. Under sterile conditions, it was rinsed in DPBS 1X and subsequently obvious vessels, coagulated blood, and necrotic tissue were removed. Tumor specimen was dissociated into small pieces using scalpels and further enzymatically dissociated by incubation with Collagenase Type II (250 U/mL, Sigma Aldrich, St. Louis, Missouri), 0,25% of trypsin (GIBCO, Ivitrogen Corporation, CA, USA) in DPBS 1X at 37°C for 18 h in agitation. At the end the incubation period, trypsin activation was stopped by adding to the tissue from medium cointaining 10% fetal bovine serum (FBS, Thermo Fisher Scientific, Waltham, Massachusetts)). Centrifugation at 300g for 5 minutes at 4°C was performed to recover the cells from the enzyme, and resuspended in Dulbecco′s Modified Eagle′s Medium (DMEM 1X, GIBCO; Ivitrogen Corporation, CA, USA), supplemented with 10% FBS, and then the cells were filtered with a 70 micron cell strainer. After washed by centrifugation and seeded in cell culture flask with a medium composed of DMEM, 10% FBS, 100 U/mL penicillin (GIBCO Invitrogen Corporation, CA, USA), and 0.1mg/mL

streptomycin (GIBCO Invitrogen Corporation, CA, USA) at 5% CO_2 atmosphere at 37°C. For suspension culture and adherent culture T25 cell culture flask was used. After a 1-day resting phase, the cell culture supernatant was removed, the cells were washed with DPBS 1X (if there was cellular debris in the culture), and a new cell culture medium was added. Change of cell culture medium and microscopic monitoring (phase contrast) was performed routinely every 2 days.

7.3.2 Tumoral cell line

In this study, we used the cell lines G166, isolated from malignant glioma (ISENET Biobanking Cell Lines) showing stem cell properties and initiating high grade gliomas after xenograft. Cells were grown in serum-free complete medium (Euromed-N, EuroClone; code ECM0883LD), with supplements: 2% B27 (GIBCO; code 17504-044), 1% N2 (GIBCO; code 17502-048), 20ng / mL epidermal growth factor (EGF, Peprotech; code 100-15) added fresh; 20ng / mL basic fibroblast growth factor (FGF2, Peprotech; code 100-18B) fresh added; on the laminin coating at 1 µg/mL (Invitrogen; code 23017-015). The cells were split typically once for week after dissociation with Accutase solution (Sigma Aldrich) and centrifugation at 1000xg for 3 minutes, and seeded in laminin-coated flask obtained with gentle agitation for at least 2 hours at room temperature. The cells were incubated at 37 ° C in a humidified atmosphere with 5% CO_2 until confluence in monolayer.

7.4 Hematoxylin and eosin staining

Five thousand cells per well were plated in chamber slids and allowed to attach and proliferate for 24 or 48 hours. After fixation (ice-cold methanol for 30 minutes, Carl Roth, Karlsruhe, Germany) were staining with Hematoxylin and Eosin (E&E), using stain in hematoxylin solution (Papanicolaou Ematossilina Harris, Bio-Optica: code: 05-12011) for 1 h RT; following counterstain in Eosin Y (Eosina Y soluzione acquosa 1%, Bio-Optica; code: 05-M10002) for 1.5 minutes. Then mounted with histologic mounting medium and a coverglass, and finally

observed with an optical microscope (Microscope Axioscope 5/7 KMAT, Carl Zeiss) connected to a digital camera (Microscopy Camera Axiocam 208 color, Carl Zeiss).

7.5 Immunofluorescence and confocal analysis

For immunofluorescence, the cells were placed in eight-well chamber slides, cultured for 24 h and fixed with ice cold methanol for 30 min. The fixated cells were washed with DPBS pH 7.4 and then incubated with unmasking solution (trisodium citrate 10 mM, 0.05% Tween 20, pH 6) for 10 min at RT. After rinsing twice with DPBS, the cells were blocked with 3% (w/v) bovine serum albumin (BSA, Sigma Aldrich, St Louis, MO, USA) in PBS for 30 min at RT. Next, the incubation in a humidified chamber overnight at 4 °C with primary antibodies (***Table 3***). The day after, the cells were washed twice in PBS and were incubated with a fluorescent secondary antibody (mouse IgG antibody conjugated with FITC, Sigma-Aldrich 1:100; goat IgG antibody conjugated with FITC, Sigma-Aldrich 1:150; mouse IgG antibody conjugated with TRITC, Sigma- Aldrich 1:100). The nuclei were counterstained with DAPI 33342 (1:1000, Sigma-Aldrich) for 15 min at RT. Finally, the slides were covered with drops of DPBS and mounted with coverslips. The images were captured using a Leica Confocal Microscope TCS SP8 (Leica Microsystems). Cell lines with cells immunopositive for GFAP and negative for NSE were defined as "primary glioblastoma cell lines ".

Table 3. *Primary Antibody used for IHC, and IF*

Methods	Antigen	Type and source	Clone	Supplier	Dilution
IHC	Hsp10	Mouse monoclonal	clone D-8	Santa Cruz Biotechnology, Dallas, TX, USA	1:100
IHC	Hsp27	Goat polyclonal	clone F- 4	Santa Cruz Biotechnology	1:100
IHC	Hsp60	Rabbit polyclonal	H-300	Santa Cruz Biotechnology	1:100
IHC	Hsp70	Mouse monoclonal	5A5	Abacam, Cambridge, UK	1:100
IHC	Hsp90	Mouse monoclonal	ab13492	Abcam	1:100
IF	GFAP	Mouse monoclonal	2E1	Santa Cruz Biotechnology	1:50

IF	NSE	Mouse monoclonal	MRQ-55	Ventana Medical System, Arizona, USA	1:50
IF	VIM	Mouse monoclonal	V9	Biocare, Dallas, USA	1:50
IF	β-tubulin	Mouse monoclonal	TUB 2.1	Sigma-Aldrich, St Louis, MO, USA	1:50
IF	ALDH1	Mouse monolconal	H-8	Santa Cruz Biotechnology	1:50
IF	PCNA	Mouse monoclonal	F-2	Santa Cruz Biotechnology	1:50
IF	FLT-1	Rabbit polyclonal	C-17	Santa Cruz Biotechnology	1:50
IF	FLK-1	Mous emonoclonal	A-3	Santa Cruz Biotechnology	1:50
IF	FLT-4	Rabbit polyclonal	C-20	Santa Cruz Biotechnology	1:50
Abbreviations: IHC, immunohistochemisry; IF, immunofluorescence,					

7.6 Extracellular vesicles isolation and characterization

7.6.1 Liquid biopsies

During the drafting of the project, we also considered as samples the liquid biopsies (plasma) of patients with GBM enrolled for the isolation of the EVs. Whole blood was collected from patients with GBM at different follow-ups: before and after surgical resection (7days), indicated T0 and T1 respectively (***Table 4***). The plasma was obtained by centrifuging samples at 2,500xg for 15 min, and then stored at -80°C until isolation procedure. The same number of samples from healthy subjects were used as controls and treated in the same way.

Before Surgery	**After Surgery (7 days)**
T0	T1
Liquid biopsy sample collection times	

7.6.2 EVs isolation by size exclusion chromatography (SEC)

Briefly, the starting volume of platelet-free plasma used for each isolation method was 2 mL. The isolation of the EVs was made packed the Sepharose CL-2B300 (cod.65099-79-8, Sigma Aldrich, Bologna, Italia) onto a plastic syringe (Becton Dickinson (BD), San Jose, CA) stacked with 10 mL washed sepharose (Figure 1) to create a column with height of 10 cm. Frozen plasma sample were thawed on ice for the first time after freezing, centrifugated at 500xg for 10 min at 4°C to pellet cellular debris, and then at 13.000xg for 15, at 4°C. The samples obtained were further concentrated with Amicon® Ultra centrifugal Filters (100,000 NMWL of regenerated cellulose, Millipore Corporation, Cat. No. PLHK02510) until at the final retentate (1mL) at 3200xg, at 4°C. Subsequently, the samples were loaded onto column, followed by elution with DPBS 1X.

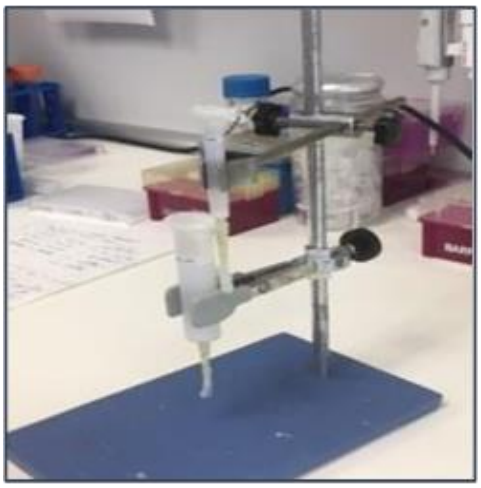

***Figure 4**. Image shows chromatography*

column made by packing inside the sepharose CL-2B.

Before proceeding with SEC isolation, the column was placed in a holder, left equilibrate at room temperature with DPBS 1X filtered. Once equilibrated the column, with the lower cap still on, excess of DPBS 1X filtered was pipetted out from the top filter and 1 mL of sample were loaded. The lower cap was removed and 20 fractions of 0,5 mL each were collected in 1,5 mL plastic vials. Each plastic vial, containing the eluate, was weighed and read at the Nanosight Instrument. Fractions containing vesicles, specifically fraction 7-8-9-10, were pooled together

and concentrated through Amicon® Ultra-0,5 centrifugal Filters Unit, at 13,000 x g, at 4 °C. The final eluated was then used for further experiments or stored at -20 °C for further analysis.

7.6.3 Nanoparticle tracking analysis (NTA)

The concentration and size distribution of particles in collected fractions was measured with a Nanosight LM10 Instrument (Malvern Instrument Ltd, Malvern, UK), equipped with 638 nm laser and CCD camera, and data were analysed with the Nanoparticle Tracking Analysis (NTA) software. Silica beads (100 nm diameter; Microspheres-Nanospheres, Cold Spring, NY) were used to configure and calibrate the instrument. Fractions were diluted 10–1,000-fold in DPBS to reduce the number of particles in the field of view below 200/image. Of each fraction, 10 videos, each of 30-seconds duration, were captured with the camera shutter set at 33.31 ms and the camera gain set at 400. All fractions were analysed using the same threshold.

7.6.4 Transmission electron microscopy (TEM)

After thawing, samples from 7, 8, 9, 10 fractions undiluted, were subjected to overnight fixation, in 0.1% final concentration (v/v) paraformaldehyde (Electron Microscopy Science, Hatfield, PA). Then, a 200-mesh formvar and carbon coated copper grid (Electron Microscopy Science) was placed on a 10 µL droplet to allow adherence of particles to the grid (7 minutes, room temperature). Thereafter, the grid was transferred onto drops of 1.75% uranyl acetate (w/v) for negative staining. Each grid was studied using a transmission electron microscope (Jeol JEM 1010, Thermo-Fisher Talos Artica) operated at 100 kV equipped with a 1k x 1k Gatan CCD camera (MegaScan model 794) and uses a tungsten filament as its electron source. Images were recorded on a Gatan Ultrascan 890 CCD camera with the current MegaScan 794.

7.7 EVs proteins analysis

7.7.1 Protein quantification

The protein concentration was determined using a Micro-BiCinchoninic Acid Assay (Pierce BCA protein assay kit, #23225; Thermo Scientific, Waltham, MA, USA) protein assay

according to the manufacturer's instructions. Briefly, intact EVs resuspended in DPBS were quantifcated using the Micro BCA Protein Assay Reagent Kit. A standard curve (range 0–2000 μg/mL) was derived with nine points of Bovine Serum Albumin (BSA) and a working reagent. The samples (100 μL each) were mixed with 2.0 mL of working reagent and incubated at 37 °C for 30 min. After cooling to room temperature, each absorbance difference, which was subtracted by averaged absorbance of blank standard replicates at 562 nm, was measured by a spectrometer (DS-11; Denovix, Wilmington, DE, USA), and the absorbance differences were converted to μg/mL via the standard curve. If a protein concentration exceeded the upper limit of the standard curve of 2000 μg/mL, the sample was diluted until it could be measured within the standard range, and the final concentrate was calibrated considering the dilution factor. All samples and standard points were replicated three times.

7.7.2 Immunoblotting analysis

The Tris glycine-SDS-PAGE method was employed to separate proteins from SEC fractions and vesicle preparations. From each fraction, equal volume of each collected fraction (40 μl) were dissolved in reducing conditions, boiled for 6 min at 96°C, and then loaded on 12% gradient PAGE gels (Bio-Rad, USA), and proteins were transferred to PVDF membrane (Millipore, Billerica, MA) for 1 h at 15 Volt using Trans-Blot® SD semi-dry transfer (Bio-Rad, USA). Subsequently, the membrane washed twice with DPBS and incubated with Blocking Buffer at RT for 1h, and then blots were incubated overnight with primary antibodies at 4°C in Tris-Buffered saline (20 mM Tris, 137 mM NaCl, pH 7.6) containing 0.05% Tween-20 (T-TBS). We used the following primary antibodies: mouse anti-CD81 (1:1000; clone B-11, Santa Cruz Biotechnology, Dallas, TX, USA), mouse anti-GFAP (1:1000), mouse anti-Hsp70 (1:1000) (see above). Afterwards, membranes were rinsed three times in T-BST for 5 min follwed by incubation with secondary antibody at 1:10000, for 1 h at RT. Finally, the protein bands were analyzed using an enhanced chemiluminescence (ECL) reagent and ChemiDoc™ XRS + System (Bio-Rad, Hercules, CA, USA).

7.8 Proteomic analysis

For proteomic analysis, the EVs samples were dried in and rotary evaporator and dissolved with 22.5 L of 2 mM DTT in 50 mM ABC and processed. Digestions were stopped with 10% TFA at a final concentration of 1%, and then 5 g of the digestion mixture were dried in a vacuum centrifuge and re-suspended in 10 L of 2% ACN 0.1% TFA. In turn, the samples were tested with Liquid Chromatography and Tandem Mass Spectrometry (LC–MS/MS). Single LC-MS/MS experiment that was performed on Orbitrap Elite (Thermo, CA) equipped with Aquity Nano HPLC (Waters, MA) Nano HPLC pump. Peptides were separated onto a 150 μm inner diameter microcapillary trapping column packed first with approximately 3 cm of C18 Reprosil resin (5 μm, 100 Å, Dr. Maisch GmbH, Germany) followed by analytical column ~20 cm of Reprosil resin (1.8 μm, 200 Å, Dr. Maisch GmbH, Germany). Separation was achieved by applying a gradient from 5%–27% ACN in 0.1% formic acid over 90 min at 200 nL min^{-1}. Electrospray ionization was enabled by applying a voltage of 2 kV using a home-made electrode junction at the end of the microcapillary column and sprayed from fused silica pico tips. The Elite Orbitrap instrument was operated in a data-dependent mode for the mass spectrometry methods. The mass spectrometry survey scan was performed in the Orbitrap in the range of 410 –1,800 m/z at a resolution of 12 × 104, followed by the selection of the twenty most intense ions (TOP20) for HCD/CID-MS2 fragmentation in the Elite Orbitrap using a precursor isolation with window of 2 m/z, AGC setting of 50,000, and a maximum ion accumulation of 200 ms. Singly charged ion species were not subjected to HCD fragmentation. Normalized collision energy was set to 37 V and an activation time of 1 ms. Ions in a 10 ppm m/z window around ions selected for MS2 were excluded from further selection for fragmentation for 60 s. Samples were analyzed by a single 180 min mass spectrometry run. Each sample was injected in triplicate, in order to assess the reproducibility of the MS data. MS calibration was performed using the Pierce ® LTQ Velos ESI Positive Ion Calibration Solution (Thermo Fisher Scientific). MS data acquisition was performed using the Xcalibur v. 3.0.63 software (Thermo Fisher Scientific). Searches for matches between the MS data and proteins in the

NCBI nr and Swiss-Prot databases (human taxonomy) were performed with the Mascot Server v2.3 (Matrix Science, Boston, MA, USA). Searches were conducted with carbamidomethylation of cysteine as a fixed modification; oxidation of methionine, pyroglutamate formation from glutamine and pyro-carbamidomethyl as variable modifications of proteins; a peptide mass tolerance of ±10 ppm; a fragment mass tolerance of ±0.6 Da; and an allowance for up to two missed tryptic cleavages. Proteins identified by LC-MS / MS were searched on ExoCarta (http://exocarta.org, accessed February 8, 2021), an online database of exosomal proteins, RNAs and lipids. In addition, a symmetric Venn diagram was generated (http://bioinformatics.psb.ugent.be/webtools/Venn/, accessible on 26 March 2021) to show shared and non-shared proteins between samples obtained before and after surgery.

7.9 Statistical analysis

Statistical analyses were carried out using the GraphPad Prism 4.0 package (GraphPad Inc., San Diego, CA, USA). Comparisons were made by using Student's t-Test. All data are presented as the mean ±SD, and the level of statistical significance was set at $p < 0.001$.

8 Results

8.1 The immunohistochemical evalution

This study conducted a semiquantitative immunohostochemical analysis for Hsp10, Hsp27, Hsp60, Hsp70 and Hsp90 in GBM tissue sections of the enrolled patients by comparing them with non-tumor tissues. Histopathologically, we observed an immunopositivity for Hsp10 in the cytoplasm in GBM tissue, with an average percentage of positive cells of 61.6 ± 1.8%, compared to the control tissue (CTR) which, on the other hand, showed a positivity of 5.5 ± 0.6% (***Figure 5A***). As shown in the ***Figure 5B***, Hsp27 immunohistochemical staining in tumor tissue was much higher than the CTR; we obtained a mean percentage of positive cells of 86.5 ± 2.1% versus 5.7 ± 0.7%, respectively (***Figure 5B***). The immunolocalization of Hsp27 was cytoplasmic. The percentage of tissue immunopositivity for Hsp60 was 66.5 ± 2.1% in the pathological tissue and 5.3 ± 0.3 in CTR, with exclusively cytoplasmic localization (***Figure 5C***). ***Figure 5D*** shows a representative staining of low / almost absent expression of Hsp70 in both groups studied, i.e. GBM tissue and healthy control, with a mean percentage of 4.2 ± 0.57% in the GBM group and 4 ± 0,7% in the CRT (***Figure 5D***). The immune reaction for Hsp90 was also cytoplasmic; we obtained a mean positive percentage of 72 ± 2.9% in the GBM samples, while in the CTR it shows a percentage of 4 ± 0.55% (***Figure 5E***). Finally, the statistical analysis showed a significant increase ($p < 0.001$) in the levels of Hsp10, Hsp27, Hsp60 and Hsp90 in the GBM compared to the control group. In contrast, no difference was found in the evaluation of the immunopositivity of Hsp70.

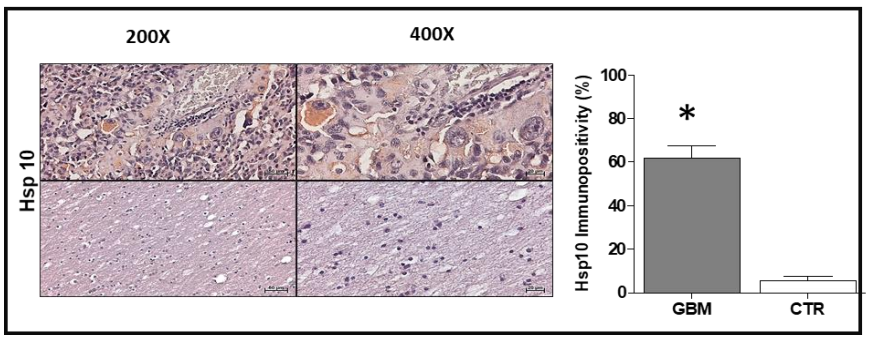

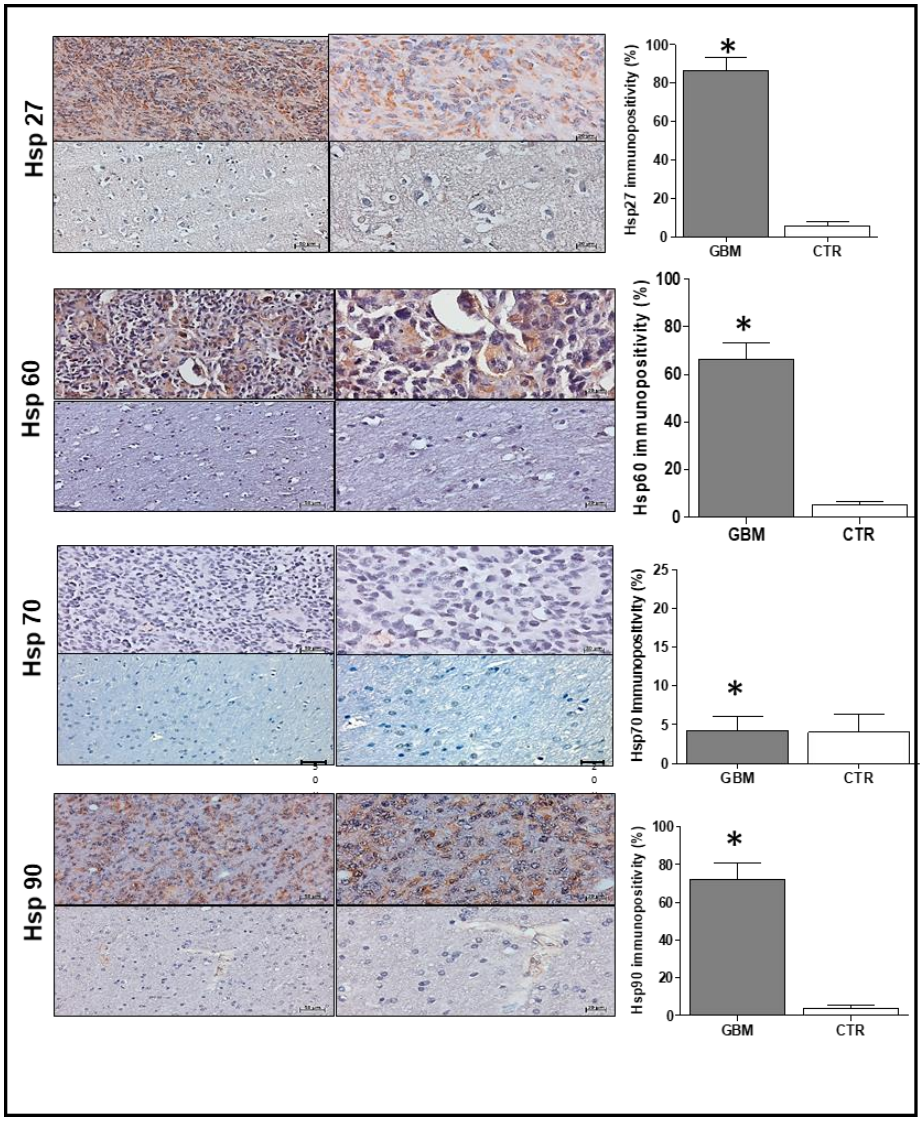

Figure 5. *Detailed images for Hsp10, Hsp27, Hsp60, Hsp70 and Hsp90 in GBM samples(up) and CTR (down). Mmagnification 200X and 400X. (A), (B), (C) and (E) the staining pattern for the Hsp10, Hsp27, Hsp60, and Hsp90 proteins was cytoplasmic, with strong intensity in GBM tissue. (D) Low immunopositivity was observed for Hsp70 in GBM tissue.*

8.2 Cultivation efficiency of primary cell lines of GBM

One of nine glioblastoma tissue resulted in short-term primary cell cultures, which did not further stored. The remaing five/nine tumor samples did not attach and proliferative after disaggregation (non cultivable). By contrast, we successfully established four primary cell lines derived from GB with continuous proliferation that could be passed regularly. It is assumed that the area of tumor

which the sample originates can cause the differences in cultivability. If the sample was taken in a necrotic area, it is not possible to cultivate cells. If the tumor samples originate from the transitional area between necrosis and proliferating tumor, cultivation is possible, but often such large amounts of cellular debris are found in the culture that the cells die. The presence of erythrocytes during the cultivation of samples with a high blood supply also leads to cell death. Time from explantation (p0) of the tumor samples to the first subscultivation step (p1) differed between the primary cells lines. We report here the establishment of four novel human cell lines, designated as GBM1, GBM2, GBM3, and GBM4, derived from a glioblastoma tumor.

8.3 Morphology classification and growth characteristics of primary and secondary cell lines of GBM

H&E staining is performed for a morphological evaluation, to identify the cytomorphological diversity expected in the GBM cell lines. It was noticeable that the adherent cell layers of the out growing primary cell lines developed into two growth types: a- monolayer cells growing side by side, and b- focal growth, where the cells grew in inslets connected by cellular protrusion. The commercial cell line grew as a monolayer. The primary cell lines exhibited three different main cellular shapes during cultivation: a- polygonal (***Figure 6AB***), b- spindle or glia-like (***Figure 6CD and Figure 6EF***), and c- amorphous morphology with cellular protrusion (***Figure 6GH***), but multinucleated giant cells were also present at a low frequency. The secondary cell line showed the glia-like morphology (***Figure 6IL***). Independently of cell density, the cells tend to grow without contact inhibition.

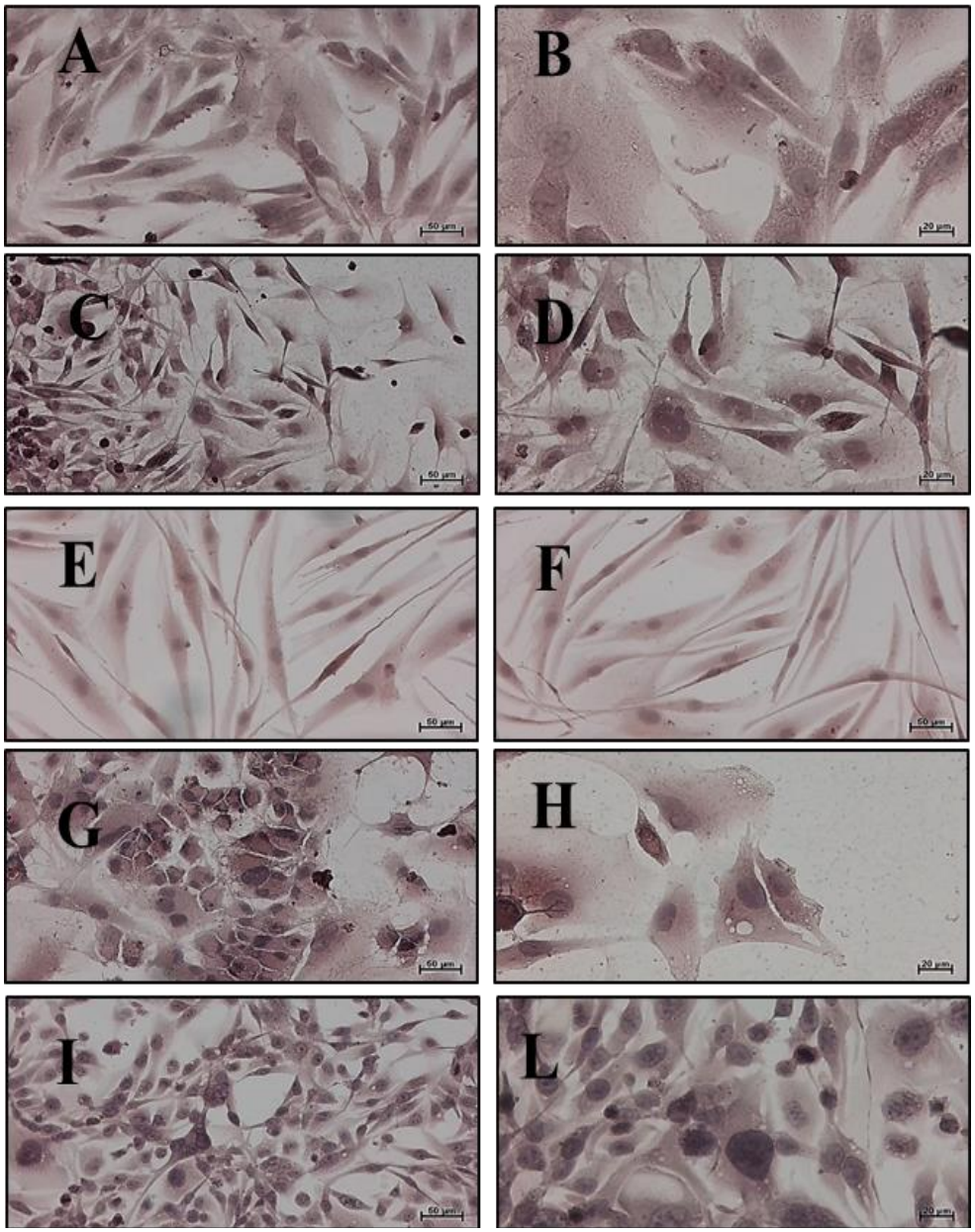

Figure 6*. H&E staining of GBM cell lines. (AB) GBM1 cell line; (CD) GBM2 cell line; (EF) GBM3 cell line; (GH) GBM4 cell line; (IL) G166 cell line. Original magnification: 200X (left) and 400X (right).*

8.4 Evaluation of GFAP, NSE, VIM, β-TUBULIN, ALDH1, and PCNA expression in primary and secondary cell lines of GBM

To specify criteria for the definition of primary GBM cell lines and to ascertain whether the GBM- derived primary cell lines have similarities to GBM tissue, we undertook an immunocytofluorescence staining for markers used in glioma diagnosis, using confocal microscopy. The markers expression was compared to the commercially available GBM stem

cell line (i.e. G166). The primary cell lines were characterized raitened the expression of glial fibrillary acidic protein (GFAP) as reliable marker of astrocytes or glial cells, Vimentin (VIM) as a neuroepithelial precursor marker, β-tubulin as marker associated with tumor resistance to microtubule-targeting agents (MTAs), neuron-specific enolase (NSE) as neuronal marker, and aldehyde dehydrogenase 1 (ALDH1) as a novel stem cell marker. Positive GFAP, Vimentin, and β-tubulin immunoreactivity, and negative staining for NSE was observed in all GBM- derived cell lines, helping to categorize them as primary (***Figure 7***). Anyhow, the levels of GFAP-expressing cells varied in the primary cell lines with highest in GBM2, GBM3 and GBM4 compared to GBM1. Almost all the primary cell lines displayed a negative staining signal for NSE marker (***Figure 7***). The levels of the immunofluorescence reaction positivity for the VIM was observed in all lines, with highest in the GBM1 probably looked at a high passage (p5). Accordingly, was classified almost senescent. Immunostaining for the class β-tubulin revealed that malignant GBM cell lines vary in the positivity, and the decreased expression is associated with lack of cell differentiation and increased expression of stemness markers. GBM1 and GBM4 cell lines express higher levels of β-tubulin regard the GBM3 and even more respect GBM2 cell line (***Figure 7***). Intensive staining for GFAP, VIM, and β-tubulin were found in the cytoplasm of in all primary GBM cultures, whereas no signal for NSE was found in the nuclei (***Figure 7***). Immunofluorescence staining was, also, performed to confirm ALDH1 expression in GBM-derived primary cell lines. ALDH1 immunoreactivity were found in GBM2 and G166 cell lines, and the other cell lines were negative (***Figure 7***). We also examined PCNA expression in glioma cells and we found that PCNA was upregulated in all GBM lines. PCNA immunoreactivity was largely confined to nuclei (diffuse or granular stained nuclei) of the proliferating cell populations in GBM1, GBM2 and GBM4 primary cell lines, whereas cytoplasmic staining was seen in GBM2, GBM3, GBM4, and G166 cell lines. The nuclear staining was granular and diffuse (***Figure 7***). The expression of the studied markers was compared with the expression in the stabilized G166 line. A greater positivity was observed for the stemness marker, ALDH1, in the G166 cell line compared to the primary lines obtained in this study; whereas the

immunopositivity relative to the other markers was similar in both the primary and secondary lines.

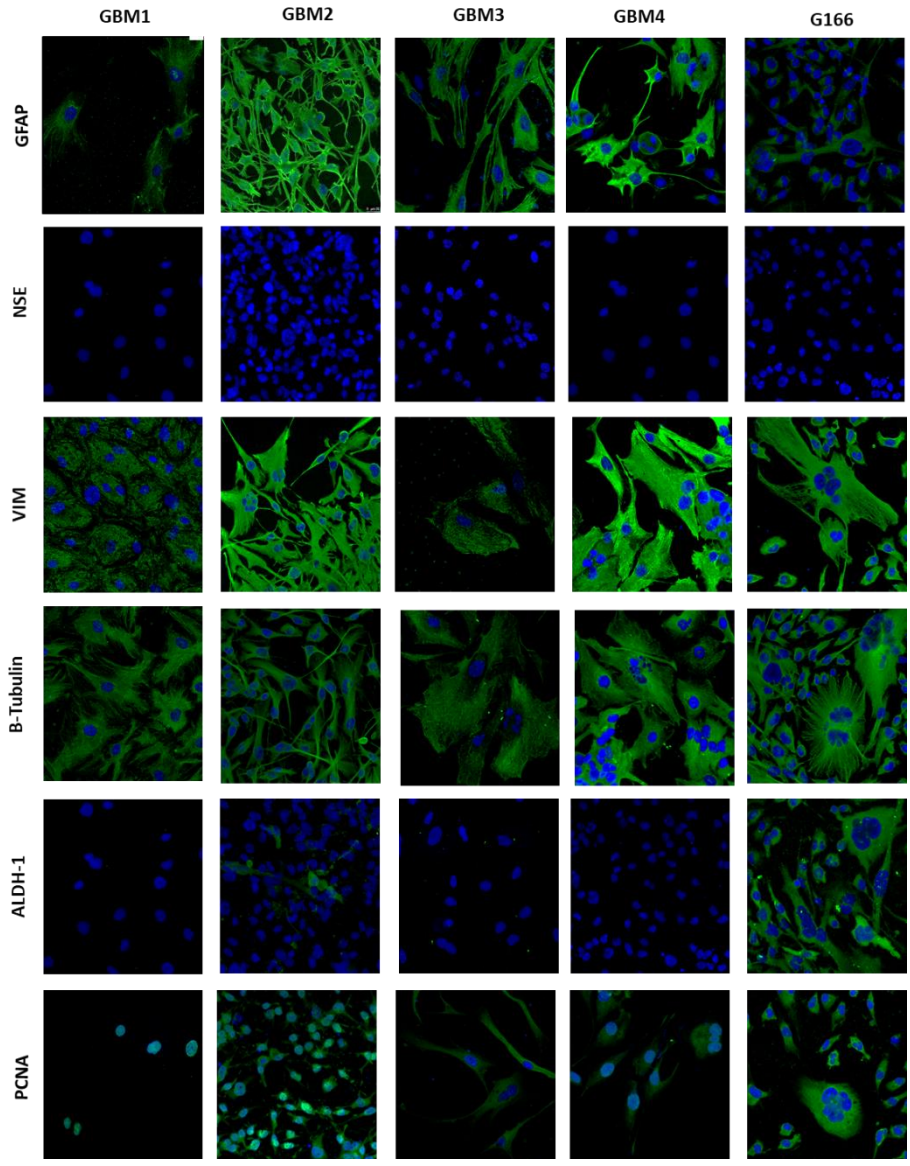

Figure 7. *Immunofluorescence staining for GFAP, NES, VIM, β-tubulin, ALDH1, and PCNA markers in GBM1, GBM2, GBM3, GBM4 tumoral cell lines compared with to the G166 cell line. The cell nucleus was identified via blue fluorescence using DAPI. Magnification 400X.*

8.5 Evaluation of Hsps expression in primary and secondary cell lines of GBM

To evaluate Hsps expression in human malignant glioma cells in *vitro*, all primary GBM cell lines were also examined for expression of Hsp10, Hsp27, Hsp60, Hsp70, and Hsp90 by single immunofluorescence assay (***Figure8***). With the exception of Hsp70, all Hsps examined were

expressed in all primary GBM cell lines studied. Immunofluorescence staining observed for Hsp10, Hsp27, Hsp60, and Hsp90 were high in all cell lines studied, both primary and secondary (***Figure 8***). Although, we found a higher level of immunopositivity for Hsp27, Hsp60, and Hsp90 in all cell lines examined (both primary and secondary) (***Figure 8***), while the immunopositivity for Hsp10 is lower compared to them (***Figure 8***). Surprisingly, Hsp70 was only slightly expressed in GBM3 and GBM4 cell lines, whereas was absent in the other primary cell lines, however we observed a high positivity in the secondary G166 line (***Figure 8***).

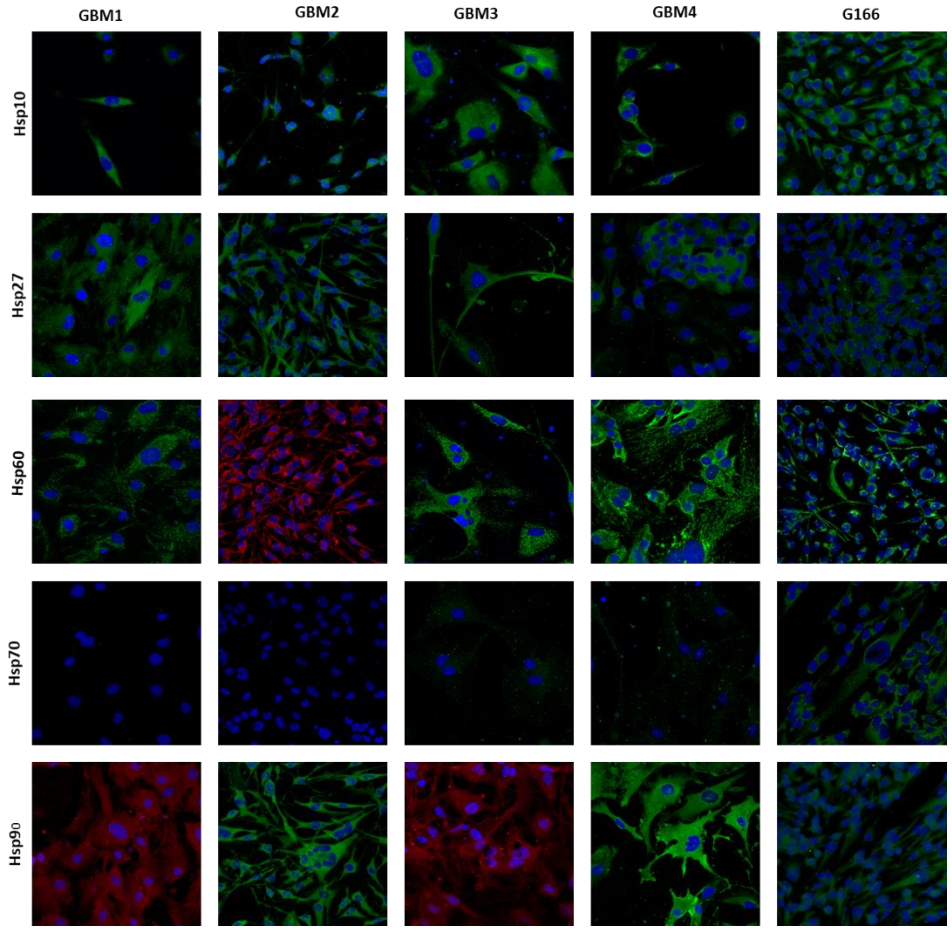

Figure 8. *Immunofluorescence staining of GBM primary and secondary cultures for Hsp10, Hsp27, Hsp60, Hsp70, and Hsp90. Cell nuclei were counterstained with DAPI (blue). Magnification 400x.*

8.6 Evalution VEGFRs expression in primary and secondary cell lines of GBM

In order to assess the clinical relevance of our findings, we also have characterized the four GBM cell lines obtained in regard to alterations in the expression of VEGF Receptor 1 (VEGFR1, Flt1), VEGFR2 (KDR/Flk1), and VEGFR3 (Flt4) expression. These data allowed used to examine possible links between Hsps expression and the previously examined parameters. Overall, there was elevated expression of Flt1 and Flk1 proteins in all four primary GBM cell lines, confirming the importance of angiogenic process as a significant biological feature of this tumor, as well as possible associations of these levels with proliferation and tumor invasion. There was no relevant expression in the level of Flt4 among the GBM2 and GBM3 cell lines, whereas there also was expression in GBM1 and GBM4 cell lines. (***Figure 9***).

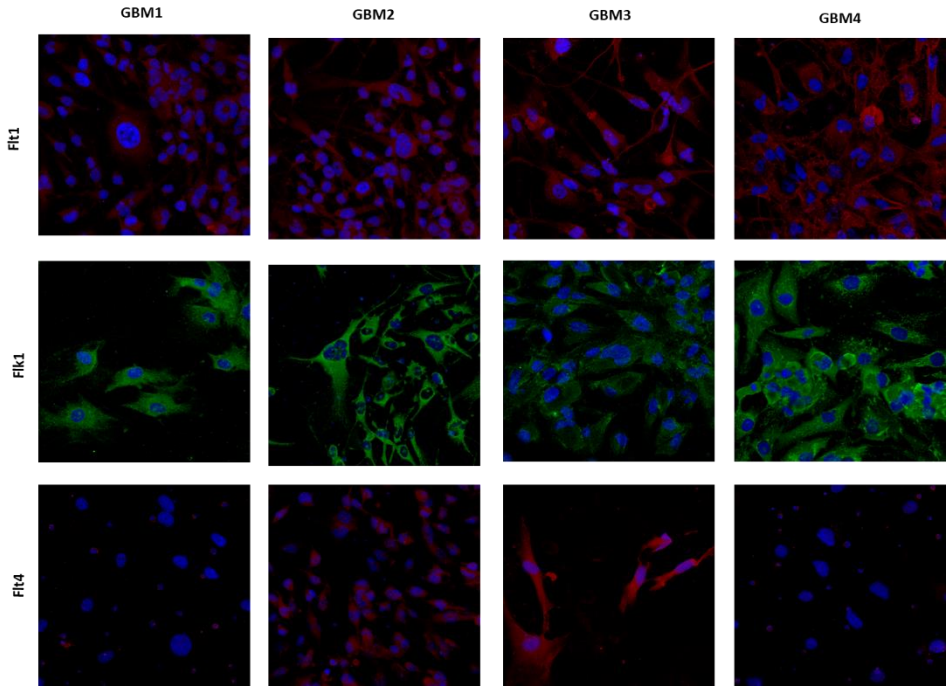

Figure 9*. Immunofluorescence images for Flt1, Flk1, and Flt4 in GBM primary cell lines. Cell nuclei were counterstained with DAPI (blue). Magnification 400x.*

8.7 EVs analysis

8.7.1 NTA analysis

The analysis of the size and concentration of the EVs, obtained with the method mentioned in Materials and Methods, i.e. SEC, was performed using the NTA instrument. NTA successfully addresses one of the key problems (i.e., polydispersity), in that it can resolve and accurately measure different-size particles simultaneously within the same solution. This is an essential prerequisite for analyzing cellular EVs in biological fluids, such as plasma. The overlap of the peaks in ***Figure 10*** is due to the inherent limitation of measuring a stochastic process (brownian motion) by sampling over a finite time period (the time for which each particle can be tracked). NTA also allows you to directly estimate the concentration of particles, finding a good linearity between the actual concentration and that measured by NTA in a given interval. With our settings, NTA detected single particles with a diameter larger than 70 nm. After SEC, the highest concentration of particles was found in fractions 7-10 (***Figure 10).***

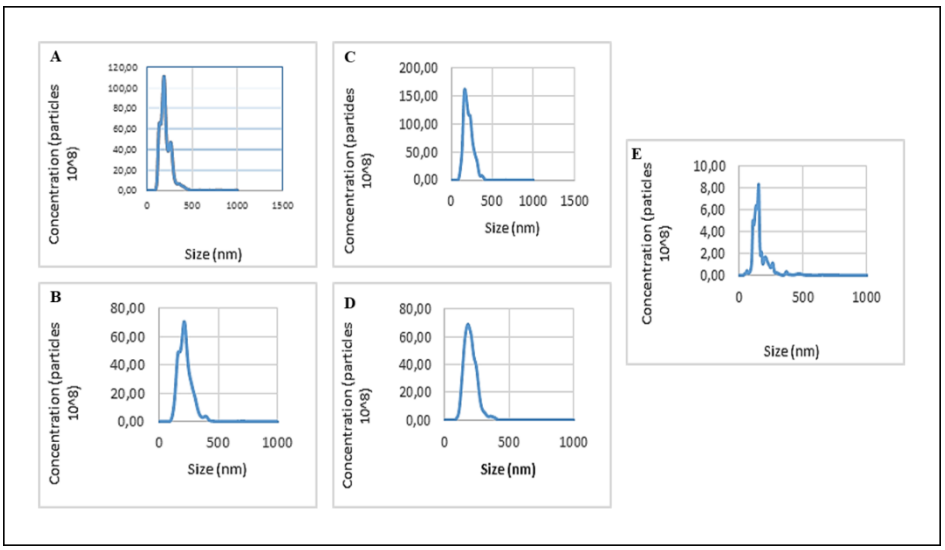

Figure 10. *NTA measurement of EVs isolated from plasma of GBM patients compared at non-pathological controls (CTR). (AB) T0- pathological samples; (CD) T1- pathological samples; (E) non-pathological samples.*

The recovery of particles measured by NTA was 76%±38, and 46%±6 of the recovered were present in fractions 7-10. In our study, we have not found a significant difference in the size and

concentration of the EVs isolated at T0 and T1 from plasma of pathological samples, whereas we observed a significantly difference between the size of the EVs present in the plasma of the pathological samples compared to the non-pathological samples (***Figure 10***).

8.7.2 Electron Microscopy Observation

We used Transmission Electron Microscopy (TEM) to confirm the presence of EVs. Figure (***Figure 11***) shows a representative images of the fraction particularly enriched in EVs, i.e. F8, of GBM samples at T0 and T1, compared with at CTR (***Figure 11***). As expected, in F8, the EVs (cup shaped) were clearly visible, but also visible were low numbers of lipoproteins (ragged structures), whereas were not present the proteins (***Figure 11***). EVs were also observed in F6, F7, F9, and F10 (data not showed).

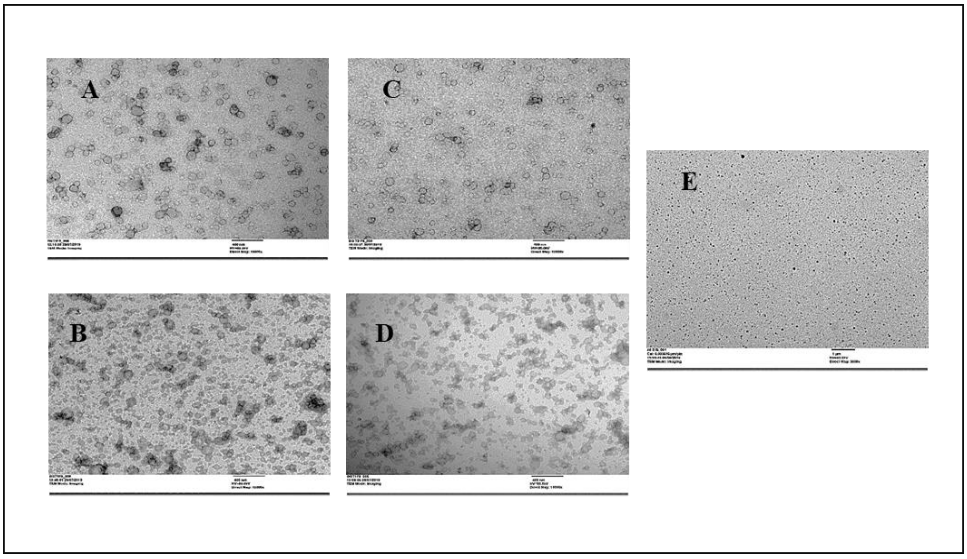

Figure 11. *Representative electron microscopy negative staining images of EVs obtained from plasma showing round-shaped EVs. Scale bar reflect the magnification at the camera 100k magnification, scale bar 200 nm. (AB) T0 samples; (CD) T1 samples; (E) CTR.*

Thus, TEM analysis confirms that SEC separates the EVs from proteins and lipoproteins, resulting one of the best separation methods. In addition to direct and immediate evaluation of the size of the EVs during observation, we measured the size of the EVs using ImageJ 1.53a with Java 1.8.0_172 (64-bit).

Electron micrographs show rounded vesicles (***Figure 11***) with a mean (median) size of 82,741nm in T0 sample, and 91,225 nm in T1 sample; whereas the CTR samples were 68,029 nm.

8.7.3 Protein quantification of EVs

In this study, we used BCA assay to determine the total protein content of EVs isolated from plasma before and after surgery. ***Figure 12*** showed that the amount of proteins differed significantly across T0 and T1 samples, with higher protein concentration at T1 compared T0, probably for the inflammation conditions post-surgery. Moreover, pathological samples were enriched in EVs in contrast at non pathological samples (***Figure 12)***.

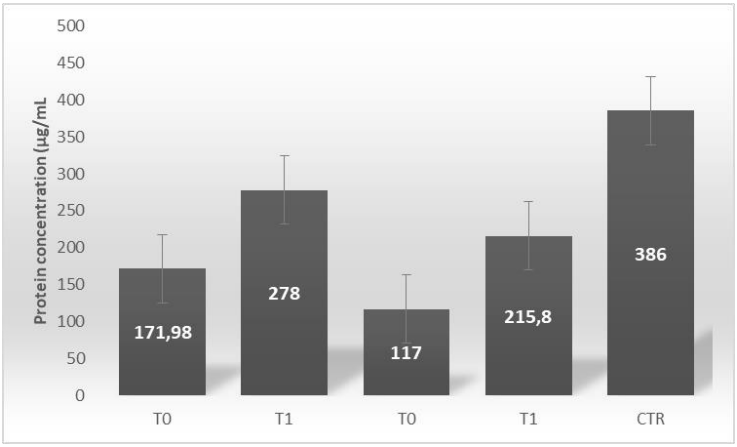

Figure 12. *Determination of the protein concentration of the EVs by BCA assay*

8.7.4 Yield of EVs enrichment from plasma

As mentioned, most vesicles were present in fractions 7-10. To gain insight into the extent of purification of the vesicles present in the fractions, we measured the recovery of EVs by calculating the ratio of particle count and protein concentration as described by Webber and Clayton 2013 in order to assess the level of contaminating non- EVs protein retrieved using SEC method. We conducted this analysis why a large numbers of protein aggregates may contribute to the particle counts potentially skewing the ratio. Pooling fractions 7-10 recovered 43%±23 of EVs and give a 70±19-fold enrichment of EVs compared to protein (***Figure 13***), and a 8±3-fold

enrichment of EVs compared to CTR. Results revealed that before surgery yielded higher particle to protein ratios. In contrast, after surgery resulted in a lower particle to protein ratio, which can be explained as lower particle yield obtained after remove mass tumoral (***Figure 13***), while the low particle to protein ratio observed in the CRT was due to a high level of co-isolated protein (***Figure 13***). In particular, it has been suggested that highly pure vesicle preparations exhibit particle-protein ratios on $3x10^{10}$ particles per microgram of protein. Considering this, the method produced highly pure preparations, exceeding the purity ratios of $3x10^{10}$. Thus, sepharose CL-2B SEC results in a 562±337-fold enrichment of EVs compared to proteins.

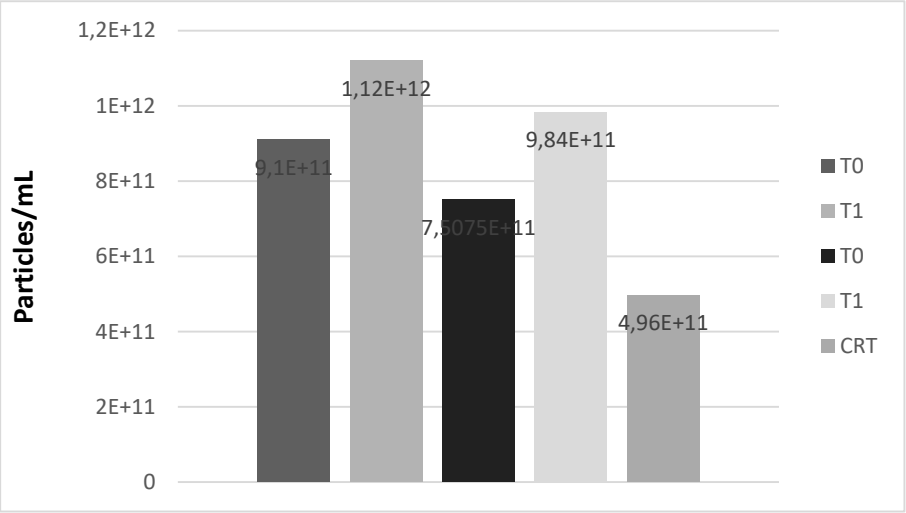

Figure 13. *The ratio of EVs count and protein in the pool of fractions considered (i.e.F7, F8, F9, and F10).*

8.7.5 Immunoblotting Validation for CD81

Immunoblotting is a standard method whereby probing for different EV markers in conjunction with a biomarker of interest can be carried out. EV markers that can be used include CD63, CD81, CD9, and TSG101, amongst many others. These markers do not differentiate between different EV subtypes but do confirm the presence of EVs. Immunoblotting, to some extent, can also be useful in the analysis of EVs purity. The abundance of CD81 selected protein (vesicle-associated tetraspanins) was examined by immunoblotting of pooled plasma EV proteins (relatively at F7,

F8, F9, F10) (***Figure 14***). This analysis confirmed higher levels of CD81 in EVs derived from plasma of pathological samples with a low level in EVs obtained from control groups. CD81 was also identified in cell lysate of the G166 stem line (***Figure 14***).

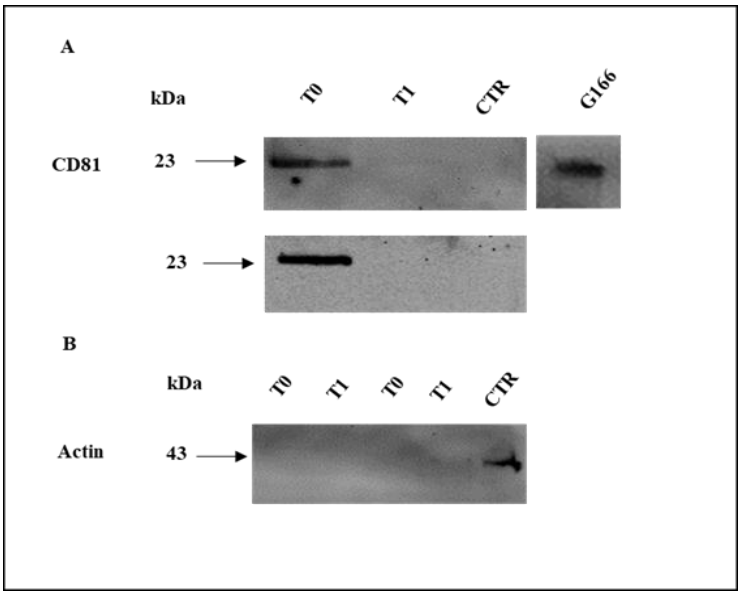

Figure 14. *Immunoblotting detection of CD81 in EVs isolated before and after surgery in GBM groups compared to CTR (protein names on the left), and in G166 cell line, by upon excitation with the Chemidoc system (300s). A: immunodetection for CD81 in T0, T1, and CTR; B: immunodetection for actin in T0, T1, and CTR. Actin was used as an internal control in the experiment.*

8.7.6 Immunoblotting Validation for Hsp70

Afterwards, we sought to assess which Hsps are expressed in EVs derived by plasma in T0, T1, and CTR samples by immunoblotting. We found Hsp70 abundantly expressed in the before surgery in all samples studiated (***Figure 15***) compared to after surgery and CTR. Hsp70 was also identified in cell lysate of the G166 stem line (***Figure 15***).

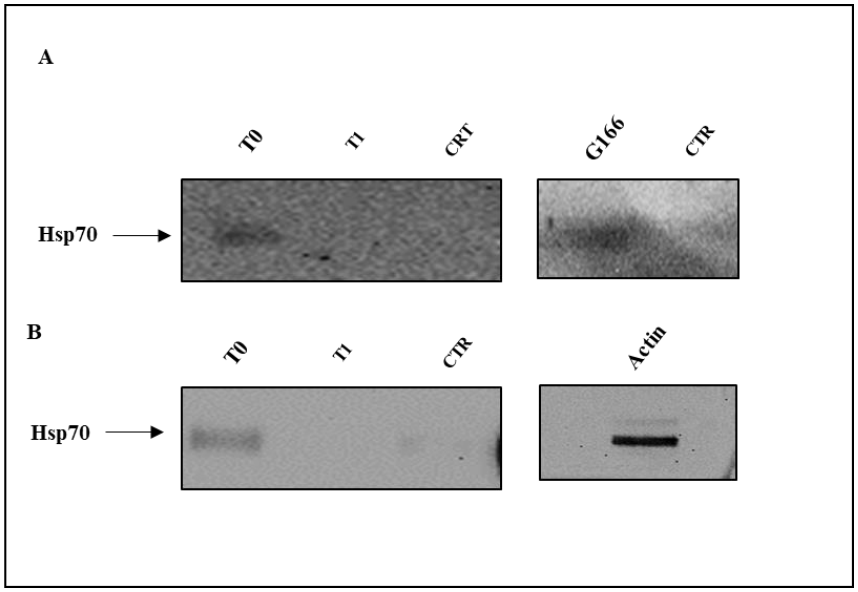

Figure 15. *Immunoblotting detection of Hsp70 before and after surgery in GBM patients, CTR groups, and in G166 cell line by Chemidoc system (300s). Actin was used as an internal control in the experiment.*

8.7.7 Immunoblotting Validation for GFAP

Expression of GFAP after staining with immunofluorescence, as astrocyte marker, led us to evaluate its expression in the plasma-derived EVs, in order to confirm the real origin of the tumor EVs (***Figure 16***).

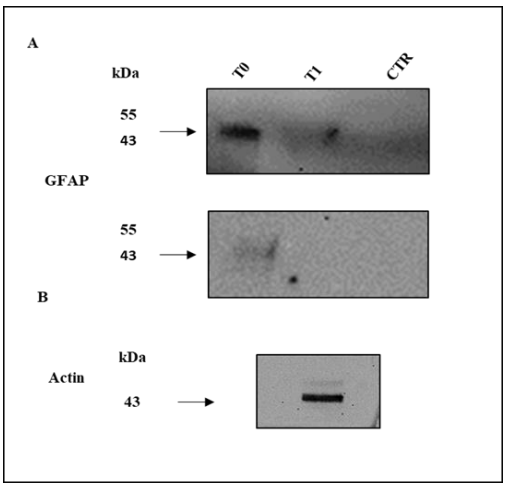

Figure 16. *Detection by immunoblotting of GFAP in EVs samples isolated from plasma before and after surgery in the GBM groups comparing to non-pathological control.*

Immunoblotting data revealed that the GFAP expression level was higher in the pathological groups compared to the healthy controls (***Figure 16***). Consequently, we can assume that GFAP is a valid marker of EVs released by the tumor mass, i.e. GBM, and therefore could be used for the purpose of diagnostic examination.

8.8 Proteomic analysis by LC/ESI-MS/MS

For proteomic analysis, EVs isolated LC/ESI-MS/MS analyses and subsequent database search against the UniProt database, as well as ExoCarta and Vesiclepedia databases, that show the total number of different proteins identified in EVs representing almost half of the human proteome. ***Figure 17*** reports the Venn diagram grouping of the different proteins relationships in T0, T1, and CTR groups. In this study, we identified 102 proteins associated to the T0 samples, 90 proteins associate to T1 samples, and 122 proteins associated to CTR groups; including also human ENO1 used as internal standard to quantify relative protein abundance (***Figure 17***). As it can be observed in the Venn diagram, the overall number of unique protein elements identified was higher in T0 groups compared at T1groups, corresponding to 60 total, whereas 48 unique proteins were identified in T1. Consequently, these proteins will be under investigation in diagnostic research relative at GBM. As depicted in the Venn diagram of ***Figure 17***, the majority of the protein elements resulted in common between T0, T1, and CTR.

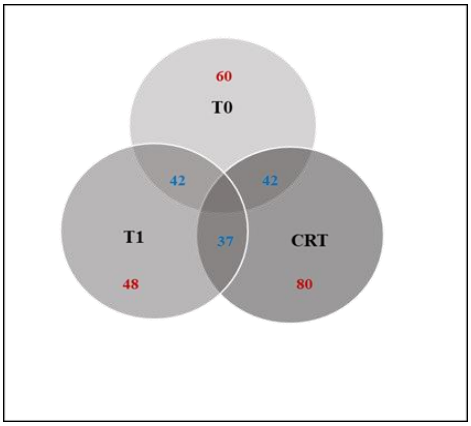

Figure 17. *Venn diagram illustrates proteins shared by TO, T1, and CRT; also, those unique in plasma-derived EVs isolted by pathological groups, healthy groups, and CTR.*

Proteomic analysis confirmed the results obtained from immunoblotting study regarding the expression of EVs markers, such as CD81 (Homo sapiens, Uniprot Acc. P60033), and Hsp70 (Uniprot Homo sapiens, Acc. P17879 and P16627), as well as for GFAP. In details, significant differences in CD81 and Hsp70 expression were observed between the T0 and T1 samples, and respect to healthy controls. Interesting, Exo-Carta database interrogation revealed that these proteins had already been identified in EVs of variuos human tumor samples. In addition, we compared our list of plasma-derived EV proteins of the three samples of EVs revealing that the 55% had not been identified in EVs of healthy plasma in any of the studies and, therefore, could be plasma EV proteins related to GBM cancers. Only 19 of our EV proteins were common to all three other studies, including complement C4A and C4B, clusterin, haptoglobin, and others. Consequently, our study identified a differential protein display that could be to use as potentially predictive of GBM.

9 Discussion

GBM is characterised by invasive capacity and a high proliferation rate (Lee., 2006). GBMs are histologically heterogeneous tumours comprising numerous and diverse types of cells. Current GBM management consists of MRI and surgery or brain biopsies; however, both of these strategies have certain limitations. MRI has a short resolving power, which implies that small lesions could be unseen. Additionally, it is difficult to distinguish between a tumour recurrence and postsurgical necrotic regions, while it remains even more difficult to establish the precise tumour without histological examination (Lottaz, 2010) (Verhaak, 2010) (Keerthikumar, 2016). The ability to frequently monitor cancer progression, as well as development an early diagnosis could contribute to informed clinical decisions and personalized treatment of cancer. This may be possible with liquid biopsies, given that liquid biopsies might allow to survey tumor heterogeneity and clonal evolution. The term "liquid biopsy" refers to a test performed on a sample of biofluid including blood or urine aiming to detect cancer cells or cancer-derived molecules (Babayan A. , 2018). Liquid biopsies are obtained by non-invasive or minimally invasive means that allow serial sampling, therefore they have a potential utility for the detection of minimal residual disease (MRD) or recurrence, tracking tumor evolution and predicting the emergence of chemoresistance in solid tumors. Although several diagnostic tests have been approved by regulatory authorities and are available for clinical use, there are still many scientific, technological and regulatory challenges that still need to be overcome to introduce liquid biopsies into standard clinical workflows. In line with these results, the aim of the PhD project focused on the execution of preliminary experiments for the development of a real-time monitoring tool for diagnostic cancer by isolating EVs befor and after surgery from patients con GBM.

So, the first step was to define distinct signatures to describe the GBM. We reported the establishment and characterization of GBM primary cultures derived from the primary tumor tissue of patients surgically treated for the presence of the tumor. Although numerous human glioma cell lines have been cultivated only, some were successfully established and propagated.

Four cell types with different cell morphology are permanently observable in the culture: most cells exhibit spindle or glia-like morphology, although multinucleated giant cells are also present at a low frequency. Heterogeneity in glioblastoma histomorphology is well known, and the presence of different cell types reflects that this phenomenon also occurs in *vitro* conditions. The detailed immunofluorescence analysis proved the expression of main neuroglial protein markers in cells of GBM during the cultivation, i.e. GFAP and VIM, which confirm that they derived from transformed glial cells, as well as confirming they neuroectodermal origin of these cell lines. The strong expression of GFAP was stable during long-term cultivation, thus confirming the glial origin of the cell lines. These results suggest that the expression of GFAP could be a potential marker for distinguishing undifferentiated GFAP-negative glial tumors. During the cultivation, other markers have assessed. In particular, no reaction was detected for NSE in all the cell lines, whereas we observed a low positivity for ALDH1 and strong positivity for PCNA. The absence of expression for NSE, as a neuronal marker, confirmed that these cell lines represent cell populations with features of glioblastoma cancer cells. Although ALDH1 has recently been suggested as a novel stem cell marker in a small series of GBM (Yoon, 2020), its expression and function in the central nervous system (CNS) and tumors deriving thereof are largely unknown. We therefore sought to examine the role of ALDH1 in multiple passages of cultivation to get a closer insight into the role of this suggested prognostic stem cell marker, and we ascertained a low or absent expression suggesting that the majority of the cell lines does not feature stem cell characteristics. By contrast, a strong immunopositivity reaction we noticed in the G166 staminal cell line, as expected. Subsequently, we also analyzed the expression of PCNA, i.e. a marker involved in DNA replication which allows the evaluation of the tumor grade, recurrence span and malignancy in cancer diagnosis. We observed a strong positive reaction in all cell lines, with both nuclear and cytoplasmic localization. The markers analyzed were also expressed in the stabilized G166 line, confirming that the primary line studied reflected the condition of the tumor.

A proper molecular characterisation of the tumour is required to provide more effective treatment. Therefore, we proceed with evaluating by immunohistochemistry and immunifluorescence to

determine the presence, subcellular localization and relative abundance of Hsp10, Hsp27, Hsp60, Hsp70, and Hsp90 markers. The current study sought to explore Hsp27 levels revealing a high expression in the cytosol of all primay cell lines. Specifically, Hsp27 protein expression levels showed a more intense immunostaining in GBM cases with short survival, confirming the possible usefulness of Hsp27 as a predictive factor of worse prognosis. Moreover it has been reported in the literature that, Hsp27 overexpression in cancer cells is responsible for chemoresistance and poor prognosis (Webber, 2013), and when works with Hsp90 is able perpetuate the malignant nature of GBM, thus becoming as targets for new cancer therapies. A significant expression of Hsp10 and Hsp60 was observed in all primary culture cells of GBM. The presence of a diffuse immunostaining positivity for Hsp60 in the cytoplasm has already been described in other forms of solid tumors (Théry, 2018). The high expression of Hsp10 and Hsp60 is maintained from the first passages of cell growth, and it remains elevated until the end of the treatment. This suggests that, these chaperonins are implicated in the onset and/or progression of cancer from the beginning to the early stages. Of note, we identified Hsp10 and Hsp60 only in the cytosol, where they could contribute to both anti-apoptosis and pro-apoptosis processes. Regarding Hsp70, it is overexpressed in most human cancers (Gourlay, 2017), even if some tumor types present a lower expression when compared to healthy controls, thus indicating a correlation between Hsp70 levels and survival that is lacking (De la Garza-Ramos, 2016). Herein, we observed a non-significant positivity reaction for Hsp70 in primary tumor cells, probably attributable to an increased presence of free or associated with EVs of Hsp70, as discussed in the previous work (Klekner, 2019). However, we found a high expression of Hsp70 in the stem line, demonstrating that the stem nucleus of the tumor maintains an intracellular localization of Hsp70, while, probably, the surrounding tumor tissue relaxes it in the extracellular environment (where stem cells have not been observed yet). So, we speculated that the low or almost absent expression of Hps70 in the primary cell lines studied is probably due to its release into the extracellular environment through EVs. Only very few studies have assessed Hsp90 expression in GBM. Siegelin et al reported a higher expression in tumour tissue compared to adjacent brain tissue

(Solárová, 2015). In our study, we confirm connections between a high expression of Hsp90 and an advanced disease stage.

Liquid biopsy represents a new minimally invasive technique, which is rapid, cheap, and can be performed multiple times and at an earlier phase before tumours become macroscopically visible, facilitating the surveillance of tumour progression over time (Campanella, 2012). Interestingly, differences could be observed when looking closely at the expression levels of EV specific proteins that can become significant diagnostic and prognostic markers for GBM. According to the studies in the literature, we thought that GBM signatures might be associated with exclusive expression levels of a few selected EV-associated markers that could provide cancer diagnostic signatures from biofluids. Along with CD81, our results suggest that a relatively large fraction of CD81+ EVs were also positive for GFAP. Thus, GFAP-containing EVs can appear in the plasma of individuals with GBM, making it a relatively informative marker by itself. Data confirmed by not detectable levels of GFAP-containing EVs in their plasma of healthy controls (***Figure 16***). Consequently, in combination with CD81 expression, and considering this clinical context, GFAP may add to the specificity of detection of GBM-derived EVs.

As previously reported, blood Hsp70 levels are correlated with the intracellular Hsp70 levels and match the membrane-Hsp70 status of the tumor cells from which they originate. In this study, we observed a significant decrease in the intracellular Hsp70 levels in patients with GBM, through immunohistochemistry and immunofluorescence analysis (***Figure 5*** and ***Figure 8***, respectively). The decrease of Hsp70 expression may indicate an increased presence of hsp70, probably, free or associated at EVs derived by a large variety of highly aggressive cancer cells. Therefore, Hsp70 may be considered a valuable biomarker for determining the viable tumor mass at diagnosis and during or after surgery. Accordingly, we isolated EVs from patients with GBM, and from healthy controls. By immunoblottiing anlysis, we demonstrated that the levels of Hsp70-positive EVs were significantly decreased following surgical resection of the tumor in all patients analyzed, while were significantly higher in patients before surgery compared to patients controls (***Figure 15***). These data was in line with other studies that reporting elevated levels of chaperone-

containing EVs in tumor patients (Yáñez-Mó, 2015). To the best of our knowledge, this is a important results demonstrating the relevance of circulating EVs for monitoring tumor burden. According to our data, EVs may to validate the diagnostic value of Hsp70 as markers of EVs isolated from patients with GBM, and in the same way, the follow-up could also benefit.

This study pinpoints EVs as a major determinant for diagnsotic phenotype in the clinical setting. Unfortunately, so far none promising clinical studies established the actual clinical value of these EV-based biomarkers for the interest of patients and also for economic benefit. Indeed, the accreditation of research laboratories under ISO standard 15189 would certainly improve the reproducibility and standardization of current EV-based biomarkers for clinical use. This will ultimately facilitate the implementation of randomized trials involving multicenter validation and clinical approval of these promising EV-based biomarkers for diagnosis. Only then, EV research may grant clinicians the opportunity to make better-informed therapeutic decisions and, eventually, target both cancer cells and the EV-mediated communication for improved therapeutic outcomes. There is a growing belief that the EV-based industry is poised for growth as observed by the recent market activity. Only last year, EV-based start-up companies have been the recipients of more than $386.2 million in investor funding. More importantly, most of these cancer EV-based startup companies became the focus of strategic acquisitions, partnerships, collaborations, and agreements by large industrial players between 2016 and 2018. Thus, novel technological platforms capable of enriching cancer-derived EVs or specific EV subpopulations from human biofluids are urgently needed to move this field forward.

In this regard, we propose a technological idea based on EVs able to cover macro- and micro-scale approaches. The technology could be used for the isolation and detection of specific markers of EVs isolated from liquid biopsies obtained from cancer patients. So, we first performed an analysis of EV-based technologies and existing of commercial products in the market relatively at isolation methods of EVs from biofluids. We found that, despite the growing interest in the use of EVs, an inherent drawback in most of the platforms are scalability, validation, and standardization. A challenge is related to the isolation phase of the EVs, which is important for

downstream analysis processes. Certainly, using a devices efficiency and reliability for the isolation of EVs, would allow fewer steps and less time, accelerating the analysis on EVs, thus reducing the cost of isolating EVs as a point-of-care tool. Over this challenges, there are still hurdles in the quantification and detection of EVs.

In line with the data presented in this study, SEC method represents a technology widely used to separate heterogeneous samples based on their size, constituting one of the most promising isolation methods in the field of EVs. Indeed, as compared to the classical ultracentrifugation technology, SEC is easy to perform. SEC does not need specific pieces of equipment (e.g. ultracentrifuge) and provides a higher quality of isolated EVs, keeping their shape intact, which can instead be damaged by centrifuge force. Nowadays, various research groups have already widely used this technology, demonstrating its ability to obtain sorted purer vesicles subpopulations than ultracentrifugation (Mandrekar., 2008). Moreover, it has been shown that EVs can be isolated by SEC without significant albumin content (Santos-Junior, 2018). However, one of its main drawbacks is the initial dilution of the sample, causing its dispersion in several fractions, thus influencing the final yield and subsequent EVs analysis. However, despite this, in the "single step" the EVs can be isolated, and the plasma can be loaded onto a sepharose CL-2B column to execute SEC without the need for expensive equipment. In this study, the sepharose columns were made manually, packaging the Sepharose matrix in plastic syringe separately (***Figure 4***), and the isolation of vesicles was rapid, low-cost, and manageable. However, this process may be labor and time consuming, as well as only small volumes to be processed in a single step. Therefore, technological evolution comes to our aid. Indeed, the technology market features the latest development in SEC automation, namely the Automated Fraction Collector (AFC), substantial development of the qEV platform, i.e. Izon AFC, which enables fast, accurate and automated isolation of EVs (***Figure 18***).

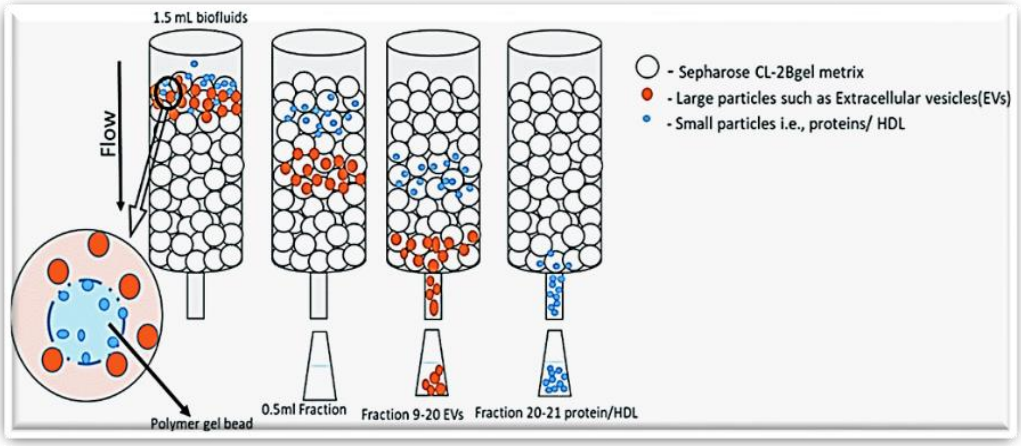

Figure 18. *qEV platform with Automated Fraction Collector (AFC) able to separate EVs from proteins, by pooling them in a specific range of fractions*

In details, a commercial Izon qEV 70 nm column and an automatic fraction collector (AFC) (Izon Science Ltd.) with a 1ml/min flowrate, to permit of separate the EVs from contaminating proteins. The optimal sample volume to obtain pure samples is 0.5 mL, which consistently results in vesicles eluting in the 1.5 mL EVs-zone. However, loading higher sample volumes than recommended volumes lower level of purity in the later vesicle volumes, and greater overlap between protein and EV elution peaks, and higher protein levels within the EV zone. There are different Izon qEV columns with recommended volumes, which can be use for isolation of EVs (https://www.izon.com/application/extracellular-vesicles) (***Table 5***). Overall, isolation of EVs with Izon qEV represent a robust and standardised technique to purify EVs from liquid biopsies. Specifically, Izon qEV allows to automate the isolation process and, at the same time, allows to analyze large volumes of biofluids.

Optimal input volume	qEV column	Output volume
150 µL	qEV single	600 µL
0.5 mL	qEV original	1.5 mL
2 mL	qEV2	8 mL
10 mL	qEV10	20 mL
100 mL	qEV100	200 mL

Table 5. C*ommercial Izon qEV columns with the specifications relating to optimal imput and outup volumes.*

Once isolated, the protein characterization represents the next step for the identification of specific markers. In this study, we used the heat lysis method, as we believe that the heat supplied to the EVs is sufficient to denature the membrane proteins and lyse the EVs. An advantage of thermal lysis is that it can be performed in simple devices without additional modifications, are sufficient small chamber to capture and lyse EVs, and a resistive heater to heat the chamber themselves. Following the lysis, the protein content can be analyzed. In separation sciences, to analyze complex samples there is always a trend toward high-resolution separations. Indeed, methods allowing in parallel were developed to increase sample to sample reproducibility, and this parallelism is still very widely used today. Based on our experiments, we believe that two-dimensional electrophoresis (2-DE) represents the goal for the analysis of the protein profile of EVs. It is a method that involves the separation of proteins by, first, isoelectric focusing and, in the second phase, SDS electrophoresis. Although the order of the two steps may vary, the classical order is the best choice both for economic reasons (the large, second separation is better to be the cheapest one, i.e. SDS electrophoresis) and for technical reasons, since gels for SDS electrophoresis are much easier to interface with downstream protein analysis techniques. 2-DE represents a unique setup that allows accurate and sensitive detection of proteins on the gel. As a result, this step plays a crucial role, as i) only what is detected can be further analyzed and ii) the quantitative variations observed in this phase are the basis for selecting the few points of interest easily. Although the manual production of gels could be the choice, it could be laborious and time consuming. For these reasons, we thought of to solve the problem using ready-to-use gels, fast, easy (within one working day, <6 h), and with lower competing prices. Conducting a market analysis, we found HPETM BlueHorizonTM flatbed gel electrophoresis unit that enables a wide range of applications in the field of protein separation. This device is composed of a central unit which is an extremely flat cooling plate. The central unit allows the separation in unprecedented resolutions, easy to operate, and low buffer consumption. To meet all needs, they are available a variety of ready-to-use SERVA precast gels, also in 2DE with vertical and horizontal migration. In addition, up to four units can be stacked and operated under the control of one power supply and one chiller. This tool is extremely beneficial, as it is versatile in IEF gels, blotting, SDS and

native PAGE, and others. Therefore, is possibly obtained a high quality of separation in a singol step.

As a next step, is analyze the results obtaimed by 2.DE. Image processing techniques commonly used to analyze gel electrophoresis require three main steps: band detection, band matching, and quantification. Although several techniques were presented in literature to automate all steps fully, gel image analysis still requires researchers to extract information manually. This type of extraction is time consuming and subject to human errors. Current in-gel protein detection methods fall into three main categories: organic dye detection, silver staining, and fluorescence. This study aimed to identify high quality and accurate detection systems, and, therefore, we initially have oriented ourselves towards fast, easy to use and competitive fluorescence methods in the market. In this regard, Bio-Rad provides several 2-DE gel imaging acquisition systems combined an image analysis software that can meet various 2-DE gel imaging requirements, thus making the analysis fully automated. Of note, analysis of high-quality 2-DE gels is an essential requirement for investigating changes in protein expression. In consider this, 2-DE gel before being used is necessary digitize them with an image evaluation system. The most commonly used devices are camera-based systems, densitometers, phosphor imagers, and fluorescence scanners. About that, Bio-Rad has imaging equipment suitable for different detection methods typology. Consequently, we conducted a market research to order identify a system for the detection of gels 2-DE, and, surprisingly, in the roundup of instruments available in market and in by Bio-Rad companie, we found GS-900 Calibrated Densitometer (***Figure 19***). This tool allows the identification of proteins in manner fast and with a low-cost quantitative analysis, which can being pushed forward to reach commercialization/clinical use by several startup companies. This tool allows to obtain highly safe, reliable, and high quality results in manner quickly and accurately.

Figure 18. *GS-900 Densitometer is a high-quality with accurate detection system*

The GS-900 Calibrated Densitometer is designed to reproducibly image gels, blots, and film and quantitate proteins across a wide dynamic range. The GS-900 Densitometry System uses transmissive and reflective imaging to scan chromogenic samples at the optimal detection wavelength. The three-colour red, green, and blue CCD imaging technology enable accurate, reproducible quantitation with a wide variety of common stains (https://www.bio-rad.com/it-it/applications-technologies/imaging-analysis-2-d-electrophoresis-gels?ID).

In this study, we aimed at developing an "integrated device" for isolating and quantification of EVs from plasma for initial screening of GBM. Coupling 2-DE gels with isolation and enrichment of EVs in an inexpensive, disposable device significantly streamline the analysis of EVs from biofluids. Finally, we developed a devices idea for isolation, enrichment and quantification of EVs based on the principle of size-exclusion capable to fraction and enrich EVs within of a specific size range. More importantly, the concentration of EVs from patients with GBM may significantly elevated compared to healthy controls, and SEC methos differentiated cancer patients from healthy controls with a high sensitivity. The captured EVs coul be analyzed using 2-DE gels and densitometer approches, which might greatly streamlined the process for point-of-care (POC) testing. The captured EVs coul be analyzed using 2-DE gels and densitometer approches, which might greatly streamlined the process for point-of-care (POC) testing. The idea developed in this proof-of-concept study can be broadly applied to isolate of EVs from cancer patients cancer patients in the most convenient and immediate way.

From a perspective of POC testing, the developed EV quantification modality is advantageous over traditional methods for isolating and detecting EVs from samples, considering insufficient infrastructure and inexperience operators. In addition, our idea is based on size-exclusion, which eliminates the use of capture antibody to isolate EVs and obviates the tedious optimization of flow rate. The device might eliminat the need for an ultracentrifuge to isolate EVs from plasma, which is costly and time-consuming. Moreover, the densitometer proposed in this study to accommodate convenient detection/quantification of proteins without reference to a complex instrument. Compared to other existing EV analytical methods, our integrated EV analytical device is more cost-effective. This integrated approach might to be the proof-of-concept of using the concentration of EVs to differentiate cancer from healthy controls in a non-invasive manner. Furthermore, this idea has potential to be integrated with advance technologies. Nevertheless, future studies will benefit from clinical validation in a larger population and applications in other cancers. Finally, this integrated device has great potential to be subsequently registrated by the European Economic Community according to Regulation (EU) 2017/746 on in *vitro* diagnostic medical devices (IVDR), in order improve clinical diagnosis of GBM in clinics and at point-of-care settings.

10 Conclusion

Despite recent therapeutic advances and improved imaging techniques, GBM diagnosis is frequently effectuated in the advanced stages of the illness. At this point, the impact on patients'quality of life is severe. Furthermore, GBM tumors are still difficult to manage, and MRI follow-ups are expensive and sometimes misleading, as it is difficult to develop the diagnosis and prognosis. Despite ongoing efforts to develop new diagnostic and therapeutic tools, minimal advances have been made, and no reliable biomarkers are being used in clinical practice. Develop devices for rapid detection of tumor-related biomarkers can improve time to diagnosis and treatment planning, and pave the way for more glioma-targeting FDA-approved IVDRs that can help researchers and clinicians parse through the cellular and genetic heterogeneity, which makes these tumors difficult to treat. These diagnostics tools and methods are particularly important with respect to GBM due to the unique molecular profile that varies from patient to patient, and this information is necessary for the application of precision medicine for the patient's best chance at survival. The continued research and development of targeted therapies, combined with advancements advanced screening and detection tools, hold immense potential for increasing survival and prognosis of GBM patients.

11 References

Acunzo. (2012). HSP27 (HspB1), αB-crystallin (HspB5) and HSP22 (HspB8) as regulators of cell death. . *Int J Biochem Cell Biol.*

Acunzo, J. (2012). Small heat shock proteins HSP27 (HspB1), αB-crystallin (HspB5) and HSP22 (HspB8) as regulators of cell death. *Int J Biochem Cell Biol.*, 44(10):1622-31. doi: 10.1016/j.biocel.2012.04.002.

Albakova, Z. (2020). HSP70 Multi-Functionality in Cancer. *Cells*, 9(3):587. doi: 10.3390/cells9030587.

Al-Khallaf, H. (2017). Isocitrate dehydrogenases in physiology and cancer: biochemical and molecular insight. *Cell Biosci*, ;7:37. doi: 10.1186/s13578-017-0165-3. .

Almeida-Souza, L. (2010). Increased monomerization of mutant HSPB1 leads to protein hyperactivity in Charcot-Marie-Tooth neuropathy. *J Biol Chem*, 285(17):12778-86. doi: 10.1074/jbc.M109.082644.

Al-Nedawi, K. (2008). Intercellular transfer of the oncogenic receptor EGFRvIII by microvesicles derived from tumour cells. *Nat Cell Biol*, 10(5):619-24. doi: 10.1038/ncb1725.

Al-Samadi, A. (2017). Crosstalk between tongue carcinoma cells, extracellular vesicles, and immune cells in in vitro and in vivo models. *Oncotarget.*, 8(36):60123-60134. doi: 10.18632/oncotarget.17768.

Anthony, C. (2019). The evolving role of antiangiogenic therapies in glioblastoma multiforme: current clinical significance and future potential. *Expert Opin Investig Drugs*, ;28(9):787-797. doi: 10.1080/13543784.2019.1650019.

Arrigo, A. (2007). Hsp27 (HspB1) and alphaB-crystallin (HspB5) as therapeutic targets. *FEBS Lett.*, 581(19):3665-74. doi: 10.1016/j.febslet.2007.04.033.

Arvold, N. (2014). Treatment options and outcomes for glioblastoma in the elderly patient. *Clin Interv Aging*, ;9:357-67. doi: 10.2147/CIA.S44259.

Babayan. 2018. Advances in liquid biopsy approaches for early detection and monitoring of cancer. *Genome Med.*

Babayan, A. (2018). Advances in liquid biopsy approaches for early detection and monitoring of cancer. *Genome Med*, 10(1):21. doi: 10.1186/s13073-018-0533-6.

Babu, R. (2013). Outcome and prognostic factors in adult cerebellar glioblastoma. *J Clin Neurosci*, 20(8):1117-21. doi: 10.1016/j.jocn.2012.12.006.

Bao, S. (2006). Glioma stem cells promote radioresistance by preferential activation of the DNA damage response. *Nature*, ;444(7120):756-60. doi: 10.1038/nature05236.

Becker, A. (2016). Extracellular Vesicles in Cancer: Cell-to-Cell Mediators of Metastasis. *Cancer cell*, 30(6):836-848. doi: 10.1016/j.ccell.2016.10.009.

Behnan, J. (2019). The landscape of the mesenchymal signature in brain tumours. *Brain*, 142(4):847-866. doi: 10.1093/brain/awz044.

Bell, E. (2018). Association of MGMT Promoter Methylation Status With Survival Outcomes in Patients With High-Risk Glioma Treated With Radiotherapy and Temozolomide: An Analysis From the NRG Oncology/RTOG 0424 Trial. *JAMA Oncol*, 4(10):1405-1409. doi: 10.1001/jamaoncol.2018.1977.

Benedikter. (2017). Ultrafiltration combined with size exclusion chromatography efficiently isolates extracellular vesicles from cell culture media for compositional and functional studies. *Sci Rep.* , 15297.

Bepperling, A. (2012). Alternative bacterial two-component small heat shock protein systems. *Proc Natl Acad Sci U S A.*, 109(50):20407-12. doi: 10.1073/pnas.1209565109.

Bergmann, N. (2020). The Intratumoral Heterogeneity Reflects the Intertumoral Subtypes of Glioblastoma Multiforme: A Regional Immunohistochemistry Analysis. *Front Oncol*, 10:494. doi: 10.3389/fonc.2020.00494.

Bohn, A. (2018). The association between race and survival in glioblastoma patients in the US: A retrospective cohort study. *PLoS One*, 13(6):e0198581. doi: 10.1371/journal.pone.0198581.

Boussadia. (2018). Acidic microenvironment plays a key role in human melanoma progression through a sustained exosome mediated transfer of clinically relevant metastatic molecules. . *J Exp Clin Cancer Res*, 245.

Brennan, C. (2013). Research Network. The somatic genomic landscape of glioblastoma. *Cell.*, 155(2):462-77. doi: 10.1016/j.cell.2013.09.034.

Brennan, C. (2013). The somatic genomic landscape of glioblastoma. *Cell*, 155(2):462-77. doi: 10.1016/j.cell.2013.09.034.

Brocchieri, L. (2000). Conservation among HSP60 sequences in relation to structure, function, and evolution. *Protein Sci.*, 9(3):476-86. doi: 10.1110/ps.9.3.476.

Brocchieri, L. (2008). hsp70 genes in the human genome: Conservation and differentiation patterns predict a wide array of overlapping and specialized functions. *BMC Evol Biol.*, 8:19. doi: 10.1186/1471-2148-8-19.

Broggi, M. (2019). Tumor-associated factors are enriched in lymphatic exudate compared to plasma in metastatic melanoma patients. *J Exp Med.*, 216(5):1091-1107. doi: 10.1084/jem.20181618.

Brzozowski. (2018). Extracellular vesicles with altered tetraspanin CD9 and CD151 levels confer increased prostate cell motility and invasion. *Sci Rep.*, 8822.

Campanella, C. (2012). The odyssey of Hsp60 from tumor cells to other destinations includes plasma membrane-associated stages and Golgi and exosomal protein-trafficking modalities. *PLoS One*, 7(7):e42008. doi: 10.1371/journal.pone.0042008.

Campanella, C. (2016). The histone deacetylase inhibitor SAHA induces HSP60 nitration and its extracellular release by exosomal vesicles in human lung-derived carcinoma cells. *Oncotarget*, 7(20):28849-67. doi: 10.18632/oncotarget.6680.

Cappello., F. (2005). The expression of HSP60 and HSP10 in large bowel carcinomas with lymph node metastase. *BMC Cancer.*, 5:139. doi: 10.1186/1471-2407-5-139.

Cappello., F. (2008). Hsp60 expression, new locations, functions and perspectives for cancer diagnosis and therapy. *Cancer Biol Ther.*, 7(6):801-9. doi: 10.4161/cbt.7.6.6281.

Cappello., F. (2017). Exosome levels in human body fluids: A tumor marker by themselves? *Eur J Pharm Sci.*, ;96:93-98. doi: 10.1016/j.ejps.2016.09.010.

Chakrabart, I. (2005). A population-based description of glioblastoma multiforme in Los Angeles County, 1974-1999. *Cancer*, 104(12):2798-806. doi: 10.1002/cncr.21539.

Chargaff, E. (1946). The biological significance of the thromboplastic protein of blood. *J Biol Chem.*, 166(1):189-97. PMID: 20273687.

Chatterjee, S. (2016). HSP90 inhibitors in lung cancer: promise still unfulfilled. *Clin Adv Hematol Oncol*, 14(5):346-56. PMID: 27379696.

Chen. (2017). Glioma subclassification and their clinical significance. *Neurotherapeutics*, 14(2):284-297. doi: 10.1007/s13311-017-0519-x.

Chen, Y. (2017). Aerrant low expression of p85α in stromal fibroblasts promotes breast cancer cell metastasis through exosome-mediated paracrine Wnt10b. *Oncogene*, 36(33):4692-4705. doi: 10.1038/onc.2017.100.

Chen., P. (2001). Ethnicity delineates different genetic pathways in malignant glioma. *Cancer Res*, 61(10):3949-54.

Chiva-Blanch, G. (2016). roparticle Shedding from Neural Progenitor Cells and Vascular Compartment Cells Is Increased in Ischemic Stroke. *PLoS One.*, 11(1):e0148176. doi: 10.1371/journal.pone.0148176.

Choi, D. (2014). Extracellular vesicles shed from gefitinib-resistant nonsmall cell lung cancer regulate the tumor microenvironment. *Proteomics.*, 14(16):1845-56. doi: 10.1002/pmic.201400008.

Chun, J. (2010). Cytosolic Hsp60 is involved in the NF-kappaB-dependent survival of cancer cells via IKK regulation. *PLoS One.*, 5(3):e9422. doi: 10.1371/journal.pone.0009422.

Ciocca, D. (2005). Heat shock proteins in cancer: diagnostic, prognostic, predictive, and treatment implications. *Cell Stress Chaperones.*, 0(2):86-103. doi: 10.1379/csc-99r.1.

Clerico, E. (2015). How hsp70 molecular machines interact with their substrates to mediate diverse physiological functions. *J Mol Biol.*, 427(7):1575-88. doi: 10.1016/j.jmb.2015.02.004.

Colman, H. (2010). A multigene predictor of outcome in glioblastoma. *Neuro Oncol.*, 12(1):49-57. doi: 10.1093/neuonc/nop007.

Colombo, M. (2014). Biogenesis, secretion, and intercellular interactions of exosomes and other extracellular vesicles. *Ann Rev Cell Dev Biol.*, ;30:255-89. doi: 10.1146/annurev-cellbio-101512-122326.

Csermely, P. (1998). The 90-kDa molecular chaperone family: structure, function, and clinical applications. A comprehensive review. *Pharmacol Ther.*, 79(2):129-68. doi: 10.1016/s0163-7258(98)00013-8.

Cui, Y. (2013). Circulating microparticles in patients with coronary heart disease and its correlation with interleukin-6 and C-reactive protein. *Mol Biol Rep.*, 0(11):6437-42. doi: 10.1007/s11033-013-2758-1.

Davis. (2019). The importance of extracellular vesicle purification for downstream analysis: A comparison of differential centrifugation and size exclusion chromatography for helminth pathogens. *PLoS Negl Trop Dis.* , e0007191.

Davis, F. (2011). Medical diagnostic radiation exposures and risk of gliomas. *Radiat Res*, 175(6):790-6. doi: 10.1667/RR2186.1.

de Gooijer, M. (2018). An Experimenter's Guide to Glioblastoma Invasion Pathways. Trends Mol Med. *Trends Mol Med.*, 24(9):763-780. doi: 10.1016/j.molmed.2018.07.003.

De la Garza-Ramos, R. (2016). Surgical complications following malignant brain tumor surgery: An analysis of 2002-2011 data. *Clin Neurol Neurosurg*, 140:6-10. doi: 10.1016/j.clineuro.2015.11.005.

De la Garza-Ramos., R. (2016). Surgical complications following malignant brain tumor surgery: An analysis of 2002-2011 data. *Clin Neurol Neurosurg.*, 140:6-10. doi: 10.1016/j.clineuro.2015.11.005.

De Rubis, G. (2019). Liquid Biopsies in Cancer Diagnosis, Monitoring, and Prognosis. . *Trends Pharmacol Sci.*, 0(3):172-186. doi: 10.1016/j.tips.2019.01.006.

Deun, V. (2014). The impact of disparate isolation methods for extracellular vesicles on downstream RNA profiling. *J Extracell Vesicles*,.3. doi: 10.3402/jev.v3.24858.

Dobes, M. (2011). Increasing incidence of glioblastoma multiforme and meningioma, and decreasing incidence of Schwannoma (2000-2008): Findings of a multicenter Australian study. *Surg Neurol Int.*, 2:176. doi: 10.4103/2152-7806.90696.

Doucette, T. (2013). Immune heterogeneity of glioblastoma subtypes: extrapolation from the cancer genome atlas. *Cancer Immunol Res*, 1(2):112-22. doi: 10.1158/2326-6066.CIR-13-0028. .

D'Souza, S. (1998). Constitutive expression of heat shock proteins Hsp90, Hsc70, Hsp70 and Hsp60 in neural and non-neural tissues of the rat during postnatal development. *Cell Stress Chaperones*, 188-99. doi: 10.1379/1466-1268(1998)003<0188:ceohsp>2.3.co.

Dubrow, R. (2010). Dietary components related to N-nitroso compound formation: a prospective study of adult glioma. *Cancer Epidemiol Biomarkers Prev*, 19(7):1709-22. doi: 10.1158/1055-9965.EPI-10-0225.

Duijvesz. (2015). Immuno-based detection of extracellular vesicles in urine as diagnostic marker for prostate cancer. . *Int J Cancer.*, 2869-78.

Elsharkasy, O. (2020). Extracellular vesicles as drug delivery systems: Why and how? *Adv Drug Deliv Rev*, 159:332-343. doi: 10.1016/j.addr.2020.04.004.

Endzeliņš, E. (2017). Detection of circulating miRNAs: comparative analysis of extracellular vesicle-incorporated miRNAs and cell-free miRNAs in whole plasma of prostate cancer patients. *BMC Cancer.*, ;17(1):730. doi: 10.1186/s12885-017-3737-z.

Engelhard, H. (2010). Clinical presentation, histology, and treatment in 430 patients with primary tumors of the spinal cord, spinal meninges, or cauda equina. *J Neurosurg Spine.*, 13(1):67-77. doi: 10.3171/2010.3.SPINE09430.

Enriquez, A. (2017). The human mitochondrial Hsp60 in the APO conformation forms a stable tetradecameric complex. *Cell Cycle.*, 16(13):1309-1319. doi: 10.1080/15384101.2017.1321180.

Fais. (2016). Evidence-Based Clinical Use of Nanoscale Extracellular Vesicles in Nanomedicine. *ACS Nano.* , 3886-99. doi: 10.1021/acsnano.5b08015.

Fleckenstein, T. (2015). The Chaperone Activity of the Developmental Small Heat Shock Protein Sip1 Is Regulated by pH-Dependent Conformational Change. *Mol Cell*, 58(6):1067-78. doi: 10.1016/j.molcel.2015.04.019.

Gámez-Valero. (2016). Size-Exclusion Chromatography-based isolation minimally alters Extracellular Vesicles' characteristics compared to precipitating agents. *Sci Rep.* , 6:33641.

Gámez-Valero. (2016). Size-Exclusion Chromatography-based isolation minimally alters Extracellular Vesicles' characteristics compared to precipitating agents. . *Sci Rep.* , 6:33641.

Gammazza, A. (2012). The molecular anatomy of human Hsp60 and its similarity with that of bacterial orthologs and acetylcholine receptor reveal a potential pathogenetic role of anti-chaperonin immunity in myasthenia gravis. *Cell Mol Neurobiol.*, 32(6):943-7. doi: 10.1007/s10571-011-9789-8.

Gangoda, L. (2017). Profiling of Exosomes Secreted by Breast Cancer Cells with Varying Metastatic Potential. *Proteomics*, 17(23-24). doi: 10.1002/pmic.201600370.

Gao. (2017). Extracellular Vesicles from Adipose Tissue-A Potential Role in Obesity and Type 2 Diabetes? . *Front Endocrinol*, 202.

Garrido, C. (2006). Heat shock proteins 27 and 70: anti-apoptotic proteins with tumorigenic properties. *Cell Cycle.*, 5(22):2592-601. doi: 10.4161/cc.5.22.3448.

Gener Lahav, T. (2019). Melanoma-derived extracellular vesicles instigate proinflammatory signaling in the metastatic microenvironment. *Int J Cancer.*, 45(9):2521-2534. doi: 10.1002/ijc.32521.

Gould, S. (2013). As we wait: coping with an imperfect nomenclature for extracellular vesicles. *J Extracell Vesicles*, ;2. doi: 10.3402/jev.v2i0.20389.

Gourlay, J. (2017). The emergent role of exosomes in glioma. *J Clin Neurosci.*, ;35:13-23. doi: 10.1016/j.jocn.2016.09.021.

Gramatzki, D. (2020). Antidepressant drug use in glioblastoma patients: an epidemiological view. *Neurooncol Pract*, 7(5):514-521. doi: 10.1093/nop/npaa022.

Grech, N. (2020). Rising Incidence of Glioblastoma Multiforme in a Well-Defined Population. *Cureus.*, 12(5):e8195. doi: 10.7759/cureus.8195.

Gupta, R. (1995). Evolution of the chaperonin families (Hsp60, Hsp10 and Tcp-1) of proteins and the origin of eukaryotic cells. *Mol Microbiol.*, 15(1):1-11. doi: 10.1111/j.1365-2958.1995.tb02216.x.

Gutiérrez-Vázquez, C. (2013). Transfer of extracellular vesicles during immune cell-cell interactions. *Immunol Rev*, ;251(1):125-42. doi: 10.1111/imr.12013.

Hambardzumyan, D. (2015). Glioblastoma: Defining Tumor Niches. *Trends Cancer*, 1(4):252-265. doi: 10.1016/j.trecan.2015.10.009. .

Hanahan, D. (2011). Hallmarks of cancer: the next generation. *Cell*, 144(5):646-74. doi: 10.1016/j.cell.2011.02.013.

Hansen, J. (2003). Genomic structure of the human mitochondrial chaperonin genes: HSP60 and HSP10 are localised head to head on chromosome 2 separated by a bidirectional promoter. *Hum Genet.*, 112(1):71-7. doi: 10.1007/s00439-002-0837-9.

Hartmann, C. (2010). Patients with IDH1 wild type anaplastic astrocytomas exhibit worse prognosis than IDH1-mutated glioblastomas, and IDH1 mutation status accounts for the unfavorable prognostic effect of higher age: implications for classification of gliomas. *Acta Neuropathol*, 120(6):707-18. doi: 10.1007/s00401-010-0781-z.

Hasan, M. (2017). Responses of Plant Proteins to Heavy Metal Stress-A Review. *Front Plant Sci*, 8:1492. doi: 10.3389/fpls.2017.01492.

Haslbeck, M. (2015). A first line of stress defense: small heat shock proteins and their function in protein homeostasis. *J Mol Biol*, 427(7):1537-48. doi: 10.1016/j.jmb.2015.02.002.

Hayashi. (2020). Proteomic analysis of exosome-enriched fractions derived from cerebrospinal fluid of amyotrophic lateral sclerosis patients. *Neurosci Res*, 43-49.

Hedlund, .. (2011). Thermal- and oxidative stress causes enhanced release of NKG2D ligand-bearing immunosuppressive exosomes in leukemia/lymphoma T and B cells. *PLoS One*, 6(2):e16899. doi: 10.1371/journal.pone.0016899.

Hirata, E. (2017). Tumor Microenvironment and Differential Responses to Therapy. *Cold Spring Harb Perspect Med.*, ;7(7):a026781. doi: 10.1101/cshperspect.a026781.

Hisada, Y. (2019). Cancer cell-derived tissue factor-positive extracellular vesicles: biomarkers of thrombosis and survival. *Curr Opin Hematol.*, 26(5):349-356. doi: 10.1097/MOH.0000000000000521.

Holick, C. (2007). Prospective study of cigarette smoking and adult glioma: dosage, duration, and latency. *Neuro Oncol.*, 9(3):326-34. doi: 10.1215/15228517-2007-005.

Hunt, C. (1985). Conserved features of eukaryotic hsp70 genes revealed by comparison with the nucleotide sequence of human hsp70. *Proc Natl Acad Sci U S A.*, 82(19):6455-9. doi: 10.1073/pnas.82.19.6455.

IARC Working Group on the Evaluation of Carcinogenic Risks to Humans. Non-ionizing radiation, Part 2: Radiofrequency electromagnetic fields. . (2013). *IARC Monogr Eval Carcinog Risks Hum.*

Iwai, K. (2016). Isolation of human salivary extracellular vesicles by iodixanol density gradient ultracentrifugation and their characterizations. *J Extracell Vesicles.* , 5:30829. doi: 10.3402/jev.v5.30829.

Jørgensen, M. (2013). Extracellular Vesicle (EV) Array: microarray capturing of exosomes and other extracellular vesicles for multiplexed phenotyping. *J Extracell Vesicles.* , 2. doi: 10.3402/jev.v2i0.20920.

Jørgensen, MM. (2015). Potentials and capabilities of the Extracellular Vesicle (EV) Array. *J Extracell Vesicles.* , 4:26048. doi: 10.3402/jev.v4.26048.

Jovcevska, I. (2013). Glioma and glioblastoma-how much do we (not) know? *Mol Clin Oncol*, 1(6):935-941. doi: 10.3892/mco.2013.172.

JS, S. (2021). Mechanisms of Invasion in Glioblastoma: Extracellular Matrix, Ca2+ Signaling, and Glutamate. *Front Cell Neurosci*, 15:663092. doi: 10.3389/fncel.2021.663092.

Kampinga, H. (2009). Guidelines for the nomenclature of the human heat shock proteins. *Cell Stress Chaperones.*, 14(1):105-11. doi: 10.1007/s12192-008-0068-7.

Kampinga, H. (2019). Function, evolution, and structure of J-domain proteins. *Cell Stress Chaperones.*, 24(1):7-15. doi: 10.1007/s12192-018-0948-4.

Kanwar, SS. (2014). Microfluidic device (ExoChip) for on-chip isolation, quantification and characterization of circulating exosomes. *Lab Chip.*, 1891-900. doi: 10.1039/c4lc00136b.

Keerthikumar, S. (2016). ExoCarta: A Web-Based Compendium of Exosomal Cargo. *J Mol Biol.*, 428(4):688-692. doi: 10.1016/j.jmb.2015.09.019.

Keerthikumar, S. (2016). ExoCarta: A Web-Based Compendium of Exosomal Cargo. *J Mol Biol.*, 28(4):688-692. doi: 10.1016/j.jmb.2015.09.019.

Keller, L. (2019). Biology and clinical relevance of EpCAM. *Cell Stress.*, 165-180. doi: 10.15698/cst2019.06.188.

Kim, DK. (2013). EVpedia: an integrated database of high-throughput data for systemic analyses of extracellular vesicles. *J Extracell Vesicles.* doi: 10.3402/jev.v2i0.20384.

Kim, M. (2016). Development of exosome-encapsulated paclitaxel to overcome MDR in cancer cells. *Nanomedicine.*, 12(3):655-664. doi: 10.1016/j.nano.2015.10.012. .

Klekner, Á. (2019). Significance of liquid biopsy in glioblastoma - A review. *J Biotechnol.*, 298:82-87. doi: 10.1016/j.jbiotec.2019.04.011.

Ko, S. (2019). Cancer-derived small extracellular vesicles promote angiogenesis by heparin-bound, bevacizumab-insensitive VEGF, independent of vesicle uptake. *Commun Biol.*, 2:386. doi: 10.1038/s42003-019-0609-x.

Koliha, N. (2016). A novel multiplex bead-based platform highlights the diversity of extracellular vesicles. *J Extracell Vesicles.* , 5:29975. doi: 10.3402/jev.v5.29975.

Konar, S. (2016). Predictive Factors Determining the Overall Outcome of Primary Spinal Glioblastoma Multiforme: An Integrative Survival Analysis. *World Neurosurg.*, 86:341-8.e1-3. doi: 10.1016/j.wneu.2015.08.078.

Korja, M. (2019). Glioblastoma survival is improving despite increasing incidence rates: a nationwide study between 2000 and 2013 in Finland. *Neuro Oncol*, 21(3):370-379. doi: 10.1093/neuonc/noy164.

Kowal, J. (2016). Proteomic comparison defines novel markers to characterize heterogeneous populations of extracellular vesicle subtypes. *Proc Natl Acad Sci U S A.*, E968-77. doi: 10.1073/pnas.1521230113.

Kreimer, S. (2015). Mass-spectrometry-based molecular characterization of extracellular vesicles: lipidomics and proteomics. *J Proteome Res.*, 2367-84. doi: 10.1021/pr501279t.

Lässer, C. (2018). Subpopulations of extracellular vesicles and their therapeutic potential. *Mol Aspects Med*, 60:1-14. doi: 10.1016/j.mam.2018.02.002.

Lawson, J. (2017). Selective secretion of microRNAs from lung cancer cells via extracellular vesicles promotes CAMK1D-mediated tube formation in endothelial cells. *Oncotarget.*, 8(48):83913-83924. doi: 10.18632/oncotarget.19996.

Lee, JH. (2017). Role of HSPA1L as a cellular prion protein stabilizer in tumor progression via HIF-1α/GP78 axis. *Oncogene*. doi: 10.1038/onc.2017.263.

Lee, C. (2000). Gene-expression profile of the ageing brain in mice. *Nat Genet.*, ;25(3):294-7. doi: 10.1038/77046.

Lee, J. (2017). Role of HSPA1L as a cellular prion protein stabilizer in tumor progression via HIF-1α/GP78 axis. *Oncogene*, 36(47):6555-6567. doi: 10.1038/onc.2017.263.

Lee., J. (2006). Tumor stem cells derived from glioblastomas cultured in bFGF and EGF more closely mirror the phenotype and genotype of primary tumors than do serum-cultured cell lines. *Cancer Cell.*, 9(5):391-403. doi: 10.1016/j.ccr.2006.03.030.

Lee., J. (2006). Tumor stem cells derived from glioblastomas cultured in bFGF and EGF more closely mirror the phenotype and genotype of primary tumors than do serum-cultured cell lines. *Cancer Cell.*, 9(5):391-403. doi: 10.1016/j.ccr.2006.03.030.

Li, J. (2013). Structure, function and regulation of the hsp90 machinery. *Biomed J*, 36(3):106-17. doi: 10.4103/2319-4170.113230.

Liebs, S. (2019). Liquid biopsy assessment of synchronous malignancies: a case report and review of the literature. *ESMO Open.*, 4(4):e000528. doi: 10.1136/esmoopen-2019-000528.

Liu, S. (2017). Relationship between necrotic patterns in glioblastoma and patient survival: fractal dimension and lacunarity analyses using magnetic resonance imaging. *Sci Rep*, 7(1):8302. doi: 10.1038/s41598-017-08862-6.

LM., D. (2019). Overview of Extracellular Vesicles, Their Origin, Composition, Purpose, and Methods for Exosome Isolation and Analysis. *Cells*, 8(7):727. doi: 10.3390/cells8070727.

Loeb, S. (2014). Overdiagnosis and overtreatment of prostate cancer. *Eur Urol.* , 1046-55. doi: 10.1016/j.eururo.2013.12.062.

Logozzi, M. (2009). High levels of exosomes expressing CD63 and caveolin-1 in plasma of melanoma patients. *PLoS One.*, e5219. doi: 10.1371/journal.pone.0005219.

Logozzi, M. (2017). Increased PSA expression on prostate cancer exosomes in in vitro condition and in cancer patients. *Cancer Lett.*, 318-329. doi: 10.1016/j.canlet.2017.06.036.

Logozzi, M. (2019). Increased Plasmatic Levels of PSA-Expressing Exosomes Distinguish Prostate Cancer Patients from Benign Prostatic Hyperplasia: A Prospective Study. *Cancers (Basel).*, 1449. doi: 10.3390/cancers11101449.

Logozzi, M. (2019). Prostate cancer cells and exosomes in acidic condition show increased carbonic anhydrase IX expression and activity. *J Enzyme Inhib Med Chem.* , 272-278. doi: 10.1080/14756366.2018.1538980.

Logozzi, M. (2020). Immunocapture-based ELISA to characterize and quantify exosomes in both cell culture supernatants and body fluids. *Methods Enzymol.*, 155-180. doi: 10.1016/bs.mie.2020.06.011.

Logozzi, M. (2020). Plasmatic exosomes from prostate cancer patients show increased carbonic anhydrase IX expression and activity and low pH. *J Enzyme Inhib Med Chem.* , 280-288. doi: 10.1080/14756366.2019.1697249.

Logozzi, M. (2021). Plasmatic Exosome Number and Size Distinguish Prostate Cancer Patients From Healthy Individuals: A Prospective Clinical Study. *Front Oncol.*, 727317. doi: 10.3389/fonc.2021.727317.

Logozzi, M. (2018). Microenvironmental pH and Exosome Levels Interplay in Human Cancer Cell Lines of Different Histotypes. *Cancers (Basel).*, 10(10):370. doi: 10.3390/cancers10100370.

Lopes-Rodrigues, V. (2017). Identification of the metabolic alterations associated with the multidrug resistant phenotype in cancer and their intercellular transfer mediated by extracellular vesicles. *Sci Rep.*, 7:44541. doi: 10.1038/srep44541.

Lottaz, C. (2010). Transcriptional profiles of CD133+ and CD133- glioblastoma-derived cancer stem cell lines suggest different cells of origin. *Cancer Res*, 70(5):2030-40. doi: 10.1158/0008-5472.CAN-09-1707.

Lottaz, C. (2010). Transcriptional profiles of CD133+ and CD133- glioblastoma-derived cancer stem cell lines suggest different cells of origin. *Cancer Res.*, 70(5):2030-40. doi: 10.1158/0008-5472.CAN-09-1707.

Louis, DN. (2016). The 2016 World Health Organization Classification of Tumors of the Central Nervous System: a summary. *Neuropathol*. 131(6):803-20. doi: 10.1007/s00401-016-1545-1.

Louis., D. (2016). The 2016 World Health Organization Classification of Tumors of the Central Nervous System: a summary. *Acta Neuropathol*, 131(6):803-20. doi: 10.1007/s00401-016-1545-1.

Lowry, M. (2018). Can hi-jacking hypoxia inhibit extracellular vesicles in cancer? *Drug Discov Today.*, 23(6):1267-1273. doi: 10.1016/j.drudis.2018.03.006.

Maacha, S. (2019). Extracellular vesicles-mediated intercellular communication: roles in the tumor microenvironment and anti-cancer drug resistance. *Mol Cancer.*, 18(1):55. doi: 10.1186/s12943-019-0965-7.

Mandrekar., P. (2008). Alcohol exposure regulates heat shock transcription factor binding and heat shock proteins 70 and 90 in monocytes and macrophages: implication for TNF-alpha regulation. *J Leukoc Biol.*, 84(5):1335-45. doi: 10.1189/jlb.0407256.

Markov, O. (2019). Immunotherapy Based on Dendritic Cell-Targeted/-Derived Extracellular Vesicles-A Novel Strategy for Enhancement of the Anti-tumor Immune Response. *Front Pharmacol.*, 10:1152. doi: 10.3389/fphar.2019.01152.

Martincorena, I. (2018). Universal Patterns of Selection in Cancer and Somatic Tissues. *Cell*, 1823. 171(5):1029-1041.e21. PMID: 29906452.

Matsumoto, Y. (2016). Quantification of plasma exosome is a potential prognostic marker for esophageal squamous cell carcinoma. *Oncol Rep*, 36(5):2535-2543. doi: 10.3892/or.2016.5066.

McKiernan, J. (2018). Prospective Adaptive Utility Trial to Validate Performance of a Novel Urine Exosome Gene Expression Assay to Predict High-grade Prostate Cancer in Patients with Prostate-specific Antigen 2-10ng/ml at Initial Biopsy. *Eur Urol*, 74(6):731-738. doi: 10.1016/j.eururo.2018.08.019.

Menck, K. (2017). Characterisation of tumour-derived microvesicles in cancer patients' blood and correlation with clinical outcome. *J Extracell Vesicles.*, 6(1):1340745. doi: 10.1080/20013078.2017.1340745.

Momen-Heravi. (2012). Alternative methods for characterization of extracellular vesicles. Front Physiol. *Front Physiol.*, 3:354.

Mondal, A. (2019). Effective Visualization and Easy Tracking of Extracellular Vesicles in Glioma Cells. *Biol Proced Online*, 21:4. doi: 10.1186/s12575-019-0092-2.

Mondesir, J. (2016). IDH1 and IDH2 mutations as novel therapeutic targets: current perspectives. *J Blood Med.*, 7:171-80. doi: 10.2147/JBM.S70716.

Murillo, O. (2019). exRNA Atlas Analysis Reveals Distinct Extracellular RNA Cargo Types and Their Carriers Present across Human Biofluids. *Cell*, 177(2):463-477.e15. doi: 10.1016/j.cell.2019.02.018.

Musante, L. (2016). Residual urinary extracellular vesicles in ultracentrifugation supernatants after hydrostatic filtration dialysis enrichment. *J Extracell Vesicles.* , 1267896. doi: 10.1080/20013078.2016.1267896.

Naryzhny, S. (2020). Proteome of Glioblastoma-Derived Exosomes as a Source of Biomarkers. *Biomedicines.*, 216. doi: 10.3390/biomedicines8070216.

Nawaz, M. (2018). Extracellular Vesicles and Matrix Remodeling Enzymes: The Emerging Roles in Extracellular Matrix Remodeling, Progression of Diseases and Tissue Repair. *Cell*, 7(10):167. doi: 10.3390/cells7100167.

Neckers, L. (2012). Hsp90 molecular chaperone inhibitors: are we there yet? *Clin Cancer Res*, 18(1):64-76. doi: 10.1158/1078-0432.CCR-11-1000.

Nordin. (2015). Ultrafiltration with size-exclusion liquid chromatography for high yield isolation of extracellular vesicles preserving intact biophysical and functional properties. . *Nanomedicine.*, 879-83.

Noushmehr, H. (2010). Cancer Genome Atlas Research Network. Identification of a CpG island methylator phenotype that defines a distinct subgroup of glioma. *Cancer Cell*, 17(5):510-22. doi: 10.1016/j.ccr.2010.03.017.

Núñez, F. (2019). IDH1-R132H acts as a tumor suppressor in glioma via epigenetic up-regulation of the DNA damage response. *Sci Transl Med*, 11(479):eaaq1427. doi: 10.1126/scitranslmed.aaq1427.

Ohgaki, H. (2013). The definition of primary and secondary glioblastoma. *Clin Cancer Res*, 19(4):764-72. doi: 10.1158/1078-0432.CCR-12-3002.

Ostergaard, O. (2012). Quantitative proteome profiling of normal human circulating microparticles. *J Proteome Res*, 11(4):2154-63. doi: 10.1021/pr200901p.

Osti, D. (2019). Clinical Significance of Extracellular Vesicles in Plasma from Glioblastoma Patients. *Clin Cancer Res.*, 266-276.

Ostrom, Q. (2018). CBTRUS Statistical Report: Primary Brain and Other Central Nervous System Tumors Diagnosed in the United States in 2011-2015. *Neuo Oncol*, 1;20(suppl_4):iv1-iv86. doi: 10.1093/neuonc/noy131.

Ostrom, Q. (2019). CBTRUS Statistical Report: Primary Brain and Other Central Nervous System Tumors Diagnosed in the United States in 2012-201. *Neuro Oncol.*, 21(Suppl 5):v1-v100. doi: 10.1093/neuonc/noz150.

Palazzolo, G. (2012). Proteomic analysis of exosome-like vesicles derived from breast cancer cells. . *Anticancer Res.* , 847-60. PMID: 22399603.

Park, A. (2019). Subtype-specific signaling pathways and genomic aberrations associated with prognosis of glioblastoma. *Neuro Oncol.*, 21(1):59-70. doi: 10.1093/neuonc/noy120.

Parsons, D. (2008). An integrated genomic analysis of human glioblastoma multiforme. *Science*, 321(5897):1807-12. doi: 10.1126/science.

Pathan, M. (2019). Vesiclepedia 2019: a compendium of RNA, proteins, lipids and metabolites in extracellular vesicles. *Nucleic Acids Res.* , D516-D519. doi: 10.1093/nar/gky1029.

Patton, M. (2020). Hypoxia alters the release and size distribution of extracellular vesicles in pancreatic cancer cells to support their adaptive survival. *J Cell Biochem*, 121(1):828-839. doi: 10.1002/jcb.29328.

Perry, J. (2017). Short-Course Radiation plus Temozolomide in Elderly Patients with Glioblastoma. *N Engl J Med*, ;376(11):1027-1037. doi: 10.1056/NEJMoa1611977.

Phillips, H. (2006). Molecular subclasses of high-grade glioma predict prognosis, delineate a pattern of disease progression, and resemble stages in neurogenesis. *Cancer Cell.*, 9(3):157-73. doi: 10.1016/j.ccr.2006.02.019.

Piccirillo, S. (2006). Bone morphogenetic proteins inhibit the tumorigenic potential of human brain tumour-initiating cells. *Nature*, 444(7120):761-5. doi: 10.1038/nature05349.

Qi, Z. (2014). Alcohol consumption and risk of glioma: a meta-analysis of 19 observational studies. *Nutrients*, 6(2):504-16. doi: 10.3390/nu6020504.

Qian, M. (2017). Detection of single cell heterogeneity in cancer. *Semin Cell Dev Biol*, 143-149. doi: 10.1016/j.semcdb.2016.09.003.

Radons, J. (2016). The human HSP70 family of chaperones: where do we stand? *Cell Stress Chaperones.*, 21(3):379-404. doi: 10.1007/s12192-016-0676-6.

Raimondi, L. (2020). Osteosarcoma cell-derived exosomes affect tumor microenvironment by specific packaging of microRNAs. *Carcinogenesis*, 41(5):666-677. doi: 10.1093/carcin/bgz130.

Raimondo, S. (2015). Chronic myeloid leukemia-derived exosomes promote tumor growth through an autocrine mechanism. *Cell Commun Signal.*, 8. doi: 10.1186/s12964-015-0086-x.

Ramp, U. (2007). Expression of heat shock protein 70 in renal cell carcinoma and its relation to tumor progression and prognosis. *Histol Histopathol.*, 22(10):1099-107. doi: 10.14670/HH-22.1099.

Rappa, F. (2012). HSP-molecular chaperones in cancer biogenesis and tumor therapy: an overview. *Anticancer Res*, 32(12):5139-50. PMID: 23225410.

Reina, M. (2017). Role of LFA-1 and ICAM-1 in Cancer. *Cancers (Basel).*, 153. doi: 10.3390/cancers9110153.

Reinhard, J. (2016). The extracellular matrix niche microenvironment of neural and cancer stem cells in the brain. *Int J Biochem Cell Biol.*, 81(Pt A):174-183. doi: 10.1016/j.biocel.2016.05.002.

Rickert, C. (2009). Glioblastoma with adipocyte-like tumor cell differentiation--histological and molecular features of a rare differentiation pattern. *Brain Pathol.*, 19(3):431-8. doi: 10.1111/j.1750-3639.2008.00199.x.

Ricklefs, F. (2018). Immune evasion mediated by PD-L1 on glioblastoma-derived extracellular vesicles. *Sci Adv.*, ;4(3):eaar2766. doi: 10.1126/sciadv.aar2766. .

Rodrigues, K. (2018). Circulating microparticles levels are increased in patients with diabetic kidney disease: A case-control research. *Clin Chim Acta*, 479:48-55. doi: 10.1016/j.cca.2017.12.048.

Rodríguez-Martínez, A. (2019). Exosomal miRNA profile as complementary tool in the diagnostic and prediction of treatment response in localized breast cancer under neoadjuvant chemotherapy. *Breast Cancer Res.*, 21(1):21. doi: 10.1186/s13058-019-1109-0.

Rohle, D. (2013). An inhibitor of mutant IDH1 delays growth and promotes differentiation of glioma cells. *Science*, 340(6132):626-30. doi: 10.1126/science.1236062.

Rong, B. (2018). Molecular mechanism and targeted therapy of Hsp90 involved in lung cancer: New discoveries and developments (Review). *Int J Oncol*, 52(2):321-336. doi: 10.3892/ijo.2017.4214.

Roy, S. (2018). Extracellular vesicles: the growth as diagnostics and therapeutics; a survey. *J Extracell Vesicles*, 7(1):1438720. doi: 10.1080/20013078.2018.1438720.

Santos-Junior, VA. (2018). Shock Proteins: Protection and Potential Biomarkers for Ischemic Injury of Cardiomyocytes After Surgery. *Braz J Cardiovasc Surg.* doi: 10.21470/1678-9741-2017-0169.

Shao, H. (2018). New Technologies for Analysis of Extracellular Vesicles. *Chem Rev.*, 1917-1950. doi: 10.1021/acs.chemrev.7b00534.

Sharifi, G. (2020). Glioma migration through the corpus callosum and the brainstem detected by diffuse and magnetic resonance imaging:initial findings,. *Front hun neurosci*, 25;13:472. doi: 10.3389/fnhum.2019.00472.

Sharma, A. (2017). Angiogenic Gene Signature Derived from Subtype Specific Cell Models Segregate Proneural and Mesenchymal Glioblastoma. *Front Oncol.*, 7:146. doi: 10.3389/fonc.2017.00146.

Sheng, B. (2017). Increased HSP27 correlates with malignant biological behavior of non-small cell lung cancer and predicts patient's survival. *Sci Rep*, 7(1):13807. doi: 10.1038/s41598-017-13956-2.

Shiau, A. (2006). Structural Analysis of E. coli hsp90 reveals dramatic nucleotide-dependent conformational rearrangements. *Cell*, 127(2):329-40. doi: 10.1016/j.cell.2006.09.027.

Simeone, P. (2020). Extracellular Vesicles as Signaling Mediators and Disease Biomarkers across Biological Barriers. *Int J Mol Sci*, 2514. doi: 10.3390/ijms21072514.

Singh, M. M. (2018). Thermo Fisher Scientific (US) and Lonza (Switzerland) are the Leading.

Singh., SK. (2003). Identification of a cancer stem cell in human brain tumors. *Cancer Res.*, 63(18):5821-8. PMID: 14522905.

Skottvoll, FS. (2018). Ultracentrifugation versus kit exosome isolation: nanoLC-MS and other tools reveal similar performance biomarkers, but also contaminations. *Future Sci OA.* , FSO359. doi: 10.4155/fsoa-2018-0088.

Solárová, Z. (2015). Hsp90 inhibitor as a sensitizer of cancer cells to different therapies (review). *Int J Oncol*. 46(3):907-26. doi: 10.3892/ijo.2014.2791.

SongTao, Q. (2012). IDH mutations predict longer survival and response to temozolomide in secondary glioblastoma. *Cancer Sci*, 103(2):269-73. doi: 10.1111/j.1349-7006.2011.02134.

Sreedhar, A. (2004). Hsp90 isoforms: functions, expression and clinical importance. *FEBS Lett.*, 562(1-3):11-5. doi: 10.1016/s0014-5793(04)00229-7.

Sreedhar, A. (2004). Hsp90 isoforms: functions, expression and clinical importance. *FEBS Lett.*, 562(1-3):11-5. doi: 10.1016/s0014-5793(04)00229-7.

Stancheva, G. (2014). IDH1/IDH2 but not TP53 mutations predict prognosis in Bulgarian glioblastoma patients. *Biomed Res Int*, 2014:654727. doi: 10.1155/2014/654727.

Stoddard, B. (1993). Structure of isocitrate dehydrogenase with isocitrate, nicotinamide adenine dinucleotide phosphate, and calcium at 2.5-A resolution: a pseudo-Michaelis ternary complex. *Biochemistry*, 32(36):9310-6. doi: 10.1021/bi00087a008.

Szatanek, R. (2015). Isolation of extracellular vesicles: Determining the correct approach (Review). *Int J Mol Med.*, 11-7. doi: 10.3892/ijmm.2015.2194.

Taha, EA. (2019). Roles of Extracellular HSPs as Biomarkers in Immune Surveillance and Immune Evasion. *Int J Mol Sci.*, 4588. doi: 10.3390/ijms20184588.

Tan, A. (2020). Managment of glioblastoma state of the art and future directions. *CA Cancer J Cllin*, 70(4):299-312. doi: 10.3322/caac.21613.

Tanaka, Y. (2013). Clinical impact of serum exosomal microRNA-21 as a clinical biomarker in human esophageal squamous cell carcinoma. *Cancer.*, 119(6):1159-67. doi: 10.1002/cncr.27895. Epub 2012 Dec 7.

Thakkar, J. (2014). Epidemiologic and molecular prognostic review of glioblastoma. *Cancer Epidemiol Biomarkers Prev.*, 23(10):1985-96. doi: 10.1158/1055-9965.EPI-14-0275.

Théry, C. (2018). Minimal information for studies of extracellular vesicles 2018 (MISEV2018): a position statement of the International Society for Extracellular Vesicles and update of the MISEV2014 guidelines. *J Extracell Vesicles*, 7(1):1535750. doi: 10.1080/20013078.2018.1535750.

Thiery, J. (2002). Epithelial-mesenchymal transitions in tumour progression. *Nat Rev Cancer.*, 2(6):442-54. doi: 10.1038/nrc822.

Valencia, K. (2014). miRNA cargo within exosome-like vesicle transfer influences metastatic bone colonization. *Mol Oncol.*, ;8(3):689-703. doi: 10.1016/j.molonc.2014.01.012.

Venkatesan, S. (2016). Genetic biomarkers of drug response for small-molecule therapeutics targeting the RTK/Ras/PI3K, p53 or Rb pathway in glioblastoma. *CNS Oncol*, 5(2):77-90. doi: 10.2217/cns-2015-0005.

Verhaak, R. (2010). Cancer Genome Atlas Research Network. Integrated genomic analysis identifies clinically relevant subtypes of glioblastoma characterized by abnormalities in PDGFRA, IDH1, EGFR, and NF1. *Cancer Cell*, 17(1):98-110. doi: 10.1016/j.ccr.2009.12.020.

Verhaak, R. (2010). Cancer Genome Atlas Research Network. Integrated genomic analysis identifies clinically relevant subtypes of glioblastoma characterized by abnormalities in PDGFRA, IDH1, EGFR, and NF1. *Cancer Cell.*, 17(1):98-110. doi: 10.1016/j.ccr.2009.12.020.

Vilasi, S. (2014). Human Hsp60 with its mitochondrial import signal occurs in solution as heptamers and tetradecamers remarkably stable over a wide range of concentrations. *PLoS One*, 9(5):e97657. doi: 10.1371/journal.pone.0097657.

Vilasi, S. (2018). Chaperonin of Group I: Oligomeric Spectrum and Biochemical and Biological Implications. *Front Mol Biosci.*, 4:99. doi: 10.3389/fmolb.2017.00099.

Villà, S. (2014). Radiation and concomitant chemotherapy for patients with glioblastoma multiforme. *Chin J Cancer*, 33(1):25-31. doi: 10.5732/cjc.013.10216.

Vu, L. (2019). Tumor-secreted extracellular vesicles promote the activation of cancer-associated fibroblasts via the transfer of microRNA-125b. *J Extracell Vesicles.*, 8(1):1599680. doi: 10.1080/20013078.2019.1599680.

Wang, Q. (2017). Tumor Evolution of Glioma-Intrinsic Gene Expression Subtypes Associates with Immunological Changes in the Microenvironment. *Cancer Cell.*, 32(1):42-56.e6. doi: 10.1016/j.ccell.2017.06.003.

Wang, X. (2014). HSP27, 70 and 90, anti-apoptotic proteins, in clinical cancer therapy (Review). *Int J Oncol.*, 45(1):18-30. doi: 10.3892/ijo.2014.2399.

Webber, J. (2013). How pure are your vesicles? *J Extracell Vesicles*, 2. doi: 10.3402/jev.v2i0.19861.

Wesseling, P. (2018). WHO 2016 Classification of gliomas. . *Acta Neuropathol*, 44(2):139-150. doi: 10.1111/nan.12432.

Witwer, K. (2013). Standardization of sample collection, isolation and analysis methods in extracellular vesicle research. *J Extracell Vesicles.*, 2. doi: 10.3402/jev.v2i0.20360.

Wolf, P. (1976). The nature and significance of platelet products in human plasma. *Br J Haematol.* 269-88. doi: 10.1111/j.1365-2141.1967.tb08741.x.

Xia, S. (2016). Tumor microenvironment tenascin-C promotes glioblastoma invasion and negatively regulates tumor proliferation. *Neuro Oncol.*, 507-17. doi: 10.1093/neuonc/nov171.

Xie, Q. (2014). Targeting adaptive glioblastoma: an overview of proliferation and invasion. *Neuro Oncol.*, 16(12):1575-84. doi: 10.1093/neuonc/nou147.

Xu, R. (2018). Extracellular vesicles in cancer - implications for future improvements in cancer care. *Nat Rev Clin Oncol*, 15(10):617-638. doi: 10.1038/s41571-018-0036-9.

Yáñez-Mó, M. (2015). Biological properties of extracellular vesicles and their physiological functions. *J Extracell Vesicles*. 4:27066. doi: 10.3402/jev.v4.27066.

Yoon, S. (2020). Ambient carbon monoxide exposure and elevated risk of mortality in the glioblastoma patients: A double-cohort retrospective observational study. *Cancer Med.*, 9(23):9018-9026. doi: 10.1002/cam4.3572.

Yoon, S. (2020). Ambient carbon monoxide exposure and elevated risk of mortality in the glioblastoma patients: A double-cohort retrospective observational study. *Cancer Med*, 9(23):9018-9026. doi: 10.1002/cam4.3572.

Zarovni, N. (2015). Integrated isolation and quantitative analysis of exosome shuttled proteins and nucleic acids using immunocapture approaches. *Methods.* , 46-58. doi: 10.1016/j.ymeth.2015.05.028.

Zeng, F. (2018). Extracellular vesicle-mediated MHC cross-dressing in immune homeostasis, transplantation, infectious diseases, and cancer. *Semin Immunopathol.*, 40(5):477-490. doi: 10.1007/s00281-018-0679-8.

Zhang, B. (2014). Immunotherapeutic potential of extracellular vesicles. *Front Immunol.*, 5:518. doi: 10.3389/fimmu.2014.00518.

Zhang, P. (2020). Current Opinion on Molecular Characterization for GBM Classification in Guiding Clinical Diagnosis, Prognosis, and Therapy. *Front Mol Biosci*, 7:562798. doi: 10.3389/fmolb.2020.562798.

Zhao. (2018). High Expression of Vimentin is Associated With Progression and a Poor Outcome in Glioblastoma. . *Appl Immunohistochem Mol Morphol.*, 337-344.

Zorrilla. (2019). A Pilot Clinical Study on the Prognostic Relevance of Plasmatic Exosomes Levels in Oral Squamous Cell Carcinoma Patients. *Cancers (Basel).*, 429.